



1987

A mineralogical study of the Harmon lignite bed, Bullion Creek Formation (Paleocene), Bowman County, North Dakota

Christopher J. Zygarlicke
University of North Dakota

Follow this and additional works at: <https://commons.und.edu/theses>

 Part of the [Geology Commons](#)

Recommended Citation

Zygarlicke, Christopher J., "A mineralogical study of the Harmon lignite bed, Bullion Creek Formation (Paleocene), Bowman County, North Dakota" (1987). *Theses and Dissertations*. 339.
<https://commons.und.edu/theses/339>

This Thesis is brought to you for free and open access by the Theses, Dissertations, and Senior Projects at UND Scholarly Commons. It has been accepted for inclusion in Theses and Dissertations by an authorized administrator of UND Scholarly Commons. For more information, please contact zeinebyousif@library.und.edu.

A MINERALOGICAL STUDY OF THE HARMON LIGNITE BED,
BULLION CREEK FORMATION (PALEOCENE)
BOWMAN COUNTY, NORTH DAKOTA

by

Christopher J. Zygarlicke

Bachelor of Science, University of Wisconsin-Platteville

A Thesis

Submitted to the Graduate Faculty

of the

University of North Dakota

in partial fulfillment of the requirements

for the degree of

Master of Science

Grand Forks, North Dakota

August

1987

GEO
T1987
Z99

This thesis submitted by Christopher J. Zygarlicke in partial fulfillment of the requirements for the degree of Master of Science from the University of North Dakota has been read by the Faculty Advisory Committee under whom the work has been done, and is hereby approved.

Frank Kamei

(Chairman)

Steven D. Benson

Don L. Schworer

This thesis meets the standards for appearance and conforms to the style and format requirements of the Graduate School of the University of North Dakota, and is hereby approved.

Dean of the Graduate School

Permission

Title A Mineralogical Study of the Harmon Lignite Bed,
Bullion Creek Formation (Paleocene) Bowman County,
North Dakota

Department Geology

Degree Master of Science

In presenting this thesis in partial fulfillment of the requirements for a graduate degree from the University of North Dakota, I agree that the Library of this University shall make it freely available for inspection. I further agree that permission for extensive copying for scholarly purposes may be granted by the professor who supervised my thesis work or, in his absence, by the Chairman of the department or the Dean of the Graduate School. It is understood that any copying or publication or other use of this or part thereof for financial gain shall not be allowed without my written permission. It is also understood that due recognition shall be given to me and to the University of North Dakota in any scholarly use which may be made of any material in my thesis.

Signature _____

Date 7-17-87

TABLE OF CONTENTS

LIST OF ILLUSTRATIONS..... v

LIST OF TABLES..... ix

ACKNOWLEDGEMENTS..... x

ABSTRACT..... xi

INTRODUCTION..... 1

 Purpose and Objectives of Research

 Location

 Geology

 Stratigraphy at Gascoyne

 Previous Work

METHODS..... 25

 Field Methods and Sample Collection

 Megascopic Description

 Proximate/Ulimate, BTU, and Ash Determinations

 Sample Preparation

 Petrographic Methods

 Scanning Electron Microscope/Microprobe Methods

RESULTS 41

 Harmon Bed Stratigraphy and Lithologic Layers

 Proximate/Ulimate, BTU, and Ash Determinations

 Megascopic Descriptions and Lithotypes

 Petrography

 Mineralogy

INTERPRETATION OF DETRITAL AND AUTHIGENIC MINERALS..... 145

 Formation of Detrital Minerals

 Early Stage Authigenic Formation

 Late Stage or Post Compaction Authigenic Formation

ENVIRONMENT OF DEPOSITION..... 154

APPLICATION TO UTILIZATION..... 157

CONCLUSIONS..... 159

FUTURE RESEARCH..... 162

APPENDICES..... 163

 Appendix A Maceral Point Count Data..... 164

 Appendix B SEM/EMPA Sample Descriptions..... 168

REFERENCES CITED..... 180

LIST OF ILLUSTRATIONS

FIGURE

1.	Map of the Fort Union-Powder River coal region, showing the location of the Harmon lignite study area at the Gascoyne Mine and the extent of the Williston Basin (from Groenewold et al., 1979 and Kepferle and Culbertson, 1955).....	6
2.	Chart showing the age and nomenclature of Upper Cretaceous, Paleocene, and lower Eocene strata in western North Dakota.....	9
3.	Map view of Gascoyne Mine pits and location of sampling sites.....	27
4.	Cross-sectional diagram of Harmon bed lithologic layers and the pits they were sampled from.....	43
5.	Geologic column describing lithobodies in the A, B, and C seams in the White and Blue Pits.....	45
6.	Vertical distribution of fusain in the Red Pit...	51
7.	Vertical distribution of fusain in the Yellow Pit A seam.....	53
8.	Plot of total mineral matter (only discrete phases) versus total ash for all of the samples analyzed by SEM/EMPA (total of 30 samples).....	62
9.	Vertical distributions of total ash in the White Pit for all 3 seams.....	73
10.	Vertical distribution of total ash in the Blue Pit.....	75
11.	Vertical distribution of total discrete mineral phases in the White Pit, based upon weight percent of each lithologic layer.....	78
12.	Vertical distribution of total discrete mineral phases in the Blue Pit, based upon weight percent of each lithologic layer.....	80
13.	Vertical distribution of quartz in the White Pit based upon weight percent quartz in each lithobody.....	82

14.	Vertical distribution of quartz in the Blue Pit based upon weight percent of quartz in each lithologic layer.....	84
15.	Vertical distribution of total clays in the White Pit showing greater abundances near seam margins.....	86
16.	Vertical distribution of total clay minerals in the Blue Pit.....	88
17.	Vertical distribution of kaolinite in the Blue Pit showing greater abundances in lithobodies that are adjacent to inorganic-rich layers.....	90
18.	Vertical distribution of kaolinite in the White Pit showing a somewhat random arrangement.....	92
19.	SEM photograph using secondary electron imaging (SEI) of three detrital quartz grains in coal....	95
20.	SEM (SEI) photograph of a quartz grain showing euhedral crystal faces in upper right.....	95
21.	SEM (SEI) photograph of a subrounded quartz grain surrounded by pyrite.....	98
22.	SEM (SEI) photograph of dull gray quartz occurring in center of pyrite framboid.....	98
23.	SEM (SEI) photograph of subrounded- subangular detrital quartz grain observed on a fracture surface.....	100
24.	SEM (SEI) photograph of quartz grain showing conchoidal fracture.....	100
25.	SEM (SEI) photograph showing microcrystalline quartz grains within a detrital silt bands.....	103
26.	SEM (SEI) photograph of 3-4 micron angular flakes of quartz in center of photo which may be authigenic.....	103
27.	SEM (SEI) photograph of distorted kaolinite band.....	105
28.	SEM (SEI) photograph showing larger kaolinite grain in upper part of photo.....	105

29.	SEM (SEI) photograph of lenticular kaolinite lens in center of photo, which is detrital in origin.....	108
30.	SEM (SEI) photograph showing voids in fusinite maceral.....	108
31.	SEM (SEI) photograph of kaolinite infilling voids in fusinite maceral.....	110
32.	SEM (SEI) photograph showing bright colored, oval-shaped areas of kaolinite infilling fusinite voids.....	110
33.	SEM (SEI) photograph of detrital quartz and illite bands.....	112
34.	SEM (SEI) photograph of large illite grain in center of photo.....	112
35.	SEM (SEI) photograph of fine delicate flakes of what is probably authigenic illite.....	115
36.	SEM (SEI) photograph of a large illite grain as viewed in overburden sample.....	115
37.	SEM (SEI) photograph of a rounded montmorillonite grain.....	117
38.	SEM (SEI) photograph of pyrite framboids.....	117
39.	SEM (SEI) photograph showing close-up view of pyrite crystallites, each about 2 microns in diameter.....	119
40.	SEM (SEI) photograph of massive pyrite layers which are characteristic of an epigenetic origin.....	119
41.	SEM (SEI) photograph showing close-up view of the pyrite bands in Figure 40.....	121
42.	SEM (SEI) photograph showing epigenetic pyrite replacing coal.....	121
43.	SEM (SEI) photograph showing pyrite replacing cell wall structures.....	123
44.	SEM (SEI) photograph showing dendritic pyrite replacing coal or following microfractures in coal.....	123

45.	SEM (SEI) photograph of bright subrounded pyrite grain, surrounded by dull gray kaolinite.....	126
46.	SEM (SEI) photograph of small angular grains of pyrite and elongate laths of gypsum as they were viewed on a lignite fracture surface.....	126
47.	SEM (SEI) photograph of authigenic gypsum crystals on coal fracture surface.....	128
48.	SEM (SEI) photograph of rough textured siderite siderite intergrown with smooth surfaced gypsum crystals.....	128
49.	SEM (SEI) photograph showing light gray gypsum mineralization in coal.....	131
50.	SEM (SEI) photograph using SEI of massive barite mineralization in coal particle.....	131
51.	SEM (SEI) photograph of epigenetic barite crystals on lignite fracture surface.....	133
52.	SEM (SEI) photograph showing celestite crystals on coal fracture surface.....	133
53.	SEM (SEI) photograph of quartz and dolomite occurring together in single grain.....	136
54.	SEM (SEI) photograph showing a siderite crystal protruding from a gypsum crystal.....	136
55.	SEM (SEI) photograph showing oval, pellet-like particles of calcium-aluminum-phosphate minerals in cavity of coal.....	139
56.	SEM (SEI) photograph of muscovite flakes.....	139
57.	SEM (SEI) photograph of elongate strands of biotite as seen in silt-clay parting.....	142

LIST OF TABLES

TABLE

1.	Coal mineralogy categories as determined by normalized oxide percentages.....	37
2.	Proximate/ultimate data from Harmon Bed A Seam (bulk coal samples).....	46
3.	Average mineral content for lithologic layers in the White Pit.....	59
4.	Average mineral content for lithologic layers in the Blue Pit.....	60
5.	Common minerals observed in the Harmon lignite and their abundances (based on average weight percent in lithobody).....	64
6.	Elemental oxide weight percents of representative mineral species.....	65
7.	Mineral content for the individual seams and partings for the Blue and White Pits (based on average weight percent of coal).....	69
8.	Average compositions for organically bound constituents in the Blue and White Pits (weight percent calculated from EDS scan of one square micrometer of coal).....	143
9.	Origin of minerals.....	146
10.	Average sizes of major minerals in the Gascoyne White and Blue Pits (average diameter in micrometers).....	156

ACKNOWLEDGEMENTS

This study was funded by the Coal Science Division of the University of North Dakota Energy Research Center (UNDERC) under a Department of Energy cooperative agreement and the University of North Dakota Geology Department.

I would like to extend my appreciation to my thesis committee members, Dr. Frank Karner (chairman), Dr. Don Halvorson, and Dr. Steven Benson. They gave unselfishly of their time, wisdom, and support throughout this project.

I acknowledge the cooperation of the Knife River Coal Company and the staff at the Gascoyne Mine.

I would also like to thank Dr. Harold Schobert for his assistance in the development of this project, Dave Kleesattel (UNDERC) for his assistance in the field, and Ed Steadman (UNDERC) for his help in developing the SEM/EMPA technique.

Finally, I deeply appreciate the typing assistance and loving support of my wife who endured many long hours of hard work in the preparation of this thesis manuscript.

ABSTRACT

Study of the Harmon lignite bed at the Gascoyne Mine in Bowman County, North Dakota showed that most of the minerals in the coal lithobodies were detrital in origin and that variable ash deposition during combustion may be caused by variations in types and quantities of mineral phases.

The Harmon bed is part of the Bullion Creek Formation (Paleocene). Objectives of this study included: to develop scanning electron microscope/microprobe techniques for the study of minerals in coal; to determine the origins of the mineral phases; to postulate a depositional environment for the Harmon lignite; and to ascertain whether variable ash deposition behavior of the Gascoyne lignite is related to mineral content.

Scanning electron microscopy and electron microprobe analysis was used to identify and determine the abundance of minerals in the lignite. The average mineral content in weight percent was 44% quartz, 31% illite, 13% kaolinite, 5% montmorillonite, 5% pyrite, and 2% gypsum. The amount of mineral matter as discrete phases, not organically bound inorganic constituents, varied directly with total ash.

The Blue Pit has a higher inorganic content than the White Pit because of a greater amount of quartz and clays in the B seam. This result demonstrates the lateral variability in inorganic content in the Gascoyne lignite. Minerals also varied in vertical distribution. Quartz and

clay minerals were more abundant in lithologic layers that were adjacent to clay silt partings, overburden, and underclay.

Quartz, illite, and kaolinite are primarily detrital in origin. Framboidal pyrite and possibly some kaolinite and phosphate minerals formed authigenically during early peat stages. Massive pyrite, gypsum, barite, celestite, siderite, and jarosite were probably epigenetic products which formed after seam compaction and coalification. The present mineral content of the Harmon lignite is probably the result of the characteristics of the depositional environment. Authigenic processes during early peat stages or after compaction and coalification had a minor influence on the current mineral content.

The Harmon lignite was probably deposited as part of a lacustrine depositional environment. Periodic transgression and regression of the freshwater body would explain best the types of minerals observed and their distributions. Variations in ash deposition behavior within the Gascoyne Mine may be caused by the variation in types and quantities of discrete mineral phases.

INTRODUCTION

Purpose and Objectives of Research

The study of mineral matter in low rank coal is important for geological interpretations and industrial application. Minerals in coal provide a guide to interpretation of depositional environments and their associated chemical processes. Diagenetic events, including the alteration, dissolution, or addition of mineral matter in a sedimentary unit such as coal, can be interpreted by examining the composition, morphology, and distribution of the mineral matter. If the origins of the mineral matter can be accurately determined, the sequence of diagenetic events can be traced and the dominant processes identified. The relative scarcity of minerals in low rank coal deposits magnifies their importance in geological and geochemical interpretations. There may only be three or four major minerals in a given coal. More detailed study of these minerals should aid in determining the depositional or

geochemical factors governing their occurrences and distribution.

The term "mineral matter" has often been used as a general term for inorganic constituents of coal in any form. This would include both ion-exchangeable cations and discrete mineral phases. In this report, "mineral matter" or "minerals" refers only to discrete crystalline mineral phases. The terms "inorganics" or "inorganic constituents" will refer to both mineral phases and organically bonded elements.

Study of minerals in low rank coal is also important in industrial application such as its suitability as a boiler fuel. During combustion in a typical boiler furnace used by utility companies, ash deposits accumulate on the convection and radiant heat transfer surfaces. With time these deposits will enlarge to a degree dependent upon the composition, quantity, and distribution of inorganic constituents present in the coal. Large accumulations of deposits decrease the heat exchange capacity of the conduction tubes and cause temperatures inside the furnace to increase, especially at the ash deposit sites. Temperatures may increase to the fusion point of the fouling deposits causing them to agglomerate with greater losses of heating efficiency and the necessity of costly furnace-cleaning procedures.

Extensive research has shown that sodium-containing liquid phases are the main cause of ash fouling during the

combustion of low rank coal (Sondreal et al., 1977; Sondreal and Ellman, 1975; Gronhovd et al., 1967). The fouling deposits usually consist of a mixture of calcium and sodium sulfates, sodium carbonates, melilite group minerals, and silicate glass. High-sodium coals form boiler tube deposits that are believed to contain a matrix material that envelops and connects fly ash particles coming off the burning coal, forming a strongly bonded network. Low-sodium coals form deposits that appear to have no continuous matrix material and the particles are held together by weak particle-to-particle surface bonding.

Studies by Sondreal et al. (1977) on low rank coals from the Western U.S. reveal that the severity of ash fouling deposits correlates not only with sodium concentration but also with total ash contents.

Research at the University of North Dakota Energy Research Center (UNDERC) affirms the importance of certain ash constituents besides organically bound sodium, such as discrete mineral phases, which cause fouling deposits to form during low rank coal combustion (Hurley et al., 1985; Hurley and Benson, 1984; Sondreal et al., 1977; Sondreal et al., 1968). Mineral content as well as sodium content must be taken into account when attempting to predict the ash fouling tendency of a low rank coal.

The primary objective of this study is to investigate the quantity, distribution, morphology, composition, and maceral association of discrete mineral phases in the

lignite from the Gascoyne Mine in Bowman County, southwestern North Dakota. The lignite occurs in the Harmon bed which is part of the Paleocene Fort Union Group and the Bullion Creek Formation (Houghton et al., 1984; Kepferle and Culbertson, 1955).

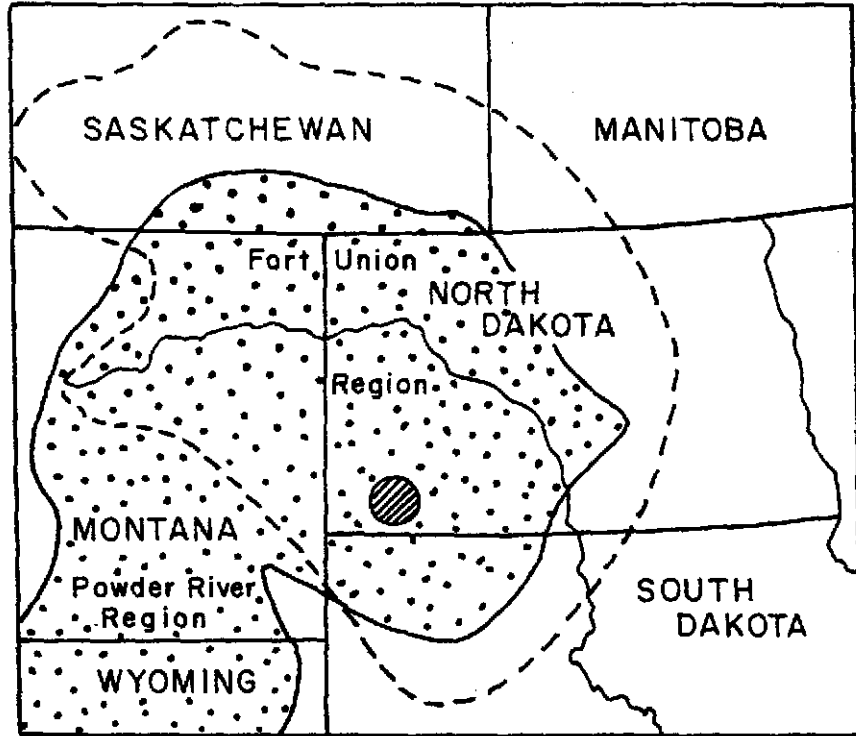
Information acquired from detailed study of the mineralogical and petrologic constituents of low rank coal can be used to interpret or better understand the following problems:

1. The use of mineral matter to characterize lignite.
2. The origin of minerals in the coal.
3. The progression of physical and chemical environments and their associated processes that occurred before, during, and after consolidation and compaction of the coal.
4. The variability in vertical and lateral distribution of minerals in the coal bed.
5. The association between minerals and macerals.
6. The variable ash deposition behavior of lignite within the Gascoyne Mine, in particular the relationship between mineral quantity and composition and ash deposition behavior.

Location

The Gascoyne Mine is located in the extreme southwestern part of North Dakota 2.5 miles east of the city of Gascoyne in Bowman County (Figure 1). The Knife River

Figure 1. Map of the Fort Union-Powder River coal region, showing the location of the Harmon lignite study area at the Gascoyne Mine and the extent of the Williston Basin (Groenewold et al., 1979; Kepferle and Culbertson, 1955).



HARMON BED (Gascoyne Mine Area)



Strippable coal deposits of the Fort Union - Powder River Coal Region



MARGIN OF WILLISTON BASIN


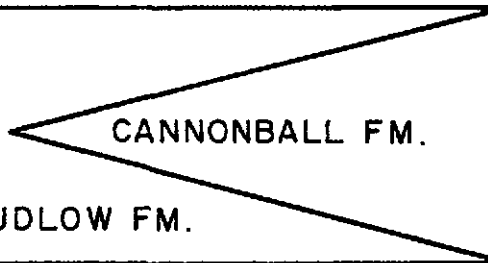
Coal Company owns and operates the mine. At the time of the study four pits were used in the Gascoyne Mine within T. 131 N., R. 99 W. including: the Red pit located in section 29, the White pit in section 28, the Blue pit in sections 26, 27, and 35, and the Yellow pit in section 33. Currently the mine is the second largest in North Dakota and is one of the most efficient strip mines in the United States with respect to the thickness of strippable coal relative to thickness of the overburden (Houghton et al., 1984).

Geology

The study area (Figure 1) is part of the Fort Union Coal region which extends through parts of North Dakota, South Dakota, Montana, and Saskatchewan. It is situated just south of the center of the Williston Basin, a broad structural and sedimentary basin which contains strata from the Cambrian through Tertiary systems (Jacob, 1976; Carlson and Anderson, 1970). Sedimentary units in the area generally dip 25-50 feet per mile north and northeast from the Cedar Creek anticline in the southwest corner of the area (Kepferle and Culbertson, 1955).

Rocks that crop out in Slope and Bowman counties, North Dakota, consist of the Pierre Shale, the Fox Hills Sandstone, and the Hell Creek Formation of Late Cretaceous Age; the Fort Union Group of Paleocene Age; the White River Formation of Oligocene Age; and surficial alluvium deposits of Pleistocene and recent age (Figure 2) (Kepferle and

Figure 2. Chart showing the age and nomenclature of Cretaceous, Paleocene and lower Eocene strata in western North Dakota (from Clayton et al., 1977).

EOCENE	WHITE RIVER FM.  GOLDEN VALLEY FM.
PALEOCENE	SENTINEL BUTTE FM.
	BULLION CREEK FM.
	SLOPE FM.
	LUDLOW FM. 
UPPER CRETACEOUS	HELL CREEK FM.
	FOX HILLS FM.
	PIERRE FM.

Culbertson, 1955; Benson, 1952). The Pierre Shale is a dark-gray micaceous and bentonitic marine shale; only the uppermost 400 feet of this unit is exposed in the extreme western part of Bowman County. Resting conformably on the Pierre Shale is the brown-gray marine Fox Hills Sandstone. The Hell Creek Formation is nonmarine in origin and unconformably overlies the Fox Hills Formation. It consists of alternating dark-gray and brown sandstones, shales, and impure lignitic beds (Kepferle and Culbertson, 1955).

The Fort Union Group in this part of the Williston Basin in Western North Dakota consists of approximately 1200 feet of Paleocene lignite bearing, sandy, silty, and clayey formations (Jacob, 1976; Kepferle and Culbertson, 1955). Formations that comprise the Fort Union Group are, in ascending order, the Ludlow, Cannonball, Slope, Bullion Creek, and Sentinel Butte formations (Figure 2). Terminology for these Paleocene units is not consistent between the United States Geological Survey and the North Dakota Geological Survey. Clayton et al. (1977), in an effort to resolve stratigraphic problems within the Fort Union Group, introduced the Slope and Bullion Creek Formations for strata below the Sentinel Butte Formation. The terminology of Clayton et al. (1977) is presently in use by the North Dakota Geological Survey and will be used in this thesis report.

The Ludlow Formation, which conformably overlies the Hell Creek Formation is comprised of carbonaceous

sandstones and shales which interfinger with marine shales of the Cannonball Formations (Houghton et al., 1984; Kepferle and Culbertson, 1955). Overlying the Ludlow are the Slope, Bullion Creek, and Sentinel Butte Formations respectively. All three of these units are gradational with one another in this area and generally consist of poorly indurated sandstones, siltstones, claystones, lignites, and small lenses of limestone (Jacob, 1976; Royse, 1967; Kepferle and Culbertson, 1955).

The youngest formational unit in the Gascoyne Mine area is the Oligocene White River Formation. Most of this unit has been eroded away, however, remnants exist capping high buttes north of the Gascoyne Mine. Comprising the White River Formation are coarse sandstones interbedded with calcareous and siliceous clays, clay beds, and impure marls (Kepferle and Culbertson, 1955; Benson, 1952).

The depositional history of the Fort Union Group and the White River Formations may be summarized as follows. During the Early Paleocene, mudstones and sandstones of the Cannonball Formation were deposited in a sea that transgressed generally westward over the Cretaceous Hell Creek Formation. The Ludlow, Bullion Creek, Sentinel Butte, and White River Formations were then deposited on an alluvial plain as it prograded generally eastward into the sea as the sea regressed. Highlands to the northwest, which developed toward the end of the Cretaceous Period, provided a source for the eastward prograding sediments (Jacob, 1976;

Royse, 1970).

Stratigraphy at Gascoyne

The Bullion Creek Formation is exposed in the immediate vicinity of the Gascoyne Mine. It consists of unbedded to finely laminated beds of clay and sand lenses. The coal beds recognized in this area include, in ascending order starting from near the base of the Bullion Creek, the H, Hansen, Harmon, Garner Creek, and Meyer lignite beds (Houghton et al., 1984; Kepferle and Culbertson, 1955; Leonard et al., 1925)

The Harmon is the only lignite bed exposed and being mined at the Gascoyne Mine. It is situated roughly 18 m above the base of the Bullion Creek Formation (Houghton et al., 1984). Total thickness of the lignite bed averages 11 m at the Gascoyne Mine. The lignite bed is comprised of three splits or seams which may be separated by clayey-silt partings or mineralized coal (black jack). Some of the seams appear to be separated only by very thinly bedded horizontal fracture zones or fusain layers. Knife River Coal Company officials have informally designated the three seams as the C, B, and A, seams in ascending order. This terminology is also employed in this study.

Previous Work

Minerals in Coal

Traditionally, research has been focused on the

identification and occurrence of minerals in coal. Over 100 different minerals are known to occur in coal, but only about 15 are relatively abundant (Harvey and Ruch, 1984). Some of the more common minerals are quartz, kaolinite, illite, montmorillonite, pyrite, marcasite, sphalerite, calcite, dolomite, hematite, gypsum, barite, zircon, and apatite (Harvey and Ruch, 1984; Stach et al., 1982).

The literature pertaining to coal minerals is primarily focused on higher rank coals and is voluminous. A survey of literature on minerals in North American coals alone yielded 439 references (Akers et al., 1978). Much of the work done in the past has been concerned simply with determining the types and relative abundances of minerals that occur in coal. The paucity, finely disseminated nature, and small size of minerals in coal has made identification difficult.

First attempts to quantify mineral content in coal were done by Parr (1932) who used total sulfur and ash contents to calculate the percent of minerals in coal. Comprehensive, pioneering studies for minerals in coal were done by Ball (1935) and Sprunk and O'Donnell (1942). Ball (1935) performed a detailed petrographic study of mineral concentrates from one coal, the Herrin (No. 6) coal seam of the Illinois Basin. In contrast, Sprunk and O'Donnell (1942) petrographically examined over 3,000 thin sections from about 100 coals. Their results included interpretations of the modes of occurrence of the major mineral types.

More recently, the development of analytical tools such as the low temperature asher (Gluskoter, 1965), scanning electron microscope (SEM), and x-ray diffractometer (XRD) has allowed for direct identification and semi-quantitative analysis of minerals in coal.

An important emphasis of coal research today is the origin of minerals in coal. This new focus has increased our understanding of coal depositional environments and diagenetic processes. Present studies suggest that minerals can occur in coal through several mechanisms: 1) detrital deposition during peat stages, 2) biogenically engendered mineral formation within plants, 3) authigenic formation from ions in solution or organometallic complexes, 4) diagenetic alteration of pre-existing minerals during coalification, and 5) post-compaction mineralization in pores, fractures and cleats (Davis et al., 1984; Finkelman, 1980; Cecil et al., 1979).

Minerals in coals are often classified as detrital, syngenetic, or epigenetic (Mackowsky, 1968). Detrital minerals are those that were deposited into the early swamp environment by wind or water action. Syngenetic minerals form during early peat stages or before seam compaction and consolidation is complete. Epigenetic minerals are mainly those that form in pores, cavities, and fractures in the coal, after compaction and consolidation (Harvey and Ruch, 1984; Mackowsky, 1968).

Mineralogic information that is useful in making

geological interpretations consists of the following: 1) the types and quantities of minerals; 2) textural evidence, that is, the relationships between different minerals and macerals (Finkelman, 1980); and 3) the geochemistry of the relative abundance of detrital and authigenic minerals that are present in coal which may aid in postulating the source of the detritus, the rate of peat accumulation, and basin subsidence. Rapid and extensive uplift of the source area would deposit more detrital minerals and allow less time for alteration and weathering. This would result in a lower relative concentration of authigenic mineral species, including altered minerals (Valkovic, 1983). Rao and Gluskoter (1973) illustrated this concept by using mineralogic data to construct a model of the depositional environments of the Herrin (No. 6) coal.

Textural evidence can be ascertained using standard SEM and optical microscopy techniques. Texture is defined here as the size, shape, and arrangement of the mineral constituents in the coal matrix. Detrital minerals are usually subrounded to subangular, often aligned parallel to bedding planes, and may have characteristics indicative of high temperature origins (i.e. rutilated quartz). Authigenic phases are found in pores, cavities, and fractures in the coal and may show crystal faces characteristic of growth in place (Güven and Lee, 1983; Finkelman, 1983; 1982;).

Güven and Lee (1983) used compositional and textural evidence, as determined by XRD and SEM analysis, to

categorize minerals in 27 core sections of Texas lignite. They determined that kaolinite, halloysite, microquartz, and pyrite were all authigenic in origin and were probably alteration products of originally detrital silicates in the acidic coal environment.

Diagenesis plays a major role in determining mineral distributions in coal. Mineral transformations begin with weathering in the source rocks, continue in the swamp environment, and further continue to occur throughout coalification (Finkelman, 1983; Ball, 1936).

Geochemical information is useful in differentiating between original detrital minerals and those that have been altered. For example, the identification of trace elements in minerals can be used to determine their origin. Characteristics indicative of high temperature origins, such as rutile needles in a quartz grain, would be indicative of detrital origin.

Cecil and others (1982) determined that the pH and ionic strength of interstitial water in the original peat environment may be major factors in determining the mineral (particularly sulfur minerals) content of the resulting coal bed. Their results were based on data from modern peat forming environments and ancient coal beds. Cecil et al., (1982) proposed that coal which formed in a peat environment having high acidity ($\text{pH} < 4.0$) and low ionic strength would show low ash and sulfur contents due to the leaching of mineral matter and minimal activity of sulfur fixing

bacteria. In contrast, a peat environment that has a near neutral pH or is slightly alkaline would develop into a high ash and high sulfur coal since the peat conditions are optimum for mineral retention and sulfur fixation. They concluded that the variation in the ash and sulfur contents for different coals depends primarily on 1) the availability of CaCO_3 in solution, which regulates the pH, 2) the ionic strength of the waters, which is in large part regulated by the availability of iron and sulfate ions, and 3) the plant paleoecology.

Studies of minerals in low-rank coals are not nearly as extensive as those for higher rank coals (bituminous and higher). As mentioned previously, Guven and Lee (1983) studied in detail the morphology and textural relationships of minerals in lignite from the Wilcox Group in East Texas. Kemezys and Taylor (1964) performed mineralogic research on Australian brown coals, which are similar to lignite.

Pioneering studies of minerals in low rank coal of the western United States were done by Fowkes (1978) who noted the uniqueness of low rank coals as compared to higher rank coals. Studies on 22 samples of lignite and subbituminous coal from the Montana-Wyoming-Dakota region indicated that most of the mineral matter was in the inorganic form and fixed in the coal as "organometallic" components by chelation or by ionic bonding. Discrete minerals comprised a much smaller percentage of the total inorganic matter and were usually observed as small, finely dispersed grains less

than 20 microns in average diameter. Fowkes (1978) noted that higher rank coals had more discrete mineral inclusions than low rank coals and usually exhibited a very small inorganic fraction that was bound to the coal by chelation or ionic forces. He concluded that, given the correct conditions for metamorphism, young coals through time lose their sites for ionic or chelation bonding of metallic ions and, therefore, higher rank coals which have undergone extensive metamorphosis have less inorganic matter that is organically bound to the coal substance (inherent mineralization).

Paulson and others (1972) used x-ray diffraction and electron microprobe techniques to identify mineral phases in North Dakota and Montana lignites. They examined mineral fractions that had been separated from the coal by float/sink methods. Examination of the sink fractions revealed the presence of nacrite (or kaolinite), barite, pyrite, hematite, quartz, calcite, gypsum, and fragments of an alpha-quartz nacrite mixture. Benson et al. (1984) studied the occurrence and distribution of minerals in the Beulah-Zap lignite (North Dakota) and made inferences about the origins of the minerals. Quantitative estimations were determined for the major mineral species present in the Beulah-Zap lignite relative to the height in the seam.

Association of Minerals and Macerals

The distribution of minerals in coal depends greatly on their association with organic coal components such as lithotypes and macerals. Sprunk and O'Donnell (1942) noted the consistent association of certain mineral phases with the four major lithotypes, vitrain, clarain, durain, and fusain, that comprise banded bituminous coal. Kaolinite was often observed lining small cracks in vitrain and filling cellular cavities in fusain, but was most commonly found in the attrital portion of the bright banded coals.

Francis (1961) summarized the relationship between the nature and amounts of inorganic constituents present in the major banded components of coal and their modes of formation. He concluded that vitrain, clarain, durain, and fusain contain increasing proportions of ash. The low proportions of ash in vitrain and the composition of the ash show that the inorganic matter in this component of coal is derived primarily from massive cellular structures of plants. This was confirmed by the high proportions of water-soluble compounds, mainly sulphates and carbonates, and the low proportions of acid insoluble compounds in the ash from vitrains. In contrast, the ash from durains consisted mainly of compounds such as impure aluminum silicates, which had compositions similar to shales in the overburden and were obviously derived from clays that had been washed into the deposit during the peat forming stage. Fusains were observed to contain many inorganic constituents

that can be deposited from solution. This is due to the open structure of the plant cells that form fusain.

Kemezys and Taylor (1964) used transmitted and reflected light microscopy, along with electron microscopy, to study the occurrence and distribution of minerals in some Australian coals. They made correlations between certain minerals and specific maceral groups. They noted that clay minerals and pyrite were commonly associated with vitrinite while chalcedony, sphalerite, chalcopyrite, and siderite were commonly associated with inertinite and fusinite.

In contrast to the more descriptive approach of Kemezys and Taylor (1964), Stanton and Finkelman (1979) correlated reflected light photomaps with SEM images of polished coal surfaces. First, the macerals were identified in reflected light and then the minerals were identified within the macerals using the SEM. Techniques were also developed to identify macerals using only the SEM. SEM identification of macerals was based on the 1) mean atomic number (contrast and difference) using backscattered electron imaging, 2) structure enhancement by mineral constituents, and 3) polishing relief that is apparent in the secondary electron image.

Finkelman (1980) conducted SEM/EDX analyses on selected minerals associated with various macerals in the Waynesburg coal. The following conclusions were drawn from his research: 1) pyrite and calcite are mostly associated with vitrinite, 2) kaolinite is mostly associated with fusinite

and semifusinite and 3) illite, quartz, and rutile commonly occur with the microlithotype termed carbominerite.

Analysis of Minerals in Coal

There are numerous analytical techniques that can be applied to the identification and characterization of minerals in coal. Optical microscopy of coal thin sections has proven to be a viable method of studying minerals in coal (Kemezys and Taylor, 1964; Sprunk and O'Donnell, 1942). Many difficulties exist, however, in the preparation of thin sections and in the identification of mineral grains. The dominantly opaque nature of coal requires that the thin sections be 10 micrometers or less in thickness so that the mineral grains can be seen. In the process of making these ultra-thin thin sections, harder mineral grains such as quartz and pyrite are often plucked off the glass slide.

Identification of minerals using optical microscopy is difficult due to the fine sizes of mineral grains, which average 10-30 micrometers. Because of its widespread availability and extensive use by mineralogists, x-ray diffraction (XRD) is probably the most commonly used technique for analyzing coal minerals (Russel and Rimmer, 1979; Rao and Gluskoter, 1973). Limitations exist when using XRD to analyze minerals in coal because it is necessary to separate the minerals from the coal. High temperature ashing (750 ° C) of coal is one method of concentrating minerals. However, this method does not

preserve the original mineralogic composition (Falcone et al., 1984). Low temperature ashing (<150 ° C) is an alternative method for concentrating minerals in coal (Gluskoter, 1965). However, minor alterations and additions of mineral matter still occur when lignite is low temperature ashed. For example, some of the pyrite in the coal may be oxidized to form hematite and bassinite is commonly produced (Miller, 1984; Rao and Gluskoter, 1973; O'Gorman and Walker, 1972; O'Gorman and Walker, 1971). Another disadvantage of low temperature ashing techniques is that samples may require up to 100 hours of ashing time to sufficiently oxidize the organic matter.

O'Gorman and Walker (1972) were some of the first to use qualitative and quantitative XRD techniques to study minerals in coal. They analyzed 57 U.S. coals, including three low rank coals from North Dakota. In a similar study, Rao and Gluskoter (1973) determined quantitative mineralogies of 65 U.S. bituminous coal samples from the Illinois Basin, using XRD. Included in their results were interpretations of the depositional environment of the Herrin (No. 6) Coal based in part on XRD mineralogical data.

Scanning electron microscope/electron microprobe analysis (SEM/EMPA) proves to be a suitable technique for examining minerals in coal. The SEM/EMPA system allows for observation and chemical analysis of very fined-grained minerals while simultaneously preserving both the original chemistry of the minerals and their relationships to the

organic constituents (Huggins et al., 1980; Raymond and Gooley, 1979; Russel and Rimmer, 1979). It should be noted that the SEM/EMPA system does not identify crystalline mineral phases as does the x-ray diffractometer; rather, the relative intensities of the elemental constituents are used to identify distinct mineral types.

The earliest and most widespread applications of SEM/EMPA to coal included: localized observation of the elemental content of macerals; determination of the morphology of organic maceral structures; identification of minerals; and description of the morphology of minerals (Finkelman, 1978; Greer, 1977; Boentang and Phillips, 1976; Augustyn et al., 1976; Vassamillet, 1972; Hughes, 1971). The qualitative use of SEM/EMPA is exemplified in the study of diagenesis of coal minerals (Stanton and Finkelman, 1979; Finkelman and Stanton, 1978). More recently, automated SEM/EMPA techniques have been developed to quantify coal minerals (Huggins et al., 1980; Moza et al., 1980; Moza et al., 1979).

Previous Investigations of the Harmon Lignite at Gascoyne

The Harmon lignite at the Gascoyne Mine typically shows pronounced within-mine variability in inorganic content and combustion behavior (Hurley and Benson, 1984; Sondreal et al., 1968). An attempt was made by Hurley et al. (1985) to correlate coal characteristics and fouling tendencies using three different coals from the Gascoyne Mine.

Concentrations of elements in the three coals varied, as did the ash fouling tendencies during combustion in a pilot scale combustor. The quantity and strength of the fouling deposits were correlated with their sodium/ash ratios, with a low ratio corresponding to a lower degree of fouling. Two of the coals correlated well with sodium ratios. The massive hard deposit formed by the third coal, however, could not be explained by the sodium/ash ratio.

METHODS

Field Methods and Sample Collection

Coal samples were collected from six locations along the three mile east-west length of the Gascoyne Mine. It was not possible to sample all three seams at any of the sampling sites; however, representative samples of lignite were collected from the four pits that mine the Harmon lignite (Figure 3). Descriptions of a columnar section of lignite at each collection site were made.

Selection of the collection sites was based on the safety and accessibility of the seam and on obtaining representative lignite samples from the entire mine. Coal collection procedures, as described by Benson et al. (1984) and Schoph (1960), were employed in the physical collection and description of the coal at each sample location site.

Channel samples (Schoph, 1960) were collected from the mine highwall at intervals defined by megascopically observable characteristics otherwise known as lithologic layers or lithobodies. Lithobodies are distinguished by: 1) thickness of individual horizontal coal layers or massiveness; 2) fracture patterns; 3) relative luster; and 4) occurrence of fusain layers greater than one centimeter thick (Kleesattel, 1984). A typical sampling site averaged 5 to 10 lithologic layers.

Each sampling channel was approximately 30 cm wide, 10

Figure 3. Map view of Gascoyne Mine pits and location of sample collection sites (Redrawn from Knife River Coal Company aerial photograph October 30, 1984).

Red Pit



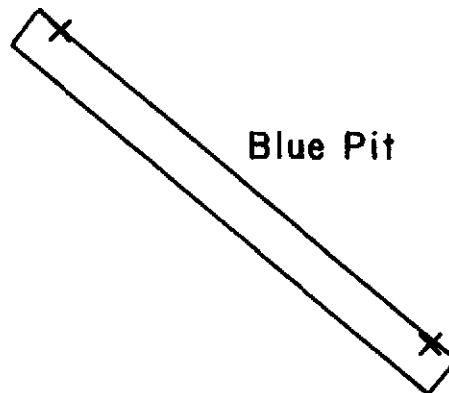
White Pit



Yellow Pit



Blue Pit

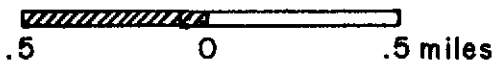


R. 99 W.

R. 98 W.

T. 131 N.

T. 130 N.



Scale 1" = .5 miles

X = Lignite Collecting Site

cm deep, and extended from the underclay below the seam to the top of the seam. A rock pick was usually the only tool needed to clear the channel. Before extracting coal from the freshly exposed surface, the channel was thoroughly swept clean of extraneous coal or mineral matter. Boundaries between lithologic layers and clay or black jack partings were then marked with tags and the entire column section was photographed.

Samples were collected beginning at the base of the seam. About 3 kg of coal were extracted from each lithologic layer and parting and sealed in plastic bags. Where accessible, overburden and underclay samples were also collected.

Megascopic Description

Detailed megascopic descriptions of individual samples were performed in the lab. Physical characteristics noted were: distance separating major bedding or banding planes, hardness, color, luster, texture, cleating or fractures, and visible mineralization. Lithotypes were distinguished on the basis of their physical characteristics. Three lithotypes, vitrain, attritus, and fusain, were classified, described, and quantified using the techniques and terminology of Stopes (1919), Thiessen and Sprunk (1935), Schopf (1960), Dutcher (1976), and Kleesattel (1985).

Proximate/Ultimate, BTU, and Ash Determinations

Routine proximate and ultimate coal analyses were performed on four bulk samples of the A seam at each of the four pits. Coal rank is often based on several characteristics such as fixed carbon and hydrogen content, BTU value, and the atomic ratios of hydrogen to carbon and carbon to oxygen.

Proximate analyses determined the moisture, ash, volatile matter, and fixed carbon contents. Ultimate analyses determined the total carbon (fixed carbon and carbon in volatile forms), hydrogen, nitrogen, ash, and oxygen contents. These analyses were performed at UNDERC using techniques comparable to the American Society for Testing and Materials (ASTM) procedures. A Fisher Coal Analyzer was used for the proximate analyses (ASTM, 1983a), while a Perkin-Elmer 240 Elemental Microanalyzer was used for the ultimate analyses (ASTM, 1983b). The lignite samples were vacuum dried for 24 hours, then crushed to pass through a 60 mesh sieve prior to analyzing. Additional ash determinations were made for each lithologic layer sample. These were done in accordance with ASTM (1979) procedures for high temperature (750 C) ashing of coal. In each case a 10 gram sample was crushed to -60 mesh and vacuum freeze dried before being ashed.

The heating value, reported in British Thermal Units (BTU), was determined for these four samples according to ASTM method D 2015-77 (ASTM, 1980). Heating value

determination involves burning a weighed sample in an adiabatic oxygen bomb calorimeter. The calorific value was calculated from the temperature difference before and after combustion. The conversion from calories to BTU values is 1 cal/g = 1.8 BTU/lb.

Sample Preparation

Quantitative mineralogy and petrography of coal lithobodies requires careful sample preparation. The objective of the following preparation procedure is to produce a sample that is representative of the true composition of the lithologic layer with a minimum of human bias. The methodology described is in accordance with standard ASTM (1980) procedures

Each sample was initially air dried for 24 hours and then crushed to a -20 mesh size using either a mortar and pestle or a Holmes Hammermill crusher. A 10 gram sample was then split from each sample using first a rotary riffler and then a small dual sample splitter. The 10 gram sample was next vacuum dried for 24 hours at a pressure of 10 to 15 micrometers of mercury.

Standard coal/epoxy pellets or briquettes (ASTM, 1980) are the most suitable type of sample for petrographic and SEM microprobe analysis and were used in this study. The 10 gram sample was mixed with several drops of epoxy to form a moist paste-like mixture. The mixture was evenly divided and pressed into 2.5 cm diameter cylindrical molds.

Additional epoxy was then poured into the coal, and, after hardening (usually 1-3 hours), a pellet 2.5 cm in diameter and 2.0 cm thick remained.

One of the base surfaces of the pellet was then ground and polished using a series of abrasives to obtain a surface suitable for microscopical examination. The grinding stage involved using a progression of 180, 320, 400, and 600 grit silicon carbide papers. The polishing stage included a progression of 9, 6, 3, and 1 micrometer diamond pastes. An oil-base lubricant was used with all of the abrasives. The samples were cleaned between each stage in an ultrasonic bath of trichloro-trifluoroethane, which is an inert solvent.

As mentioned earlier, three pellets were made for each Gascoyne coal sample. One sample was used for petrographic study and the other two for SEM/EMPA. Pellets used for SEM/EMPA were coated with a thin layer of carbon under high vacuum using a HVEC coating device.

Petrographic Methods

Petrographic examination of the coal/epoxy pellets included quantitative maceral analysis, quantitative reflectance, and fluorescence microscopy. Maceral analyses were performed using standard reflected and fluorescent light microscopy (Stach et al., 1982). The terminology employed was in accordance with the International Committee on Coal Petrology (ICCP, 1975; 1971; 1963). A Nikon

Labophot polarizing light microscope equipped with 40X and 60X oil immersion objectives and a photometer was used to identify macerals and determine quantitative reflectance values. Maceral point counting techniques, as described by Stach et al. (1982), were used to quantify macerals for each sample.

Fluorescence microscopy (blue-light excitation) is the best method for distinguishing and identifying liptinite macerals. Low-rank coals such as North Dakota lignites typically contain a high percentage of liptinite macerals (Parkash et al., 1982; Ting, 1972). Fluorescence microscopy was performed using a 100 watt, high-pressure mercury lamp.

Scanning Electron Microscope/Microprobe Methods

There were two basic stages in the examination of minerals in the Harmon lignite lithobodies. The first stage involved identifying minerals and describing their morphology and association with the coal organic matrix. The second stage involved quantifying the mineral types. The UNDERC JXA-35 scanning electron microscope/microprobe, which is interfaced with a Tracor Northern TN 5500 x-ray microanalyzer, was used to study the mineral matter.

Identification of minerals involved scanning across the polished coal/epoxy pellet at a magnification of 200-500x and noting the contrast in brightness between mineral grains and the coal organic matrix. Mineral grains have a higher

average atomic weight than coal macerals and therefore appear brighter on the SEM CRT screen. Upon locating a mineral grain, the electron beam was positioned directly over the minerals and the x-ray spectra was recorded with an energy dispersive detector. The x-ray spectra generated from the material under the microprobe beam consists of the number of counts at energy levels characteristic of each element in the material. The number of x-ray counts generated from elements in a mineral depends on the concentrations of the elements.

Representative EDS spectra of the full suites of mineral species present in this coal were stored on floppy disk, after collecting x-ray energy photons for 200 seconds using an accelerating voltage of 15 kilovolts and a beam current of 350 picoamps. The stored EDS data was then corrected using a ZAF correction routine, and printouts were generated which expressed the elemental components of the minerals as normalized equivalent oxide weight percents. The minerals were then identified by comparing their elemental oxide compositions to known mineral compositions found in the literature (Deer et al., 1966; 1962; Kerr et al., 1950). Development of this technique also involved checking SEM/EMPA mineral analyses with XRD mineral analyses performed at the Pennsylvania State University.

In addition to identifying the minerals in each lithobody sample, descriptions were made of the minerals observed. Characteristics which were noted include the

size, shape, morphology, organic association, surface texture, dissolution features, and mineral overgrowths. SEM photomicrographs were taken of the representative mineral species and unusual mineral occurrences or associations.

Other descriptive work included examining hand picked minerals and mineralized coal fragments. The specimens were prepared either as polished coal/epoxy mounts or as whole fragment mounts on carbon stubs. The whole coal fragments allowed for observation of fracture surfaces of the minerals and coal.

The final application of the SEM/EMPA system pertained to quantifying mineral species. Standard point counting methodology was employed to quantify mineral species and coal organic matrix. Epoxy, which averaged 30% of the surface area, was not included in the quantifications. The SEM automated stage, which holds the epoxy/coal pellet, was programmed to move underneath the electron beam, stopping at equal increments. A grid pattern of stopping points was created whereby 500 counts of coal or mineral matter were recorded over a 2.0-2.5 square centimeter surface area of the epoxy/coal pellet. An elemental energy spectra was acquired at each stop to determine whether the material underneath the electron beam spot was maceral, mineral, or epoxy. The identity of the material was recorded on a manual point-counting device. All potential mineral spectra were stored on floppy disk for later analysis after acquiring x-ray energy counts for 50 seconds.

The paucity of discrete mineral phases in coals makes the SEM/EMPA identification process less prone to error. From personal experience, it is noted that low rank coal usually contains only 3-4 major minerals and individual samples rarely show greater than 7-10 minerals. The spectral patterns and quantitative elemental data of the few minerals encountered in a routine SEM/EMPA analysis are usually quite distinct and follow a consistent pattern unique to a particular mineral. Deviations from this observation are found with the clay minerals, whose compositions may vary, but usually within a certain compositional range. Consistency of chemical compositions of the minerals encountered was important in developing an identification procedure.

Table 1 shows the normalized elemental oxide ranges used to categorize the minerals. The information in this table was obtained from the following sources: UNDERC microprobe analysis of known mineral standards; Huggins et al., 1980; Pough, 1976; Deer et al., 1966; and Kerr et al., 1950. As mentioned earlier, some of the minerals (e.g. quartz, pyrite, kaolinite) deviate very little from their known compositions; however, others fall more into a range of values (i.e. montmorillonite, illite). The clay minerals are categorized primarily on the group level unless the elemental analysis was of such extremely high quality that a more specific identification could be made.

X-ray diffraction (XRD) was not used for the

identification of the clays, therefore, there is some uncertainty in the identification of minerals listed in Table 1. However, the major clay minerals that were identified in this study are consistent with proprietary XRD results obtained by The Pennsylvania State University. It is possible that dickite and halloysite may have been identified as kaolinite since these three clays can only be distinguished by crystalline structure or morphology. Also, some of the material identified as illite may be muscovite. Illite and muscovite can have similar chemical compositions, but differ in crystalline structure. Positive identification of the crystalline structure of these minerals can only be done using XRD on relatively pure samples.

The actual identification procedure is explained as follows:

1. The stored elemental data of an unknown mineral was submitted to a ZAF correction procedure which corrects for absorption, atomic number, and fluorescence effects and converts the actual x-ray energy counts collected for each element to normalized oxide weight percentages.
2. The closure of the original elemental oxide data was then scrutinized to see whether the analysis was a true mineral phase. If the electron beam penetrates coal matrix before exciting the elements of a mineral grain, then the actual closure of the oxide data for the mineral will be poor. Analyses showing

Table 1. Coal mineralogy categories as determined by normalized oxide percentages.

Name	Formula	EDS Weight Percents
Quartz	SiO ₂	Si > 85
Kaolinite*	Al ₄ Si ₄ O ₁₀ (OH) ₈	Al ~ 45 Si ~ 55
Illite	K(Al,Fe) ₄ (Si,Al) ₈ O ₂₀ (OH) ₄	Al ~ 20-30 Si ~ 50-65 K ~ 3-11 Mg ~ 0-6 Fe ~ 0-6 Ca ~ 0-3
Montmorill.	(.5Ca,Na).7(Al,Mg,Fe) ₄ [(Si,Al) ₈ O ₂₀](OH) ₄ .nH ₂ O	Al ~ 18-28 Si ~ 63-74 Fe Ca ~ 5-12 Na Mg
Muscovite	K ₂ Al ₄ [Si ₆ Al ₂ O ₂₀](OH,F) ₄	Al ~ 30-40 Si ~ 45-52 K ~ 8-13 Fe ~ 0-7
Mixed Layer Aggregate		Al ~ 20-30 Si ~ 53-64 Mg ~ 1-10 Fe ~ 1-10 K ~ 1-8 Ca ~ 1-14
K-Feldspar	KAlSi ₃ O ₈	Al ~ 18-21 Si ~ 66-68 K ~ 12-17 Fe ~ 0-3
Biotite	K ₂ (Mg,Fe+2) ₆₋₄ (Fe+3,Al,Ti) ₀₋₂ [Si ₆₋₅ Al ₂₋₃ O ₂₀](OH,F) ₄	Al ~ 15 Si ~ 45 Fe ~ 15 Mg ~ 15 K ~ 7

Mineral	Formula	EDS Weight Percents
Vermiculite	$(\text{Mg}, \text{Ca},) .7 (\text{Mg}, \text{Fe}^{+3}, \text{Al}) 6 \text{Si} (\text{Al}, \text{Si}) 6 \text{O} 20 (\text{OH}) 4 .8 \text{H}_2 \text{O}$	Al ~ 15-25 Si ~ 35-45 Mg ~ 25-30 Fe ~ 10-15
Chlorite	$(\text{Mg}, \text{Al}, \text{Fe}) 2 (\text{Si}, \text{Al}) 8 \text{O} 20 (\text{OH}) 16$	Al ~ 22-28 Si ~ 24-34 Mg ~ 5-26 Fe ~ 11-51
Pyrite	FeS_2	Fe ~ 33 S ~ 67
Jarosite	$\text{KFe}_3 (\text{SO}_4)_2 (\text{OH}) 6$	Fe ~ 54 S ~ 36 K Na ~ 10
Fe Sulfate	$\text{FeSO}_4 .x \text{H}_2 \text{O}$ (x = 1, 4, or 7)	Fe ~ 45 S ~ 55
Alunite	$\text{KA}_3 (\text{SO}_4)_2 (\text{OH}) 6$	Al ~ 42 S ~ 44 K ~ 13
Dolomite	$\text{CaMg} (\text{CO}_3)_2$	Ca ~ 58 Mg ~ 42
Calcite	CaCO_3	Ca > 80
Siderite	FeCO_3	Fe > 80
Rutile	TiO_2	Ti > 65
Gypsum	$\text{CaSO}_4 .2 \text{H}_2 \text{O}$	Ca ~ 30-45 S ~ 55-70
Apatite	$\text{Ca}_5 (\text{PO}_4)_3 (\text{OH})$	Ca ~ 50-70 P ~ 25-45
Crandallite	$\text{CaAl} (\text{PO}_4) .5 \text{H}_2 \text{O}$	Ca ~ 20-30 Al ~ 45-60 P ~ 15-30
Barite	BaSO_4	Ba ~ 55-65 S ~ 30-37

Mineral	Formula	EDS Weight Percents
Celestite	SrSO ₄	Sr ~ 50-60
Titanium Mineral		Ti ~ 25-65 Si ~ 30-65 Fe ~ 0-15
Unknown	(i.e. unknown clay, titanium mineral, sulfate, etc.)	

*Those categories which do not specify a range may vary by -5 or +5 percent.

elemental oxide closures of greater than 30% were retained for identification and counted as minerals. All analyses having less than 30% closure show a very clear imprint of coal maceral material, which usually consists of nearly equal Ca and S contents and Mg, Al, and Si contents that are one-half the magnitude of the Ca-S contents. The 30% closure value was chosen after repeated experimentation on samples that were visually observed on the SEM CRT screen during the point counting procedure. In this way, minerals viewed on the sample surface could be correlated to their closures after the ZAF correction routine.

3. EDS analyses which did not correspond to any of the mineral categories were labeled as unknown minerals.

Upon completion of the microprobe point count analysis, the totals of the distinct mineral phases and organic matrix in each sample were normalized to 100%. These relative volume percents were then converted to weight percents by multiplying each constituent by its known average density value [Chemical Rubber Company Handbook of Chemistry and Physics, 1982] and normalizing the results to 100%. The quantitative results in the tables which follow were obtained using normal output procedures for analysis being developed at UNDERC. In most instances, the number of significant digits are too large.

RESULTS

Harmon Bed Stratigraphy and Lithologic Layers

Figure 4 shows the vertical and lateral distribution of the lithologic layers sampled at the Gascoyne Mine. The lithologic layers of each seam are not continuous through the extent of the mine. More detailed descriptions of the lithobodies in the Harmon bed sequence for the Blue and the White pits are found in Figure 5. The lithobodies were differentiated based on their physical properties, but the uniqueness of these units will be tested later in this report using petrographic and mineralogic data.

Proximate/Ulimate, BTU, and Ash Determinations

The results of proximate/ultimate (P/U), ash, and BTU analyses performed on four bulk samples of the A seam from each pit are found in Table 2. Comparisons of the results between the four bulk samples shows no major differences. It is possible that bulk samples from the lower B and C seams would also show little variation in P/U results since they have been subjected to similar chemical environments as the A seam.

Relative to all other coal ranks, the high volatile matter, oxygen, and sulfur contents and the low carbon content are typical of low rank coal. Mott's (1948) classification of coal rank involves plotting volatile

Figure 4. Cross-sectional diagram of Harmon Bed lithologic layers and the pits they were sampled from. The labels are explained as follows: the first letter refers to the mine name, G = Gascoyne; the second letter designates the pit name, R = Red Pit, W = White Pit, Y = Yellow Pit, and B = Blue Pit; the third letter identifies the seam, parting, or overburden layer, A = upper most seam, B = middle seam, C = lower seam, P = parting, and O = overburden.

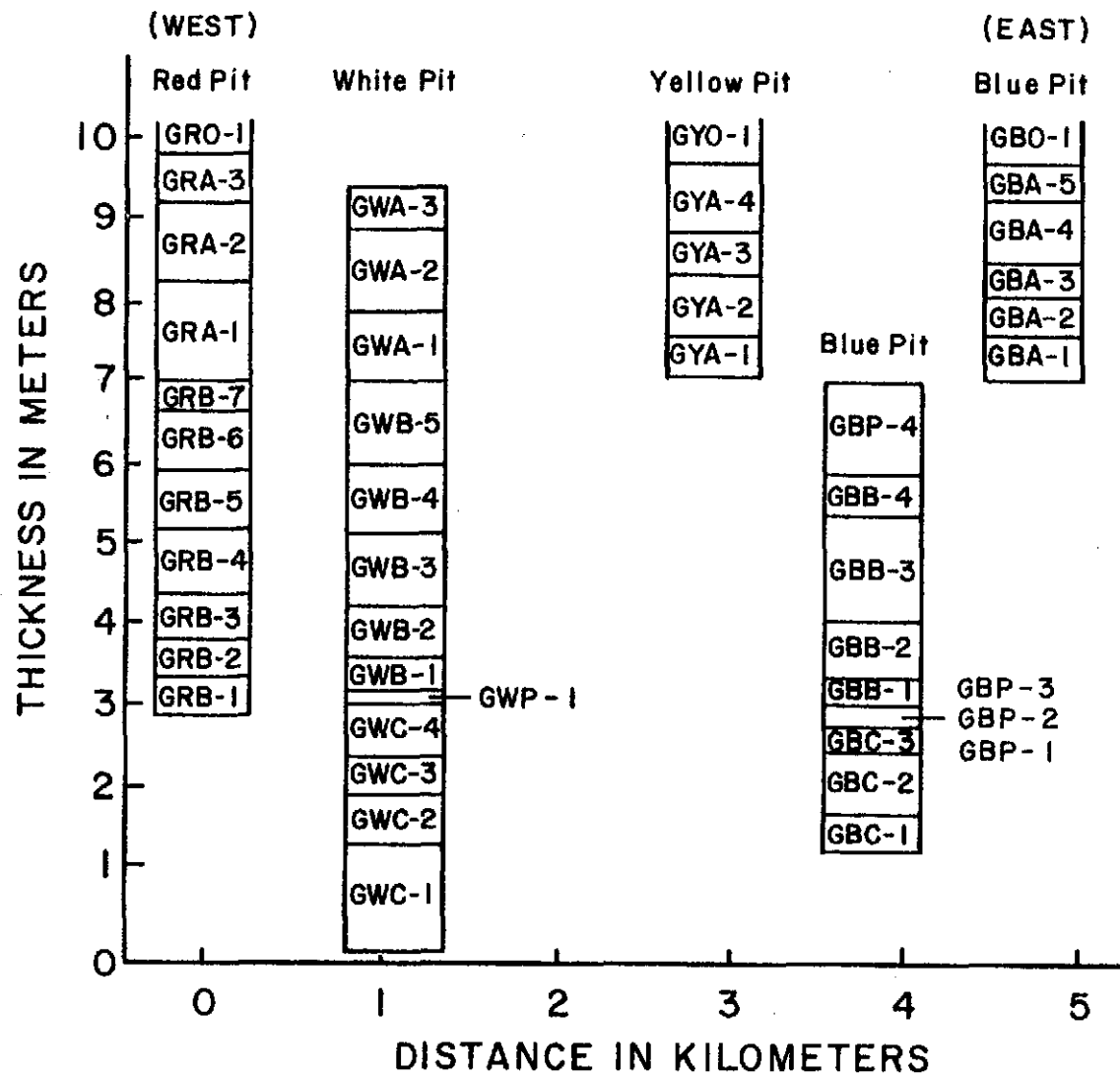
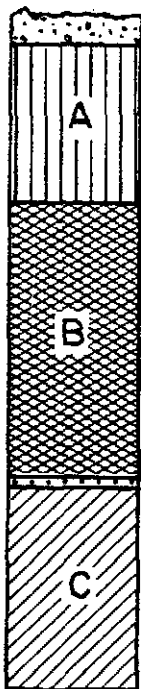


Figure 5. Geologic column describing lithobodies in the A, B, and C seams in the White and Blue pits.

White Pit



Overburden. Fine sand, silt, and clay layers. Tan colored.

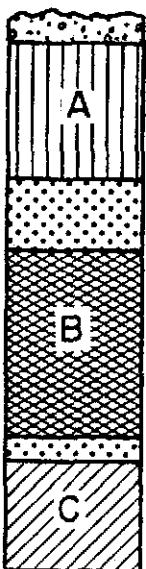
Lignite. Moderately bright and hard, woody vitrain fragments abundant. Attritus breaks easily, well-developed vertical and horizontal fractures. Scattered pyrite crystallization.

Lignite. Moderately dull and hard, fairly well-developed horizontal and vertical fractures. Fusain more abundant near top of seam. Abundant woody vitrain, though not as massive slabs. Distinct alternating vitrain-attritus bands. Yellow and white secondary minerals noted, also pyrite crystals scattered on horizontal surfaces.

Black Jack parting. Gray-black inorganic-rich coal difficult to distinguish from adjacent coal layers.

Lignite. Attritus-rich, moderately dull coal. Brittle yet very hard, especially in lower sections. Abundant woody vitrain layers at upper part of seam. No visible mineralization.

Blue Pit



Overburden. Fine sand, silt, and clay layers. Coal fragments abundant.

Lignite. Abundant fusain at margins. Abundant cleating in two directions. Woody vitrain slabs abundant in middle parts. Pyrite crystals noted in fractures.

Silt-clay parting. White-gray, silty clay, no bedding. Coal fragments common. Iron stained locally.

Lignite. Moderately dull and hard in upper sections with visible gray silt-clay bands evident. Very massive with irregular fracture. Excellently preserved woody fragments in middle parts of seam. Dull coal layers at bottom of seam that are rich in silt-clay material.

Black Jack and silt-clay parting. Three distinct inorganic-rich layers. brown silty clay with abundant plant fragments.

Lignite. Moderately dull, hard, and irregularly fractured. Tan colored clay bands in lower part of seam.

TABLE 2. Proximate/ultimate data from Harmon Bed A Seam (Bulk Coal Samples).

<u>Data Type</u>	<u>Red</u>	<u>White</u>	<u>Yellow</u>	<u>Blue</u>	<u>Average</u>
Original Moisture	4.1	8.5	15.3	19.6	11.9
Volatile Matter	44.7	44.7	49.9	42.8	45.5
Fixed Carbon	48.1	47.6	42.6	45.7	46.0
Ash	7.2	7.7	7.5	11.5	8.5
Hydrogen	4.31	4.24	3.68	4.51	4.2
Total Carbon	64.43	63.15	60.43	63.73	62.9
Nitrogen	1.04	0.87	1.07	0.97	0.99
Sulfur	1.04	1.14	0.89	1.38	4.55
Oxygen	21.97	22.90	26.43	17.91	22.3
BTU/lb	10,639	10,592	9,511	10,703	10,361

(All data based on moisture-free coal with compositions given in weight percents.)

matter content (wt%) versus calorific value (BTU/lb.) of dry, ash-free coal. When plotted, the four bulk samples averaging 49.7 weight percent volatile matter and 11,329 BTU/lb. on a dry, ash-free basis, placed the Harmon coal well within the defined limits for lignite.

Ash concentrations for the bulk samples were fairly moderate, averaging 8.5% by weight. Ash contents for each lithobody were also determined. The significance of ash concentrations for each lithobody will be more apparent when related to mineral content later in this report.

In summary, the Harmon lignite can be characterized by the proximate/ultimate (P/U) analyses as a fairly high BTU lignite with a moderate ash content. Known variability in ash deposition behavior between mine pits does not appear to be explained by any of the parameters determined using P/U.

Megascopic Descriptions and Lithotypes

There were three lithotypes that could be distinguished and quantified in hand specimen samples: vitrain, attritus, and fusain. Vitrain was observed to occur in two forms. Characteristics of the first form include a bright luster, deep black color, a hard yet brittle character, conchoidal fracture, and natural two-directional cleating (90%). Vitrain of this type commonly formed flat, medium banded lenticular bodies which were 2-5 mm thick and 10-30 mm long.

The second form of vitrain was typical of what is called anthraxylon (Thiessen and Sprunk, 1935; Thiessen and

Francis, 1929). This form was normally silky in luster, brittle yet very hard, thick banded (5-50 mm thick), lenticular, fractured conchoidally, and often showed excellently preserved woody structures such as concentric plant growth rings and tree branch forms.

Attritus occurred mainly as medium-grained massive layers that averaged .5 to 4 cm in thickness. The layers were usually moderately dull in luster, moderately hard (crumbled easily at the edge of a knife blade), fractured irregularly along horizontal planes, and commonly showed 90% cleating. The cleating was not as extensive as in vitrain. Lignite samples that were rich in attritus broke easily along irregular horizontal planes when struck with a hammer, whereas vitrain-rich lignite was much more resistant.

Classifications for higher rank coals usually substitute the terms durain and clarain for the attritus term used in this study. The overall dull luster of the Harmon lignite makes it very difficult to distinguish durain and clarain; therefore, these two constituents were grouped under the term attritus.

Fusain occurred as very soft fibrous or splintery charcoal-like patches, fragments, and lenses. Fragments of fusain were typically 2 square cm in surface area and 2-4 mm in thickness. A powdery coal residue is formed when fusain is crumbled between the fingers.

The percent concentrations of lithotypes present in each sample were estimated by randomly selecting 5 blocks of

lignite from the sample and averaging their lithotype concentrations. The average lithotype abundances for the entire Harmon bed at Gascoyne were 62.3% attritus, 33.2% vitrain, and 4.5% fusain. These results are similar to those determined for the Beulah-Zap lignite in central North Dakota which had 60% attritus, 35% vitrain, and 5% fusain (Kleesattel, 1984).

Average lithotype abundances of vitrain, attritus, and fusain are fairly consistent, varying only 5-10 % from westernmost Red Pit to the easternmost Blue Pit. This lack of lateral variation may be evidence for a fairly uniform depositional environment.

Variability in lithotype concentration was noticed when examining Harmon coal in vertical section. Some of the lignite seams appear to have higher vitrain concentrations in the middle and lower portions of the seam. Also, fusain appears to be more concentrated near the top of the seams (Figure 6).

To test the variability of lithotypes vertically and the correlation with lithobodies, samples were collected from the Yellow Pit A-seam at equal .25 meter increments. The vertical section was then examined for its megascopic physical properties and, based on these properties, 4 lithologic layers were demarcated. Figure 7 shows the 10 intervals, their respective fusain concentrations, and the demarcations of the seam into 4 lithologic layers. Each lithobody has a basal section that is rich in fusain.

Figure 6. Vertical distribution of fusain in the Red Pit. Note higher concentrations at the upper parts of the A and B seams (volume percent).

GASCOYNE RED PIT FUSAIN

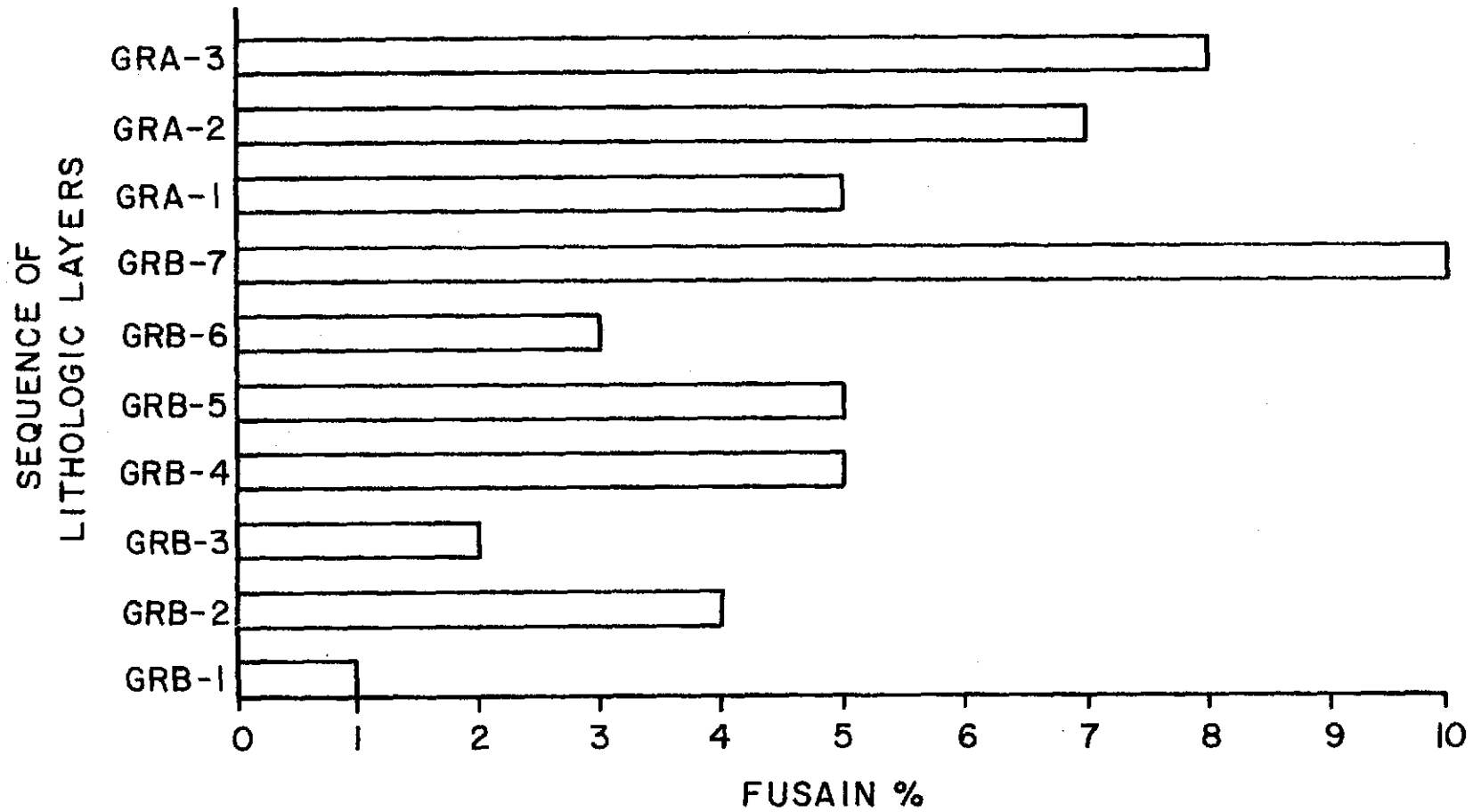
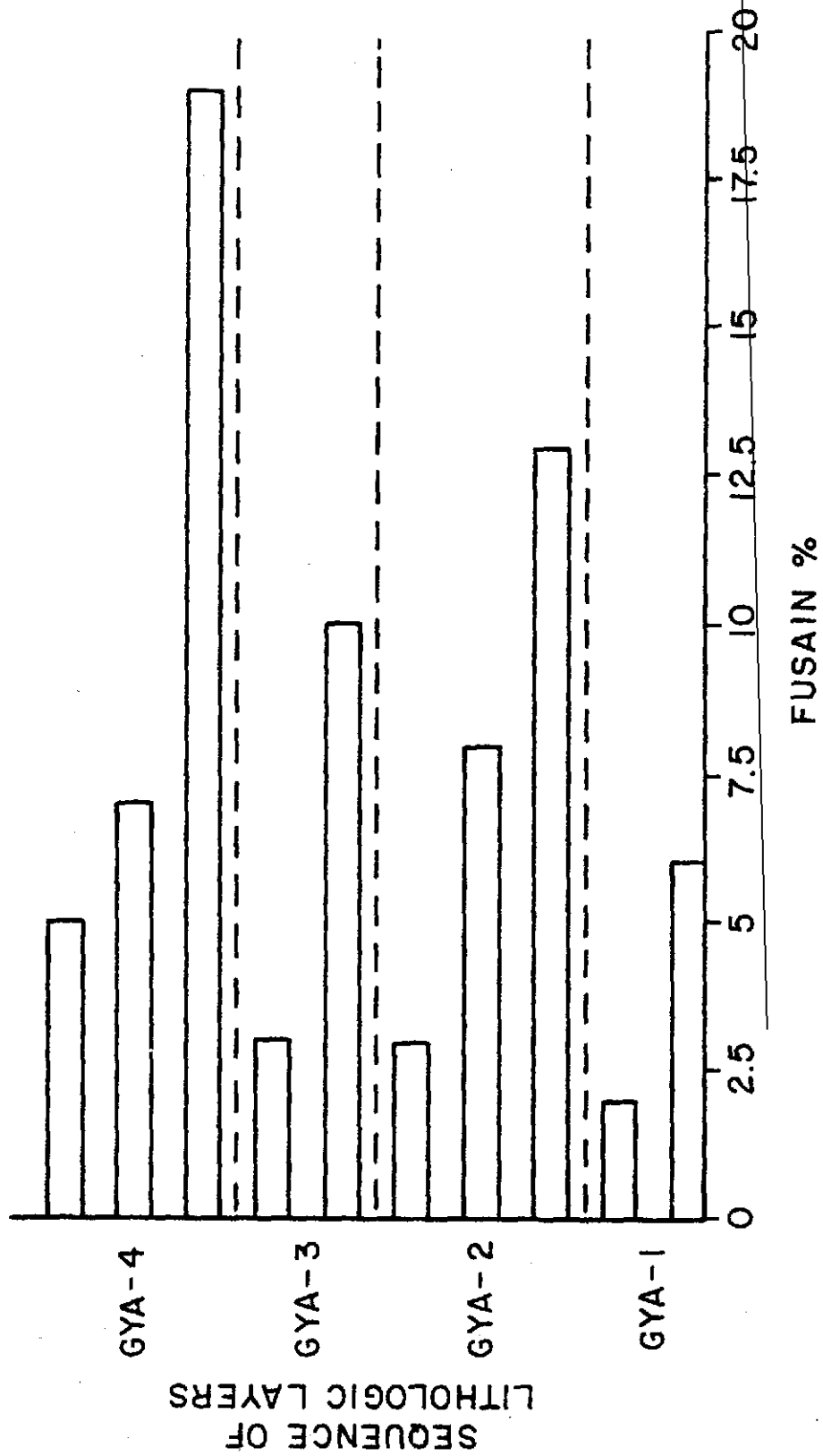


Figure 7. Vertical distribution of fusain in the Yellow Pit A seam. The dashed lines denote boundaries for lithologic layers (volume percent).

YELLOW PIT A-SEAM FUSAIN



Fusain content was a contributing factor in the megascopic designation of the lithobodies in this seam and is probably a contributing factor for the lithologic layer designations for lignite beds in general. This conclusion is not surprising because fusain can be observed forming extensive horizontal zones of weakness in most lignite coal seams, including the Harmon bed. Also, since horizontal fracture systems were one of the criteria used to differentiate lithobodies in the Harmon bed, it is not at all surprising that the vertical display of fusain content would demarcate distinct lithologic layers. The role of vitrain and attrital contents in the megascopic classification of lithologic layers is not yet clear.

Petrography

Coal lithobodies from the Blue and White pits were analyzed for maceral content. Carbonaceous or coaly clay-silt partings were excluded. Macerals were quantified and grouped under three major categories: vitrinite (also called huminite), liptinite, and inertinite. The purpose for the maceral analyses was simply to try to detect any relationship between mineral abundances and maceral groups and also to survey the association between certain macerals and minerals. Appendix A summarizes the macerals that were identified and their abundances.

The White Pit lignite maceral group averaged 68% total vitrinite, 13% total liptinite, 12% total inertinite, and 7%

mineral matter. Blue Pit maceral groups were only slightly different, consisting of 66% total vitrinite, 14% total liptinite, 16% total inertinite, and 4% mineral matter. It should be noted that the 400 power magnification used on the optical microscope in determining the maceral contents is not a high enough to recognize and differentiate certain mineral species. Therefore, the mineral content noted above may not be accurate.

Altogether, 19 maceral types were identified in the Harmon lignite. The White Pit vitrinite macerals consisted mainly of ulminite; the liptinite macerals consisted mainly of liptodetrinite and sporinite; and the inertinite macerals consisted mainly of inertodetrinite (Appendix A). The Blue Pit macerals exhibited similar maceral abundances except that the inertinite macerals were primarily represented by fusinite and inertodetrinite.

The Harmon lignite bed showed a variety of associations of minerals and macerals. Pyrite was observed as cell fillings associated with corpohuminite-rich detrital particles. Smaller framboidal pyrite (<20 micrometers) was often observed associated with ulminite. In some less common instances, pyrite framboids were seen associated with micrinite in highly gelified ulminite. Two samples had small dendritic forms of pyrite (20-30 microns) in pores of huminite group macerals. In rare cases euhedral masses of pyrite were seen in a detrital inertodetrinite matrix.

Detrital quartz grains were found associated with

detrital maceral types rich in inertodetrinite. Clay minerals were the most abundant mineral type observed in association with macerals. They occurred as aggregates approximately 50 microns in diameter, with some of the aggregates containing small inclusions of liptinite. Clay mineralization was commonly associated with cell fillings of huminite macerals such as corpohuminite and ulminite and also with the liptinite macerals such as sporinite and resinite. Clay was also found associated with coal fragments rich in inertinite group macerals such as inertodetrinite and fusinite.

Mineralogy

Effectiveness of SEM/EMPA Methodology

Much time and effort were invested in developing an effective and reliable method for determining mineral contents in the Harmon lignite. The SEM/EMPA methods were first refined and tested using twenty western U.S. coals selected from the UNDERC coal sample bank. Quantitative mineralogic results using SEM/EMPA and x-ray diffraction techniques were compared. The details of these preliminary developmental studies can not be discussed here since the studies were performed under private contracts. However, the general results can be discussed to help verify the validity of SEM/EMPA quantitative mineralogy.

In reference to SEM/EMPA quantitative mineralogy versus XRD quantitative mineralogy, it must be pointed out that

neither method has proven itself superior to the other. During the course of developing the SEM/EMPA methodology it was found that consistency or precision is just as important as striving to attain absolute accuracy. The SEM/EMPA method was found to give consistent results. For the twenty coals discussed above, the total ash content varied directly with the total of discrete mineral phases. The correlation coefficient for this relationship was calculated to be .96 at the 95% confidence level. In other words, the linear relationship between ash percent versus mineral percent was statistically significant. This result reveals that the SEM/EMPA method is consistent with current knowledge of the nature of inorganic constituents of coal. In most low rank coals, the overall mineral content varies directly with the total ash content which includes discrete mineral phases and organically bound inorganic constituents.

The mineral identification procedure used in the SEM/EMPA procedure is also fairly precise and accurate. Comparison between XRD and SEM/EMPA data for the 20 U.S. coals studied showed that the same minerals were identified, but, in different quantities.

In summary, the SEM/EMPA quantitative technique is a powerful means of determining mineral quantities in coal. The principles of modal analysis and standard point counting methodology appear to give fairly consistent results. The paucity of discrete mineral phases in coals makes the SEM/EMPA identification process less prone to error. Since

lignite usually contains only 5-6 major mineral constituents, the spectral patterns of these major species become more easily identifiable as a given coal is studied.

Quantitative and Qualitative Results

Tables 3 and 4 show the results of both the SEM/EMPA quantitative mineralogical analysis and the ash analysis. The mineral weight percentages pertain only to discrete mineral phases, whereas the ash values include minerals and organically bound inorganic constituents. As in the preliminary work mentioned earlier, the mineralogic results appear to be fairly consistent. Figure 8 shows that the total mineral matter, expressed as weight percent, for each lithobody is a function of the total ash. The least squares line was calculated to be .96 at the 95% confidence level, thereby signifying that a statistically valid relationship exists between percent mineral matter and percent ash. This information indicates that the SEM/EMPA methodology produces results that would normally be predicted knowing the geologic character of the Harmon lignite and, therefore, that the SEM/EMPA results are acceptable and useful.

By far the most abundant minerals that were observed in lignite lithobodies (not clay partings or overburden) were quartz, kaolinite, illite, montmorillonite, pyrite, and gypsum. Less common yet still significant were rutile(?) and other unknown titanium-bearing minerals, barite, iron sulfates (i.e. jarosite), carbonates (siderite, dolomite,

TABLE 3. Average mineral content for lithologic layers in the White Pit.
(weight percents)

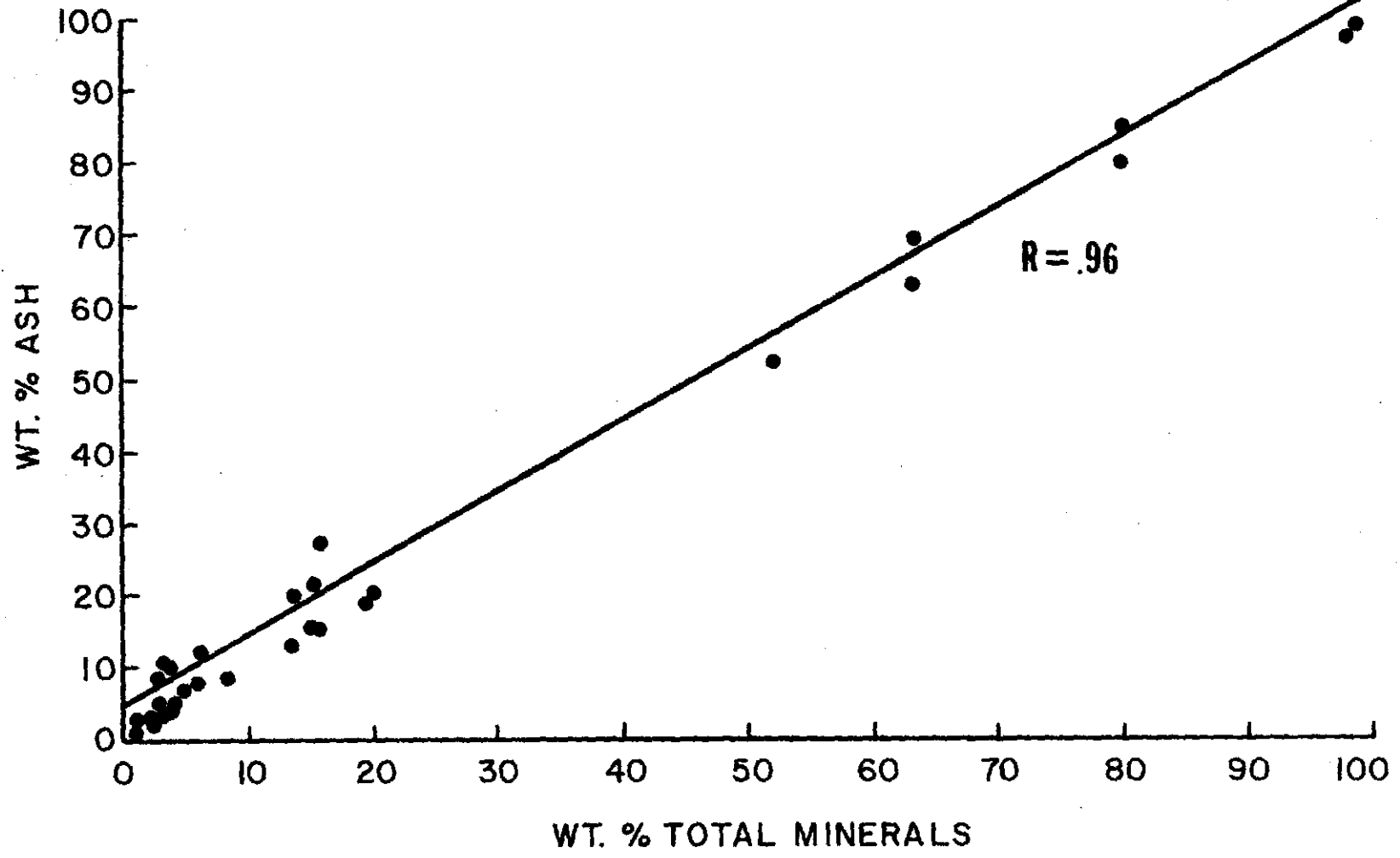
I.D.	GWC-1	GWC-2	GWC-3	GWC-4	GWP-1	GWB-1	GWB-2	GWB-3	GWB-4	GWB-5	GWA-1	GWA-2	GWA-3
Quartz	0.38	0.97	0.40	10.17	28.81	0.81	0.41	0.81	1.55	2.00	1.57	1.22	1.99
Kaol.	1.91	3.11	2.79	3.01	2.03	2.83	0.00	0.41	0.39	0.40	0.00	0.00	0.40
Illite	0.00	0.34	0.00	1.17	18.95	0.00	0.00	1.26	0.00	0.41	1.23	0.00	1.85
Mont.	0.36	0.00	0.00	2.13	0.38	0.00	0.00	0.00	0.00	0.00	0.00	0.00	0.00
Mix-clay	0.00	0.00	0.00	0.38	0.00	0.00	0.36	0.00	0.00	0.00	0.00	0.00	0.00
Pyrite	0.00	0.00	1.13	0.71	0.00	0.77	3.89	0.00	0.00	0.76	0.75	0.00	0.00
Gypsum	0.00	0.00	0.00	0.00	0.00	0.00	0.00	0.00	0.34	0.00	0.00	0.00	0.00
Barite	0.00	0.00	0.00	0.00	0.00	0.00	0.00	0.00	0.00	0.00	0.00	0.00	0.00
Siderite	0.00	0.00	0.00	0.00	0.00	0.00	0.00	0.00	0.00	0.00	0.00	0.00	0.00
Ti-Min.	0.00	0.00	0.00	0.00	1.61	0.00	0.00	0.00	0.00	0.00	0.00	0.00	0.49
Rutile	0.00	0.00	0.00	0.60	0.65	0.00	0.00	0.00	0.00	0.00	0.00	0.00	0.00
Phos.	0.41	0.00	0.00	1.61	0.00	0.00	0.00	0.00	0.00	0.00	0.00	0.00	0.00
Jarosite	0.00	0.00	0.00	0.00	0.00	0.00	0.48	0.00	0.00	0.00	0.46	0.00	0.00
Dolomite	0.00	0.42	0.00	0.00	0.00	0.00	0.00	0.00	0.00	0.00	0.00	0.00	0.00
Unknown	0.00	0.00	0.00	0.19	0.00	0.00	0.00	0.00	0.00	0.00	0.39	0.00	0.00
Total % Minerals	3.06	4.84	4.32	19.98	52.43	4.41	5.14	2.48	2.28	3.57	4.40	1.22	4.73
Total % Ash	10.83	7.68	8.78	20.63	57.32	9.02	9.55	8.26	8.13	10.17	7.42	2.82	10.33

TABLE 4. Average mineral content for lithologic layers in the Blue Pit.
(weight percents)

I.D.											Table 4 continued					
	GBC-1	GBC-2	GBC-3	GBP-1	GBP-2	GBP-3	GBP-4	GBB-1	GBB-2	GBB-3	GBA-1	GBA-2	GBA-3	GBA-4	GBA-5	GBO-1
Quartz	1.22	0.80	1.57	75.95	7.54	40.12	23.9	10.24	0.37	2.85	3.01	0.46	0.43	1.46	0.79	38.77
Kaol.	3.45	0.80	1.96	0.96	5.55	1.73	0.34	3.29	0.74	2.03	0.00	1.85	0.43	0.49	0.00	0.00
Illite	0.00	0.00	0.41	0.00	1.23	20.10	54.83	1.33	0.00	0.00	0.00	0.00	0.00	0.51	1.44	26.47
Mont.	0.00	0.00	0.00	0.30	0.37	0.68	5.40	0.00	0.00	0.00	0.41	1.31	0.00	0.00	0.00	5.78
Vermicul.	0.00	0.00	0.00	0.00	0.00	0.00	0.58	0.00	0.00	0.00	0.00	0.00	0.00	0.00	0.00	0.00
Pyrite	0.00	0.00	0.00	0.00	0.00	0.00	0.00	0.69	0.70	0.00	0.81	0.00	6.17	0.00	0.00	0.00
Gypsum	0.72	0.00	0.00	0.00	0.35	0.31	0.00	0.32	0.33	0.36	1.52	0.41	0.76	0.00	0.70	0.90
Barite	0.00	1.36	0.00	0.00	0.00	0.00	0.00	0.00	0.00	0.00	0.00	0.00	0.00	0.00	0.00	0.00
Siderite	0.00	0.00	0.00	0.00	0.00	0.00	0.00	0.00	0.59	0.00	0.00	0.00	0.00	0.00	0.00	1.64
Ti-min.	0.00	0.00	0.00	1.28	0.49	0.44	0.00	0.00	0.00	0.00	0.00	0.00	0.00	0.00	0.00	0.00
Rutile	0.00	0.00	0.00	1.54	0.00	0.00	0.00	0.00	0.00	0.00	0.00	0.00	0.00	0.00	0.00	0.00
Phos.	0.00	0.00	2.51	0.00	0.00	0.00	0.00	0.00	0.00	0.52	0.00	0.00	0.00	0.00	0.00	0.00
Jarosite	0.98	0.00	0.00	0.00	0.00	0.00	0.00	0.00	0.00	0.00	0.00	0.00	0.00	0.00	0.00	0.00
Dol./Cal.	0.00	0.00	0.00	0.00	0.00	0.00	0.73	0.00	0.00	0.00	0.00	0.49	0.91	0.00	0.42	14.28
Feldspar	0.00	0.00	0.00	0.00	0.00	0.00	0.33	0.00	0.00	0.00	0.00	0.00	0.00	0.00	0.00	1.00
Muscovite	0.00	0.00	0.00	0.00	0.00	0.00	5.59	0.00	0.00	0.00	0.00	0.00	0.00	0.00	0.00	0.00
Biotite	0.00	0.00	0.00	0.00	0.00	0.00	3.05	0.00	0.00	0.00	0.00	0.00	0.00	0.00	0.00	6.35
Chlorite	0.00	0.00	0.00	0.00	0.00	0.00	0.37	0.00	0.00	0.00	0.00	0.00	0.00	0.00	0.00	0.00
Unknown	0.00	0.00	0.00	0.00	0.00	0.00	3.23	0.00	0.00	0.00	0.00	0.00	0.00	0.52	0.00	2.31
Total % Mineral	6.37	2.97	6.44	80.03	15.54	63.36	98.35	15.87	2.74	5.77	5.75	4.53	8.68	2.98	3.35	97.5
Total % Ash	10.02	7.14	12.89	85.00	21.73	69.89	98.65	27.55	8.86	10.62	8.32	8.07	9.12	5.19	8.00	99.0

Figure 8. Plot of total mineral matter (only discrete phases) versus total ash for 30 samples analyzed by SEM/EMPA. The line drawn is a least squares best fit line.

PLOT OF ASH VERSUS MINERALS



calcite), mixed clays, and phosphorus bearing minerals. Minerals that were only rarely observed within coal lithobodies or were only observed in silty-clay partings were zircon, vermiculite, celestite, feldspar, muscovite, biotite, and chlorite. Table 5 lists, in the order of their average weight percent, the more common mineral types observed in the lithobodies of the Blue and the White pits. Quartz is the most abundant mineral species that was detected; however, if all the various clay mineral species are summed, their average is greater than the quartz averages.

The identification of minerals was based primarily upon their elemental composition and secondarily upon morphology. Table 6 gives ZAF corrected elemental compositions for representative minerals species observed in the Harmon lignite. Nearly all of the minerals identified during the course of this study had elemental compositions that were very similar to the representative types given in Table 6. Representative oxide concentrations for zircon and celestite, which were observed and identified in the coal, are not included in the table because the Tracor TN 5500 computer was not programmed to perform ZAF corrections for these elements. However, the x-ray photon counts for the elements in these two minerals were recorded and the elemental oxide percentages were calculated manually. Zircon was found to have 67% ZrO_2 and 33% SiO_2 . Celestite was observed to contain approximately 60% SrO and 40% SO_3 .

TABLE 5. Common minerals observed in the Harmon lignite and their abundances. Values were calculated as average weight percents of dry coal lithobodies.

<u>Mineral</u>	<u>Ave. Weight %</u>	<u>% of Total Minerals</u>
Total Clays	5.42	51%
Quartz	5.10	44%
Illite	3.52	31%
Kaolinite	1.55	13%
Montmorillonite	.58	5%
Pyrite	.55	5%
Gypsum	.23	2%

TABLE 6. Elemental oxide weight percents of representative mineral species.

Mineral	Location	Na ₂ O	MgO	Al ₂ O ₃	SiO ₂	P ₂ O ₅	SO ₃	ClO	K ₂ O	CaO	TiO ₂	Fe ₂ O ₃	BaO	Clos.
Quartz	GBB-4	0.0	0.0	0.0	99.56	0.00	0.00	0.0	0.0	0.0	0.0	0.44	0.00	100
Kaolinite	HPM-3	0.0	0.15	48.45	49.99	0.22	0.20	0.44	0.00	0.00	0.00	0.55	0.00	85
Kaolinite	GBB-3	0.00	0.00	44.23	54.13	0.13	0.35	0.15	0.12	0.26	0.00	0.32	0.31	90
Illite	GBB-1	0.92	0.28	40.39	51.88	0.00	0.28	0.09	5.14	0.09	0.33	0.59	0.00	97
Illite	GBA-5	0.33	2.94	27.2	56.72	0.0	0.0	0.0	10.4	0.0	0.50	1.90	0.00	99
Illite	HPM-5	0.50	2.75	27.08	51.26	0.00	1.17	0.07	8.46	1.70	1.85	5.16	0.00	82
*Illite	GBO-1	0.23	0.37	34.26	62.36	0.00	0.00	0.17	2.14	0.00	0.08	0.38	0.00	98
Na Mont.	GBA-2	6.42	2.42	21.49	61.53	0.00	0.93	0.11	3.93	0.47	0.46	2.74	0.00	85
Montmoril.	GBP-4	0.00	1.74	15.74	66.01	0.00	0.49	0.28	3.84	3.61	4.21	3.32	0.76	75
Montmoril.	GWP-4	0.37	0.27	30.70	64.59	0.22	0.66	0.33	0.94	0.51	0.87	0.20	0.34	77
Mixed Clay	GBP-4	0.59	7.71	23.69	50.88	0.00	0.00	0.29	6.70	5.83	0.41	3.91	0.00	80
Mixed Clay	GBP-3	0.62	2.12	14.33	71.20	0.00	1.45	0.00	4.78	4.64	0.86	0.00	0.00	45
Pyrite	GBB-2	0.00	0.00	0.00	0.00	0.00	67.60	0.00	0.00	0.10	0.00	32.30	0.00	100
Jarosite	HPM-2	1.63	0.00	0.00	0.42	0.00	40.33	0.10	7.83	0.23	0.00	49.45	0.00	72
Gypsum	HPM-1	0.00	0.00	0.17	0.19	0.00	58.89	0.10	0.00	39.73	0.00	0.92	0.00	100
Barite	HPM-4	0.40	0.00	0.18	0.53	0.00	32.10	0.00	0.00	0.00	0.00	0.00	66.79	80
Rutile	GBP-4	0.33	0.21	0.23	1.18	0.00	0.07	0.00	0.19	92.75	1.03	1.03	4.01	98
Ti-mineral	GBP-3	1.30	9.16	43.34	0.00	0.69	0.00	2.64	0.67	40.81	0.82	0.82	0.00	73
Ti-mineral	GBP-1	0.00	0.10	0.45	68.77	0.00	0.22	0.00	0.11	0.24	29.51	0.00	0.57	75
Calcite	GBO-1	0.00	0.50	0.00	0.00	0.57	0.53	0.00	0.00	97.80	0.00	0.00	0.63	60
Dolomite	GBO-1	0.00	43.39	0.00	0.00	0.00	0.00	0.00	0.15	56.46	0.00	0.00	0.00	55
Siderite	GBC-2	0.48	0.00	0.00	0.87	0.00	1.36	0.00	0.13	0.00	0.00	97.16	0.00	76
Muscovite	GBB-1	0.42	1.35	32.27	49.96	0.20	0.00	0.08	10.93	0.00	0.74	4.04	0.00	100
Muscovite	GBP-4	0.98	1.19	36.07	50.24	0.00	0.17	0.10	9.23	0.00	0.44	1.59	0.00	96
Biotite	GBO-1	0.00	10.24	19.20	44.51	0.85	0.00	0.28	6.35	0.49	0.71	16.42	0.94	100
Biotite	GBP-4	0.22	13.19	21.73	50.50	0.00	0.00	0.38	2.02	0.25	0.37	11.34	0.00	80
Vermiculite	GBP-4	0.00	30.25	25.80	33.69	0.12	0.00	0.00	0.09	0.11	0.18	9.77	0.00	98
Chlorite	GBP-4	0.71	11.99	20.08	34.35	0.31	0.00	0.15	0.24	0.46	1.80	29.88	0.00	97
K-Feldspar	GBO-1	0.21	1.10	23.19	57.90	0.00	0.00	0.48	11.45	0.00	0.00	1.97	3.70	100
K-Feldspar	GBP-4	0.31	1.60	19.40	62.40	0.08	0.00	0.00	13.90	0.41	1.49	1.49	0.40	91
Ca-Al-Phos	GBC-3	0.63	0.96	44.94	1.00	28.66	2.64	0.35	0.18	17.35	0.00	0.00	3.29	41
Ca-Al-Phos	GWC-4	0.19	0.17	48.43	2.26	30.15	0.00	0.00	0.00	8.03	0.00	0.24	10.54	73
Ca-Al-Phos	GBC-3	0.63	1.40	46.41	11.82	22.28	1.06	0.53	0.00	12.79	0.00	0.00	3.08	43
Fe Sulfate	HPM-6	3.52	0.11	0.21	0.31	0.00	38.70	0.12	0.00	0.00	0.00	57.03	0.00	64
Fe Al Sulf	HPM-5	0.00	0.20	20.21	0.58	0.00	67.85	0.00	0.00	0.00	0.00	11.16	0.00	70
Fe Al Sulf	HPM-5	0.54	0.00	23.24	0.68	0.00	67.68	0.00	0.00	0.27	0.00	7.60	0.00	65
Rutilated	GBP-1	0.00	0.00	0.88	91.92	0.00	0.32	0.37	0.16	0.18	5.93	0.25	0.00	72
Quartz														

*Degraded form of illite.

These oxide figures correspond well with published oxide values of 67.02% ZrO₂ and 32.51% SiO₂ for zircon and 56% SrO and 44% SO₃ for celestite (Deer et al., 1962).

For some of the minerals, more than one composition is listed. This was done to show the variation in composition that some of the minerals have, especially the clay minerals. For the clay minerals, consistency was maintained in the Si to Al ratio, but the concentrations of absorbed cations were often variable. All of the minerals identified fell into their respective elemental oxide categories as indicated in Table 1.

Several minerals had compositions that were very complex, and even though they may have matched one of the mineral categories, their identity remained speculative. A brief discussion of these minerals is given below, with a more detailed discussion of possible identities for these minerals later on. The mineral identified as chlorite had a composition very similar to that of biotite except for considerably less potassium and more iron. Illite on several occasions had the correct Si:Al ratio but was lacking the significant concentration of potassium which usually sets it apart. This form of illite was informally referred to as degraded illite (Table 6). Added to this was the problem that muscovite often resembles illite in composition. Problems were also encountered when trying to identify or classify vermiculites, due to the usual complexity of their composition.

Finally, there were some minerals which gave very high x-ray counts but were not identifiable. Included in this category are the titanium bearing minerals (Ti-mineral), calcium-aluminum phosphates (?), iron-aluminum sulfates (?), and iron sulfates (?). The titanium minerals consisted primarily of silicon and titanium. Although several rutilated quartz grains were identified, the titanium minerals identified contained far too much Ti to be called rutilated quartz. The TiO_2 component ranged from 25 to 45 percent by weight.

The presence of calcium-aluminum phosphate (?) particles presents another enigma in the mineral composition of the Harmon lignite. The particles were first thought to be contaminants. However, upon more careful examination, they were definitely an intimate part of the lignite inorganic composition. The oxide concentrations were fairly consistent, averaging 45% Al_2O_3 , 25% P_2O_5 , 11% CaO , and usually having 3% to 10% BaO . The x-ray counts were not very high, showing the degraded nature of these minerals.

The iron-aluminum-sulfur compounds are probably a sulfate mixture of some sort. The compositions were fairly consistent with 7-11% Fe_2O_3 , 20-25% Al_2O_3 , and 60-70% SO_3 . However, the x-ray counts were never very high, implying a more degraded amorphous form of mineral composition and structure. The iron sulfates (?) had compositions ranging between those of pyrite and jarosite, with 35-40% SO_3 and 60-70% Fe_2O_3 .

Distribution of Minerals

Lateral Distribution. Upon completion of the quantitative analysis of the mineral matter, efforts were made to discern the vertical and lateral distribution of minerals and ash within the Harmon bed. Lateral distribution entails the quantity of minerals and ash found in similar lithobodies but in different locations of the pit. The White and Blue pits are separated by a lateral distance of approximately 1.5 miles. Their lithobodies can not be traced or made to correspond as a clastic sedimentary member could be traced laterally. However, the three seams (A,B,C,) do correspond laterally and it is on this basis that the Blue pit and White pit mineralogies and ash concentrations will be studied for their lateral distribution.

Table 7 summarizes the average weight percents of ash, total mineral matter, quartz, kaolinite, illite, clays, and secondary-type minerals for each seam of the Blue and White pits. The average ash and total mineral content for all 3 seams is greater in the Blue Pit than the White Pit. The Blue Pit also has a greater mineral and ash content in its clay partings than the White Pit. Overall, it is obvious that the Blue Pit coal has a different character than the White Pit coal, in that it is higher in ash. Not so obvious, however, is the fact that the higher average ash content in the Blue Pit lignite is due mostly to the much

TABLE 7. Mineral content for the individual seams and partings
for the Blue and White Pits.
(based on average weight percent of coal)

Seam	Ash		All Minerals		Quartz		Kaolinite		Illite		All Clays		Secondary	
	White	Blue	White	Blue	White	Blue	White	Blue	White	Blue	White	Blue	White	Blue
A	6.86	7.74	3.45	5.06	1.59	1.23	.13	.55	1.03	.39	1.29	1.29	.15	1.04
B	9.03	16.78	3.58	9.52	1.12	5.17	.81	2.94	.33	.43	1.21	3.46	.16	.53
C	11.98	10.02	8.05	5.26	2.98	1.20	2.71	2.07	.38	.17	3.94	2.21	.61	1.86
Ave. for A, B, C	9.29	11.51	5.03	6.61	1.90	2.53	1.22	1.85	.58	.33	2.15	2.32	.31	1.14
A-B Part- ing	--	98.65	--	98.35	--	23.9	--	.34	--	54.83	--	61.52	--	.73
B-C Part- ing	57.32	58.87	52.43	52.98	28.81	47.55	2.03	2.75	18.95	7.11	21.36	10.31	--	.22

greater mineral content in the B seam (16.72% ash, 9.52% minerals).

The quantities of quartz, kaolinite, total clays, and secondary-type minerals are also greater in the Blue Pit than in the White Pit (Table 7). The average illite quantity, however, is less in the Blue Pit. Although the Blue Pit does show an overall greater amount of mineral matter than the White Pit, the C seam consistently shows a greater amount of mineral matter in the White Pit.

In summary, the Blue Pit coal shows a greater inorganic content than the White Pit coal. The A seam of both pits has similar mineral types and quantities. The B seam has a much greater mineral content in the Blue Pit than the White Pit, due primarily to greater amounts of quartz and clays. The basal C seam consistently shows slightly greater mineral contents in the White Pit. The nature of the silt-clay partings is quite different for the two pits. Ash and mineral contents are nearly identical for the B-C parting in both pits; however, the Blue Pit shows considerably more quartz and the White Pit shows considerably more clays (Table 7). Also, the Blue Pit has an A-B parting rich in illite clays (54.83%), which is missing in the White Pit.

All of these observations reveal that coal lithobodies in the Harmon lignite vary in mineral character laterally. The lateral variation is primarily due to the relative quantities of quartz and clay minerals present in the coal. Great discrepancies were also noted in the quantities and

types of minerals present in silt-clay partings. The overall inorganic content of the two pits is not only related to the relative abundance of quartz and clays in the lignite but also to the nature of the partings which separate the coal seams. Judging from the role the quartz and clay contents play in differentiating the Blue and White Pits, it may be reasonable to hypothesize that the depositional environment was a major factor in the present day inorganic character of the Harmon bed. Details will be discussed later in this report.

Vertical Distribution. To discern the vertical distribution of inorganic constituents, the quantities of ash and minerals from individual lithologic layers (lithobodies) were studied in vertical section at the Blue and White pits. Figures 9 and 10 show the vertical distribution of ash, which includes minerals and organically bound inorganics, from the base of the Harmon lignite bed (C seam) to the top of the bed (A seam). The horizontal bars represent the sequence of vertical succession of the lithologic layers and are not representative of layer thicknesses.

Both figures reveal that the quantity of inorganic constituents is less in the middle portions of the 3 seams than at the seam extremities. A reasonable explanation for this trend may be that the lignite seams are bordered by either mineral rich partings, overburden, or underclay. Lithobodies lying adjacent to these inorganic rich strata

Figure 9. Vertical distribution of total ash in the White Pit for all 3 seams. Note that the ash content is greater in lithologic layers adjacent to inorganic-rich partings, overburden, or underclay.

WHITE PIT ASH DISTRIBUTION

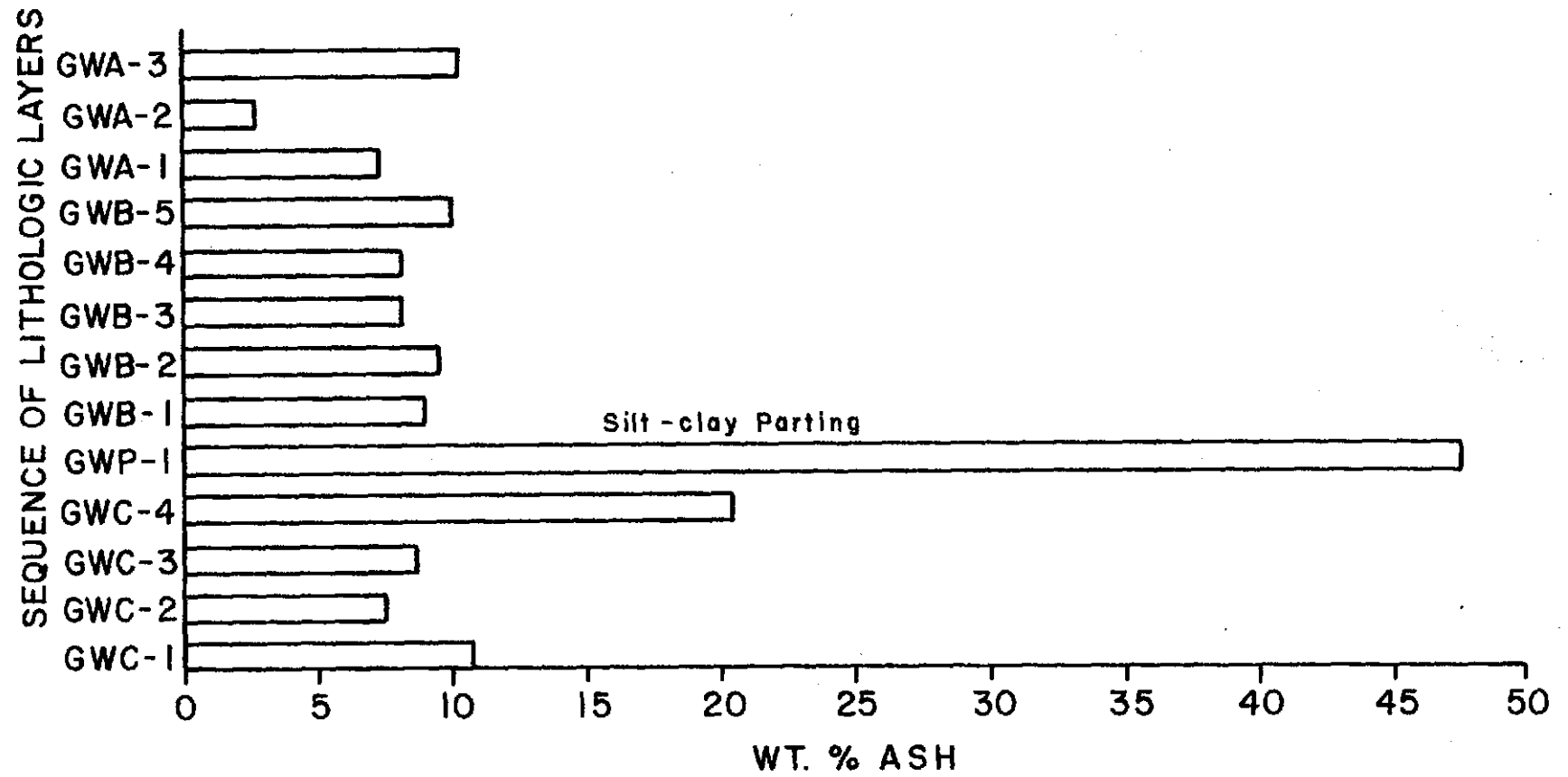
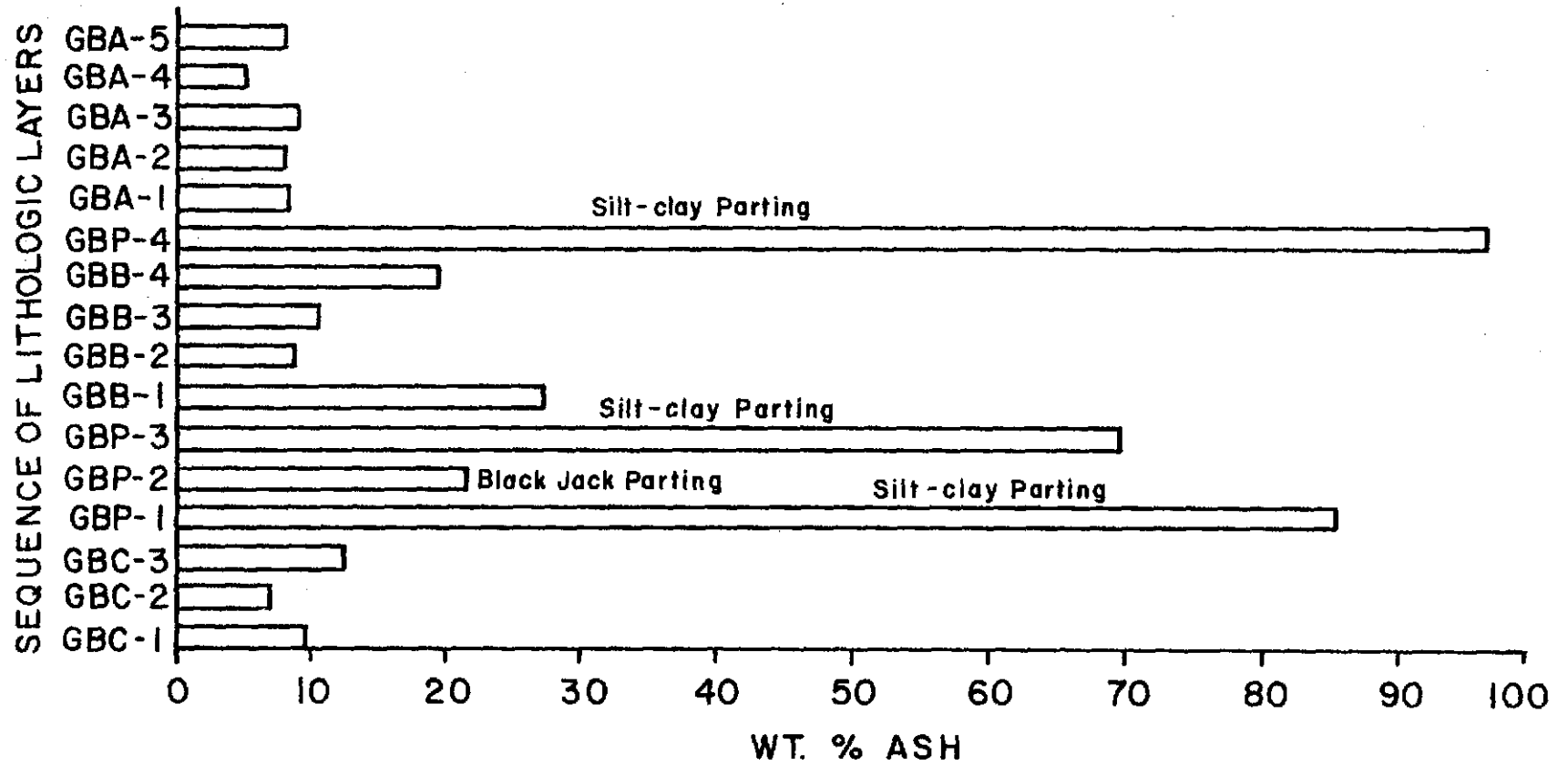


Figure 10. Vertical distribution of total ash in the Blue Pit. Ash content within coal lithobodies is greater near seam boundaries (partings, overburden, or underclay).

BLUE PIT ASH DISTRIBUTION



are, therefore, more prone to have higher inorganic contents. As an interesting note, the boundary between the A and B seam in the White Pit was not denoted by a visible clay-silt parting; however, the inorganic content of the adjacent lithobodies at this boundary still followed the general trend of having a higher inorganic content (Figure 9). In Figure 10, the clay-silt partings separating the C and B seams consist of 3 distinct lithobodies, designated GBP-1 (lowermost), GBP-2, and GBP-3. All three lithobodies contained considerable amounts of organic material, the greatest amount in the middle layer (GBP-2).

The vertical distribution of the total weight percent minerals follow a similar trend as was observed for the ash content. Figures 11 and 12 reveal that discrete mineral phases are less abundant in the middle portions of the seam and more abundant at the seam margins.

Quartz and clay minerals seemed to follow this same trend, showing greater abundances at the margins and lower quantities in the middle of the seams (Figure 13, 14, 15, and 16). Quartz and clays were also the dominant mineral phases in the parting strata GBP-1, GBP-2, GBP-3, GBP-4, and GWP-1. A closer look at the kaolinite distribution revealed that it follows the general trend as above in the Blue Pit (Figure 17) but is somewhat random in the White Pit (Figure 18).

Finally, the vertical distribution of sulphates, carbonates, and phosphates was scrutinized and no pattern or

Figure 11. Vertical distribution of total discrete mineral phases in the White Pit, based upon weight percent of each lithologic layer. Minerals are less abundant in the middle portions of the seam and greater near seam boundaries.

WHITE PIT MINERAL DISTRIBUTION

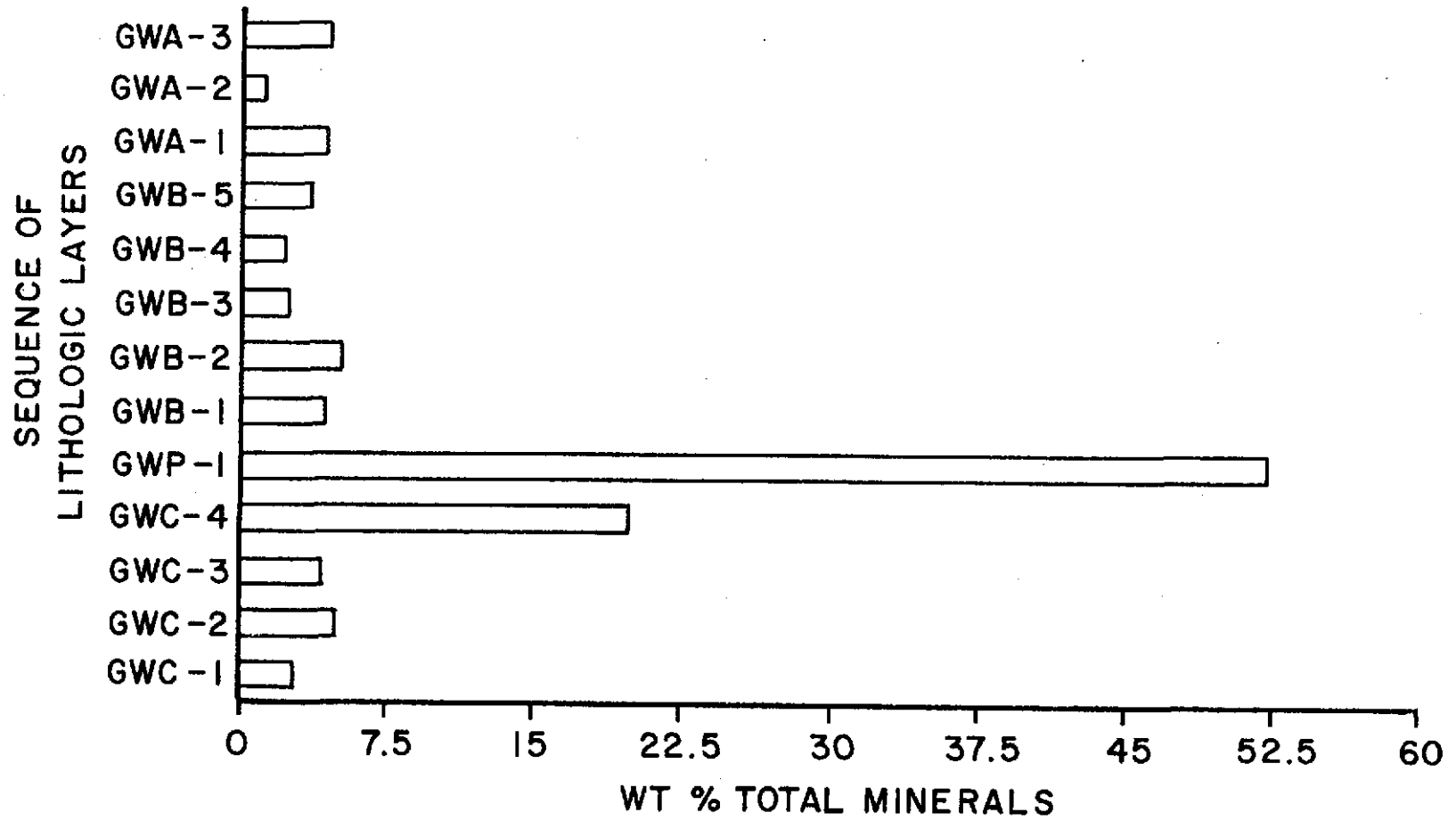


Figure 12. Vertical distribution of total discrete mineral phases in the Blue Pit, based upon weight percent of each lithologic layer. Minerals are less abundant in the middle portions of the seam and greater near seam boundaries.

BLUE PIT MINERAL DISTRIBUTION

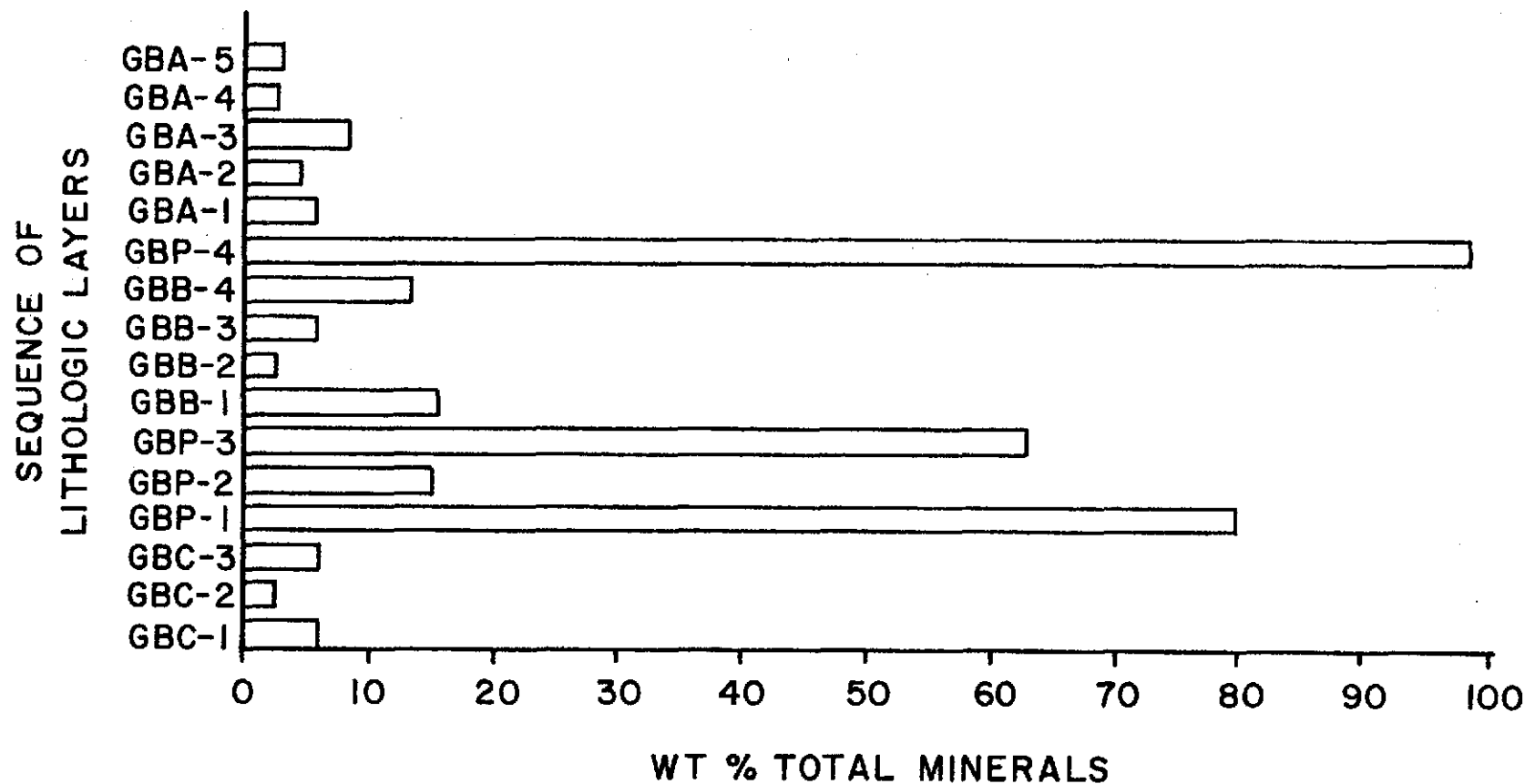


Figure 13. Vertical distribution of quartz in the White Pit based upon weight percent quartz in each lithobody. Quartz is generally more abundant near seam margins.

WHITE PIT MINERAL DISTRIBUTION

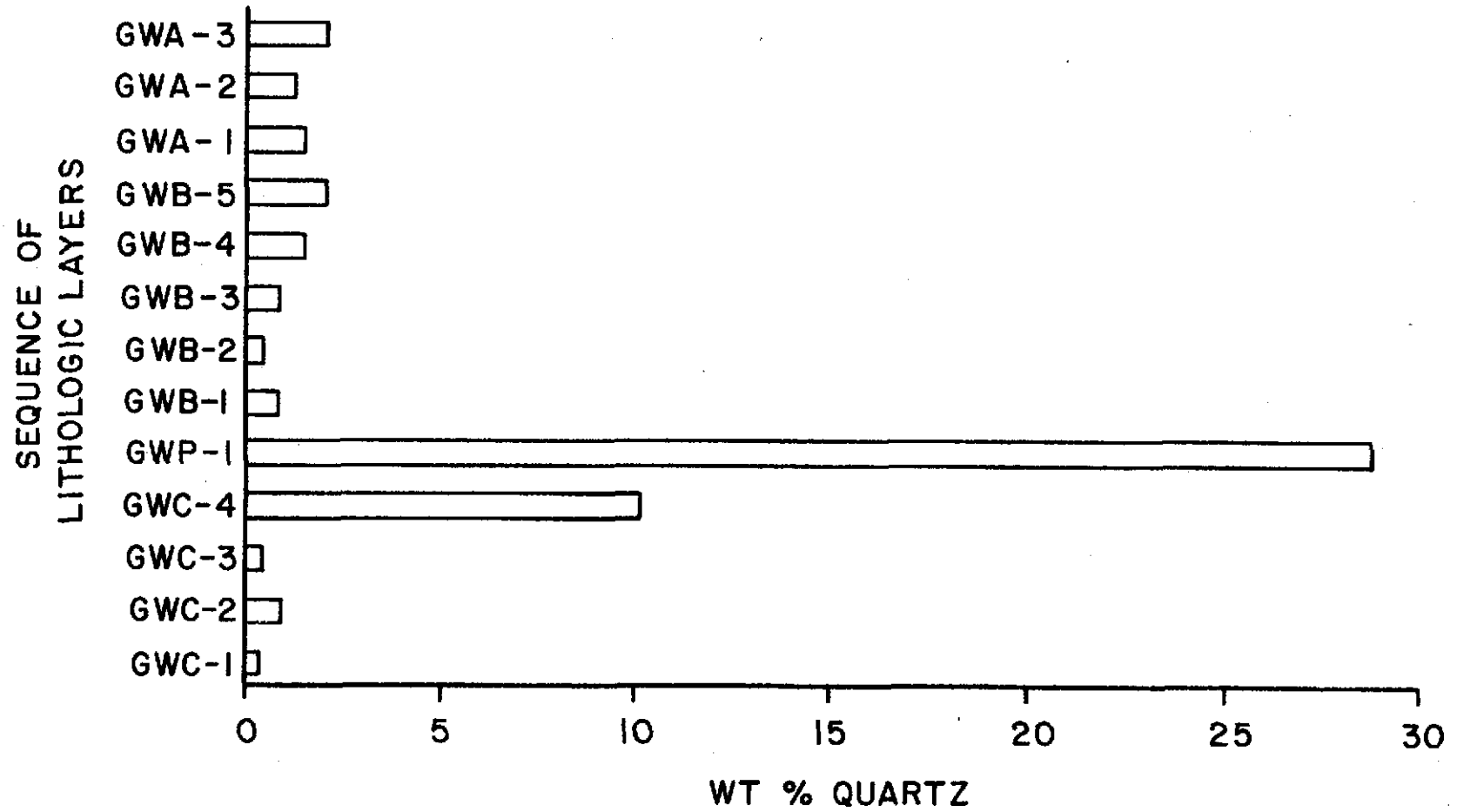


Figure 14. Vertical distribution of quartz in the Blue Pit based upon weight percent of quartz in each lithologic layer. Quartz is generally more abundant near seam margins.

BLUE PIT MINERAL DISTRIBUTION

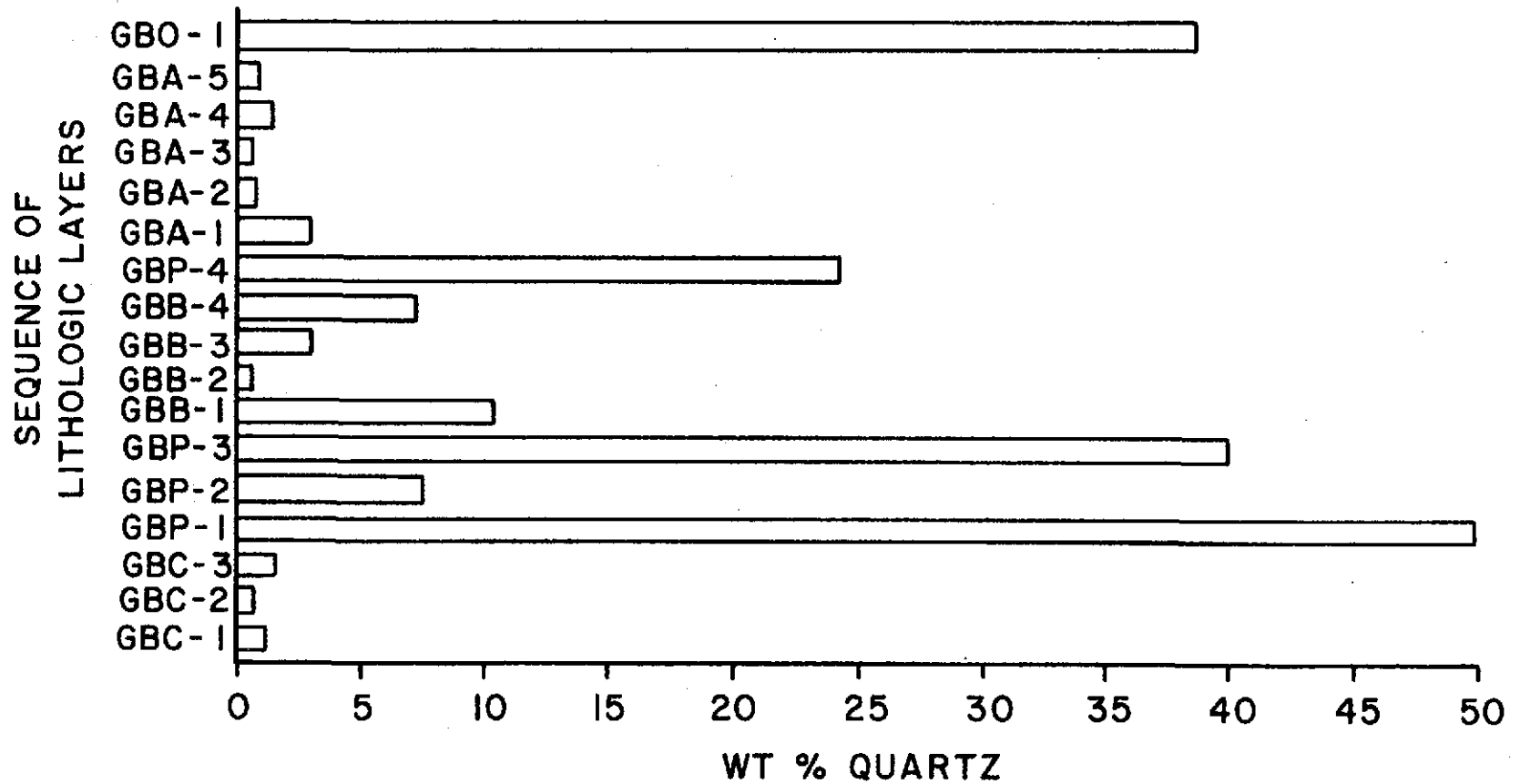


Figure 15. Vertical distribution of total clays in the White Pit showing greater abundances near seam margins.

WHITE PIT MINERAL DISTRIBUTION

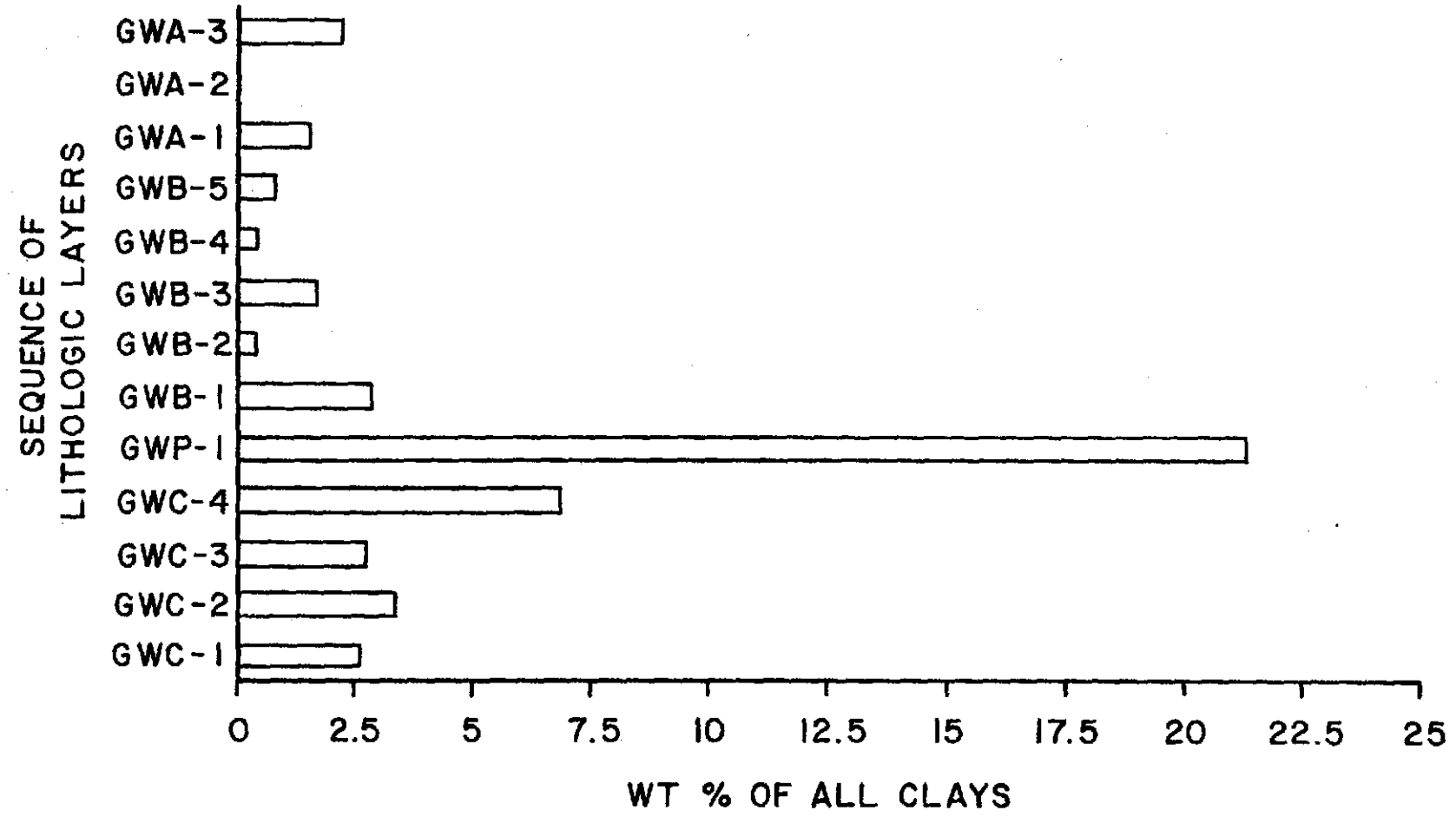


Figure 16. Vertical distribution of total clay minerals in the Blue Pit. Clay content is more abundant in lithobodies adjacent to partings, overburden, and underclay.

BLUE PIT MINERAL DISTRIBUTION

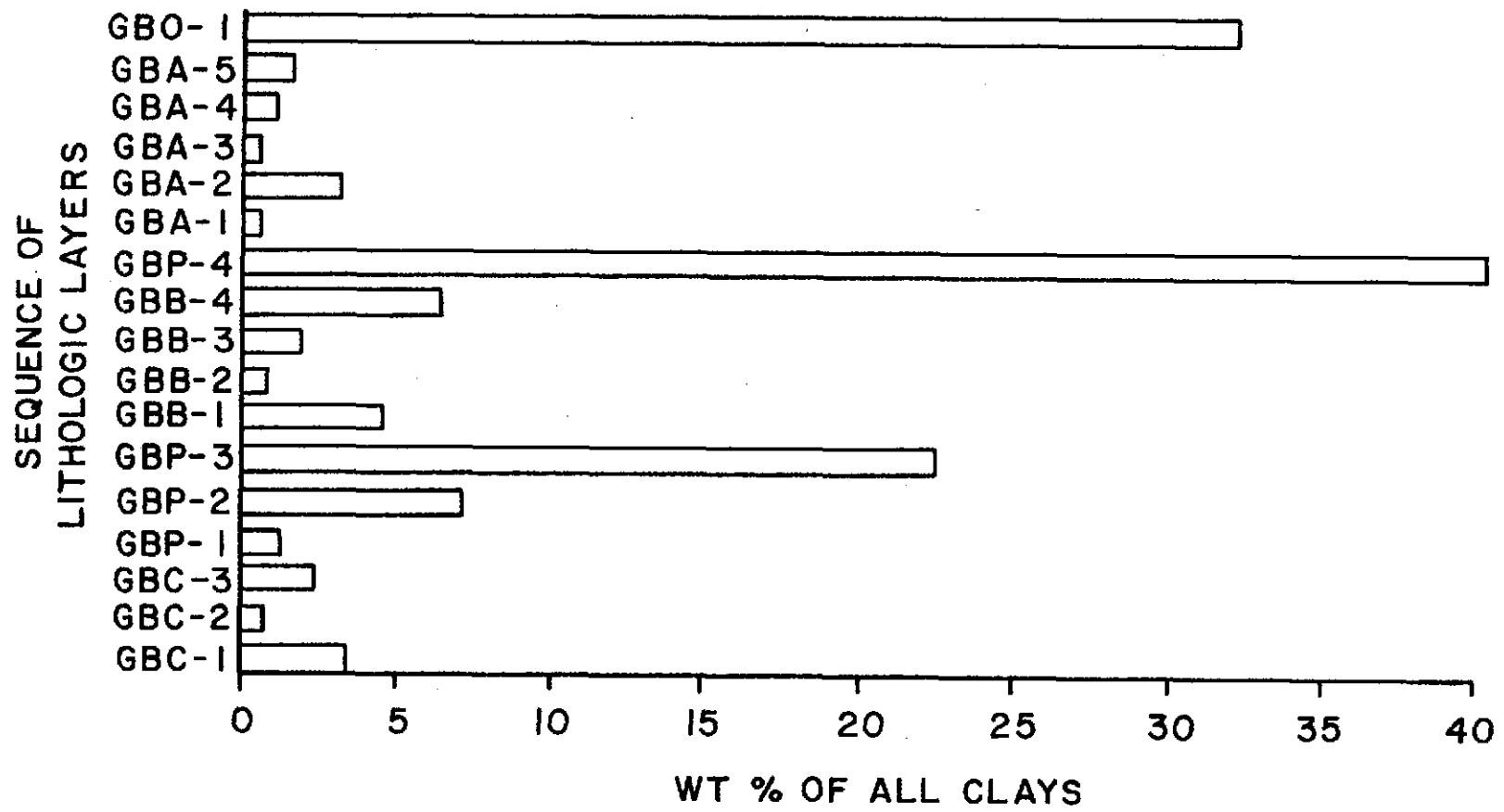


Figure 17. Vertical distribution of kaolinite in the Blue Pit showing greater abundances in lithobodies that are adjacent to inorganic-rich layers.

BLUE PIT MINERAL DISTRIBUTION

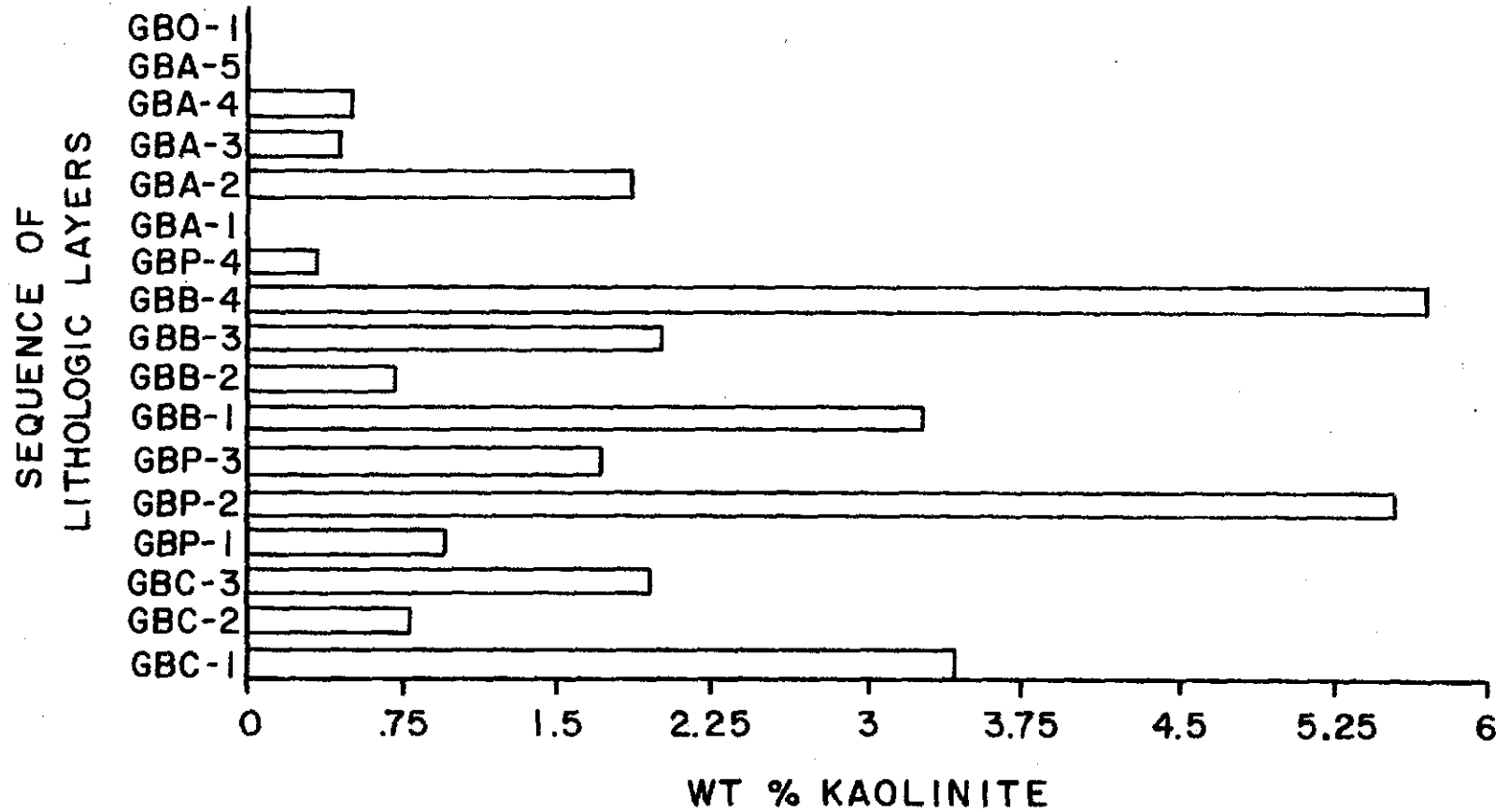
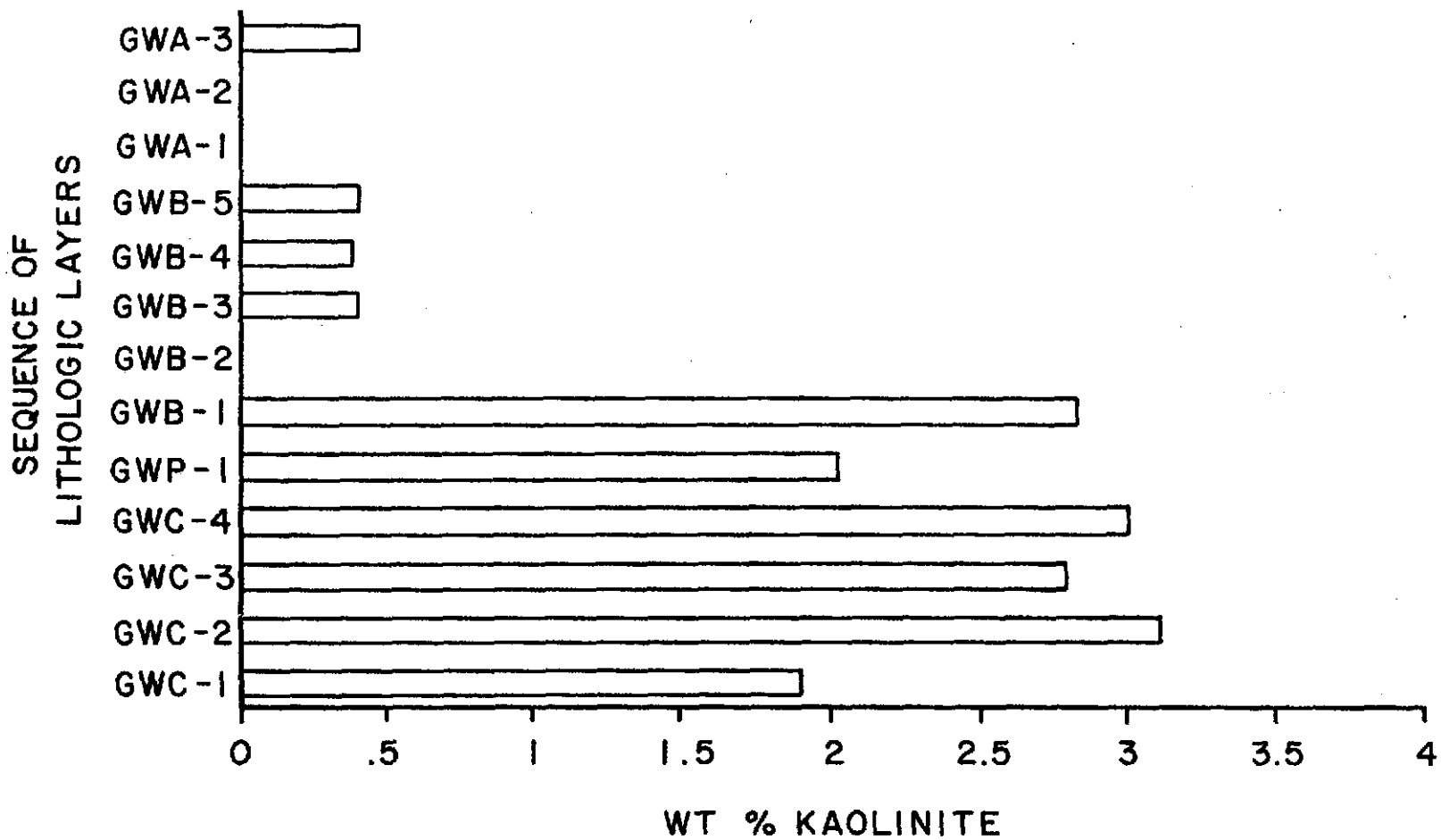


Figure 18. Vertical distribution of kaolinite in the White Pit showing a somewhat random arrangement.

WHITE PIT MINERAL DISTRIBUTION



trend was observed as above; however, these minerals did appear to be more concentrated in the lower C seam for both pits.

Morphology of Minerals and Textural Relationships

Each lithologic layer of the Blue and White pits was examined in detail using the SEM/EMPA system to discern and describe the morphology and textural relationships of the minerals they contain. In this section, all mineral species encountered in the Harmon lignite will be described in detail using SEM photographs of their representative forms as an aid. It is not the intent of this section to conclude the origin of the minerals described; however, suggestions will be made for possible origins in order to enhance the explanation later on. Appendix B summarizes the original descriptive information gathered from the microprobe analysis.

Quartz. Quartz occurred mostly as isolated and well sorted grains. The average diameter of the grains was approximately 42 micrometers for both the Blue and White pits. There was a noticeable tendency for the quartz grains to increase in size and abundance closer to silty-clay partings, overburden, and underclay. Grains that were in pure coal lithobodies were generally subangular to subrounded and showed little corrosion around the edges (Figure 19). Within parting layers, however, the quartz grains were usually rounded to well rounded and much larger

in size (averaging 130 microns).

Secondary overgrowths were not common on any of the grains within pure coal lithobodies, although some grains did show very straight euhedral faces that are often indicative of recrystallization rims (Figure 20). Another possible occurrence of secondary overgrowths may have been the secondary mineralization of pyrite around quartz grains. Quartz and pyrite were often found associated (Figure 21). On several occasions grains were observed consisting of a quartz interior with an exterior covering of pyrite crystals (Figure 22). SEM microprobe analysis gave the impression that a quartz grain substrate could be the site of pyrite mineralization.

SEM photographs of unpolished and undisturbed fracture surfaces of the lignite reveal a nonpitted smooth surface texture for most of the quartz grains (Figures 23 and 24).

Although many of the quartz grains were 30-40 micrometers in average diameter, there were several instances of microcrystalline quartz grains. Figure 25 shows a fine microcrystalline quartz layer consisting of very fine silt-sized quartz grains. These fine microquartz layers were found in a coal lithobody immediately adjacent to a quartz-rich silt-clay parting in the Blue Pit.

One of the major topics of debate concerning mineral matter in coal pertains to the origin of quartz. Detrital quartz is usually of a fine to coarse silt size (5-50 micrometers), has a subrounded to subangular shape, may be

Figure 19. SEM photograph using secondary electron imaging (SEI) of three detrital quartz grains in coal (650 X, 1 cm = 16 microns).

Figure 20. SEM (SEI) photograph of a quartz grain showing euhedral crystal faces in upper right (4800 X, 1 cm = 2.1 microns).

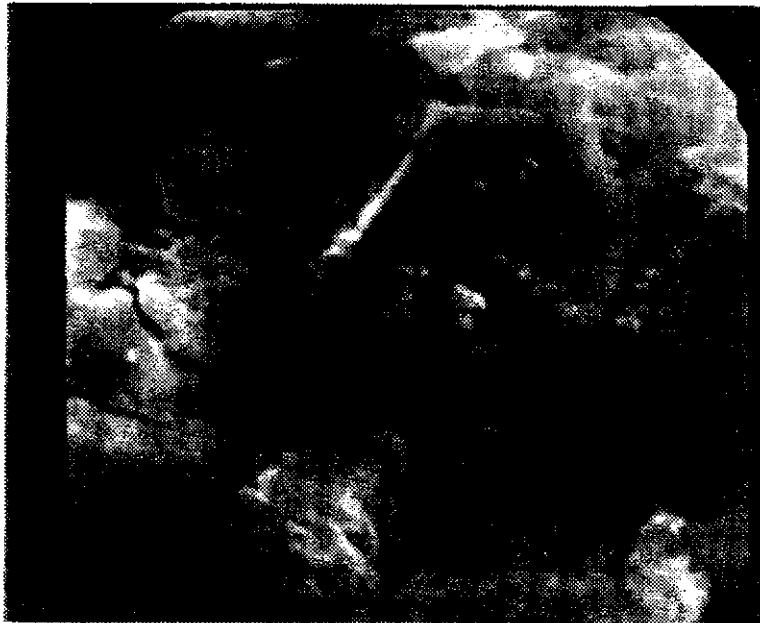
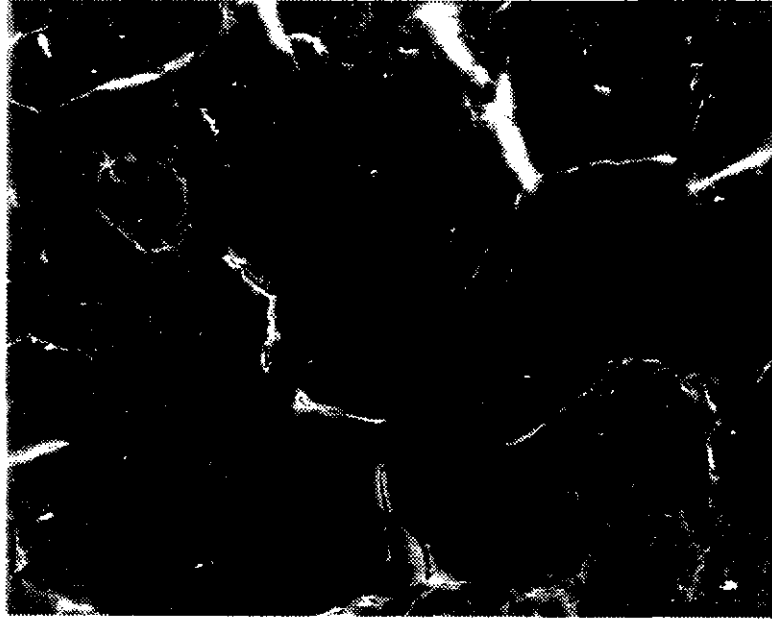


Figure 21. SEM (SEI) photograph of a subrounded quartz grain (dull gray) surrounded by pyrite (brighter gray) in lower left (360 X, 1 cm = 28 microns).

Figure 22. SEM (SEI) photograph of dull gray quartz occurring in center of pyrite framboid (3000 X, 1 cm = 4.5 microns).

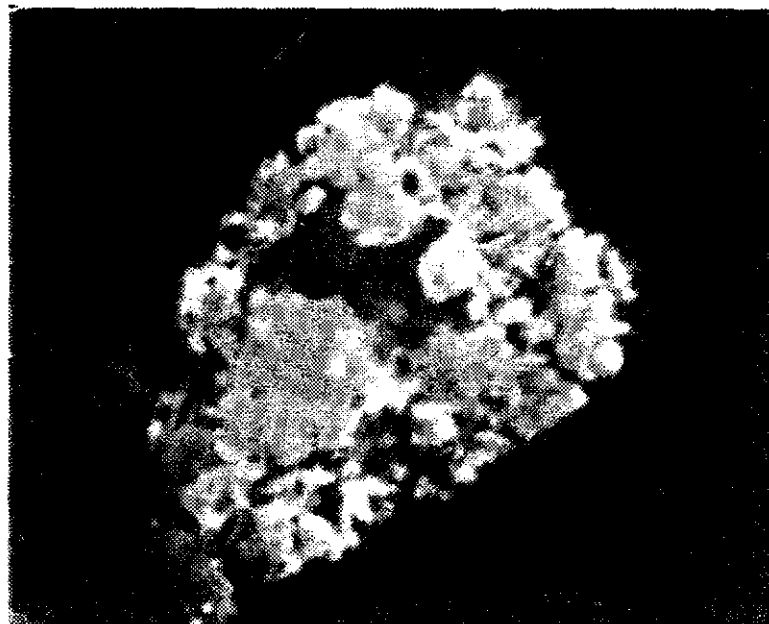
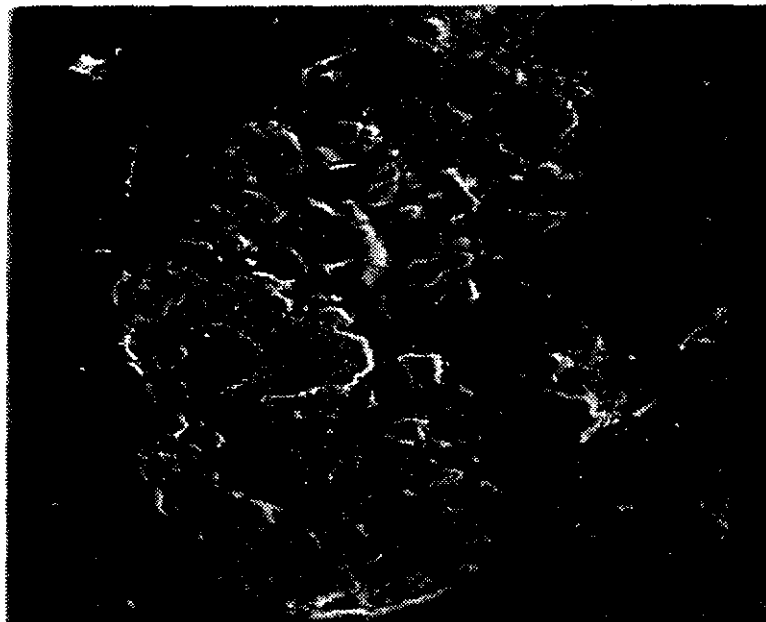
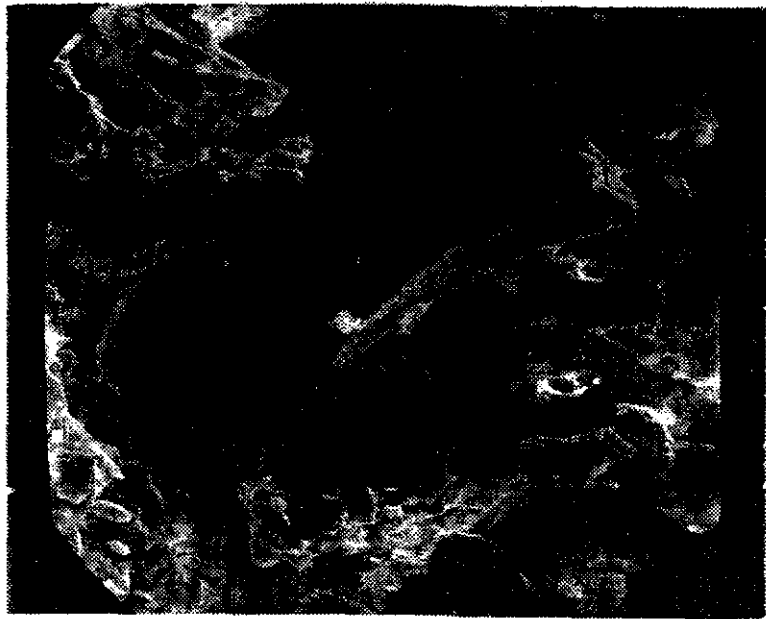


Figure 23. SEM (SEI) photograph of subrounded-subangular detrital quartz grain observed on a fracture surface (2000 X, 1 cm = 5 microns).

Figure 24. SEM (SEI) photograph of quartz grain showing conchoidal fracture (650 X, 1 cm = 16 microns).



found in microlayers of silt and clay, and generally increases in abundance nearer a clastic source. In contrast, authigenic quartz has a more delicate form, usually exhibits crystal faces or a thin, flaky form, generally consists of smaller grain sizes (less than 10 microns), and is intimately associated with the coal maceral structure. Figure 26 shows an area of microcrystalline quartz which has a much more delicate texture and appears to line a cavity of this coal fracture surface. This fits the description of authigenic quartz and is classified as such.

Kaolinite. Kaolinite usually occurs as dull aggregates 65 micrometers in average diameter, but very small (10-20 microns) evenly dispersed particles were also common. The aggregates consisted of tiny platelets less than 1 micrometer in size. These platelets are too small to obtain a good photograph using the SEM. Most of the kaolinite particles are subrounded and often distorted into various shapes (Figure 27). Several instances of kaolinite in contact with or surrounding pyrite and quartz were noted. The kaolinite aggregates sometimes consist of strands of stacked platelets. These strands pack together forming kaolinite particles. Sometimes, however, the strands are not entirely compacted and are visible (Figure 28).

Kaolinite will sometimes form massive patches or layers in the coal instead of isolated particles or aggregates. These more massive forms range from 100 to 1000 micrometers in size. Massive kaolinite mineralization commonly follows

Figure 25. SEM (SEI) photograph showing microcrystalline quartz grains within a detrital silt band (1800 X, 1 cm = 6 microns).

Figure 26. SEM (SEI) photograph of 3-4 micron angular flakes of quartz in center of photo which may be authigenic (1300 X, 1 cm = 7 microns).

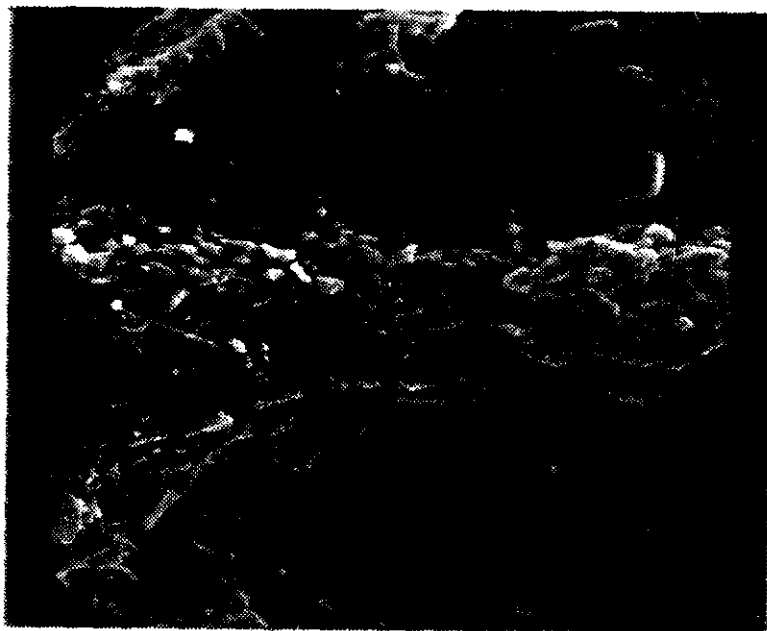
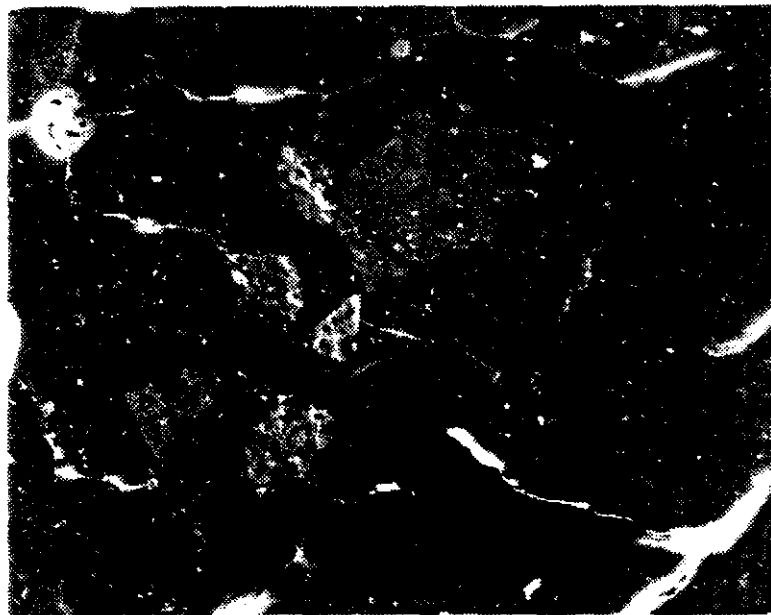
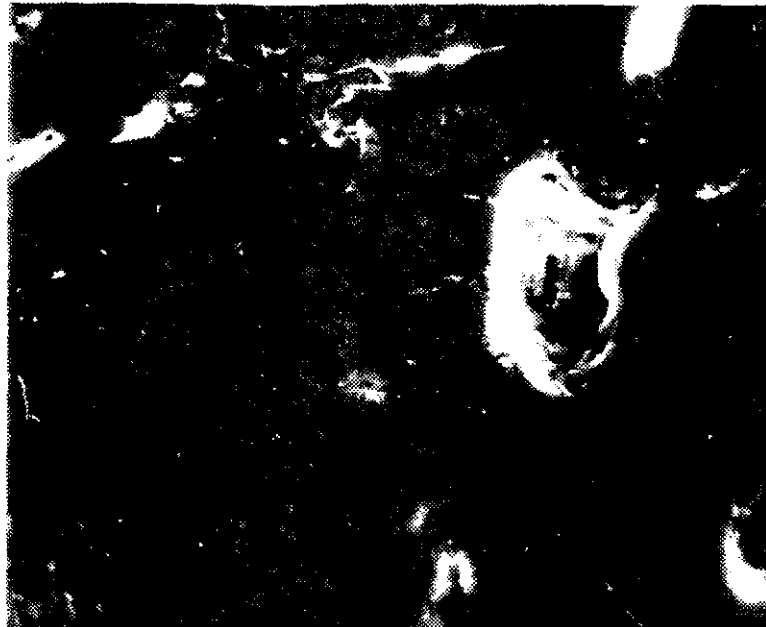


Figure 27. SEM (SEI) photograph of distorted kaolinite band (1100 X, 1 cm = 10 microns).

Figure 28. SEM (SEI) photograph showing larger kaolinite grain in upper part of photo; note the separation between the strands of stacked platelets (650 X, 1 cm = 16 microns).



the bedding plane structure of the coal. Figure 29 shows a lenticular body consisting of tiny kaolinite grains. These lenticles could be seen in a hand specimen and were probably detritally deposited.

As a final form, kaolinite was seen infilling lignite cell cavities, pores, and other maceral voids. Figure 30 is a SEM photo of cellular cavities in fusinite. Figure 31 shows similar cavities in fusinite that have been filled with kaolinite. In Figure 32, lighter colored kaolinite is shown infilling maceral voids probably in fusinite. Kaolinite of the form described above has a secondary authigenic origin.

Illite. Illite can be described as primarily isolated subangular to angular grains averaging 31 micrometers in diameter. Within pure coal lithobodies, illite is very finely dispersed and has a morphology that is difficult to distinguish from kaolinite. Unlike kaolinite, illite does not have the aggregate-like appearance.

Illite occurs more frequently when adjacent to inorganic rich layers. In Figure 33 detrital illite grains, along with quartz, form thin bands in a silt-clay parting of the Blue Pit. The uppermost silt-clay parting in the Blue Pit (GBP-4) has abundant illite grains intermixed with quartz (Figure 34). The above figure shows the platy detrital form of illite. In contrast Figure 35 reveals illite flakes intimately associated with the coal surface on which they rest. The illite here is in the form

Figure 29. SEM (SEI) photograph of lenticular kaolinite lens in center of photo, which is detrital in origin (300 X, 1 cm = 33 microns).

Figure 30. SEM (SEI) photograph showing voids in fusinite maceral (360 X, 1 cm = 28 microns).

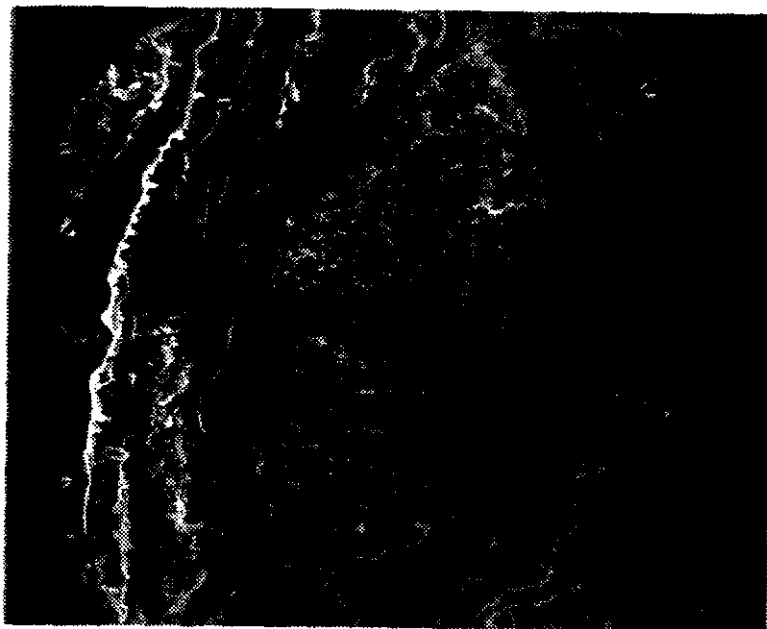


Figure 31. SEM (SEI) photograph of kaolinite infilling voids in fusinite maceral (180 X, 1 cm = 65 microns).

Figure 32. SEM (SEI) photograph showing bright colored, oval-shaped areas of kaolinite infilling fusinite voids (1000 X, 1 cm = 10 microns).

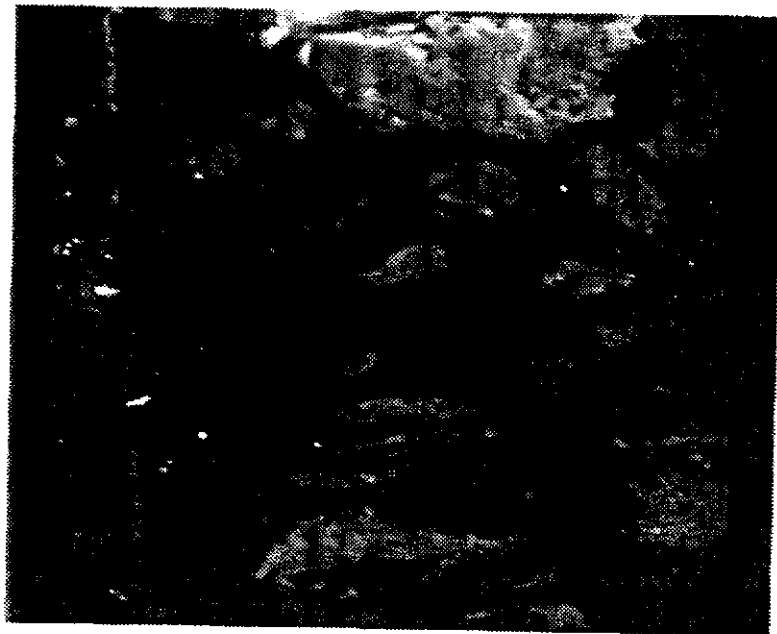
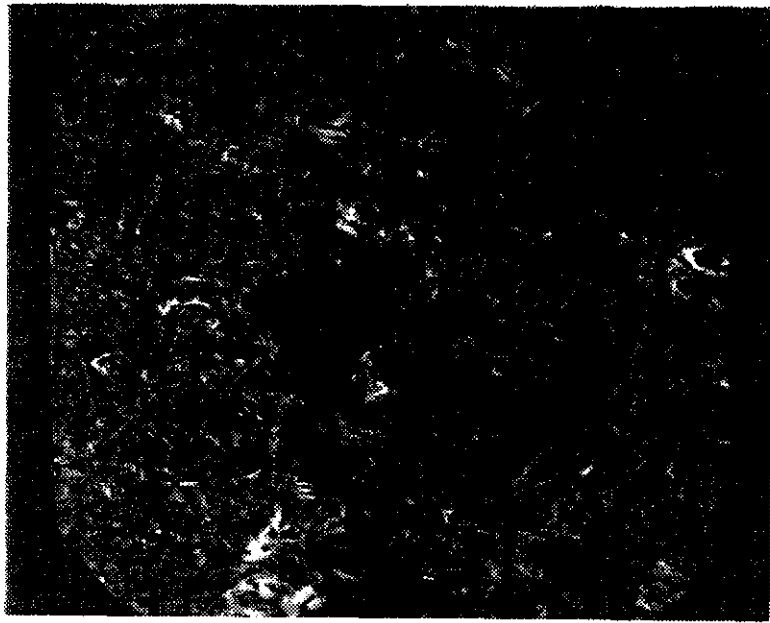
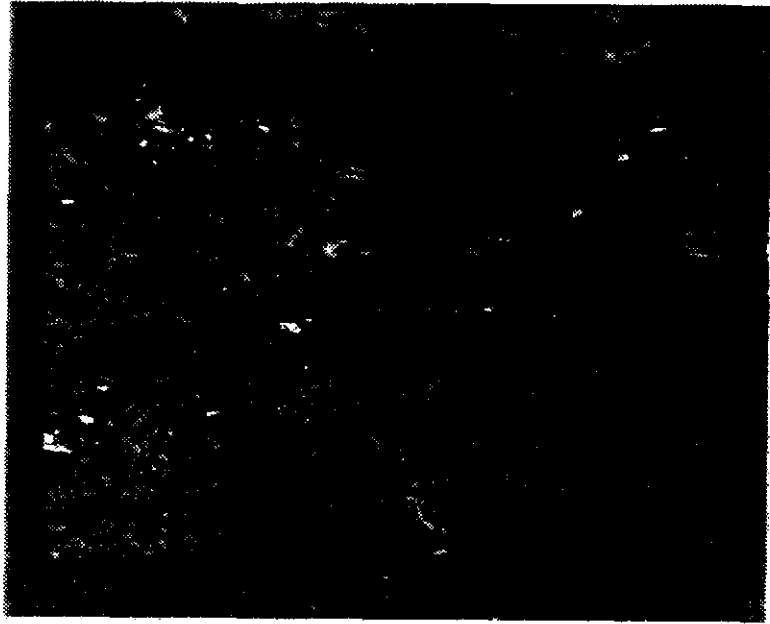


Figure 33. SEM (SEI) photograph of detrital quartz and illite bands; the elongate flakes are illite and the subrounded grains are quartz (500 X, 1 cm = 20 microns).

Figure 34. SEM (SEI) photograph of large illite grain in center; note platy strands. Rounded grain in upper right is quartz (500 X, 1 cm = 20 microns).



of fine delicate flakes which are more indicative of an authigenic origin. Overburden samples have abundant illite grains that are elongated and platy in form (Figure 36).

Montmorillonite and Mixed Clays. Montmorillonite and mixed layer clays were similar in form to isolated kaolinite aggregates. They usually consisted of dull subrounded grains that were 25-40 micrometers in size (Figure 37). It was a difficult task to find isolated examples of these clays because of their finely disseminated distribution.

Pyrite. Pyrite was found primarily as framboids with diameters averaging 45 micrometers (Figure 38). Framboids are berry-like clusters of pyrite crystallites. Figure 39 displays the form of the individual pyrite crystallites.

Pyrite was also discovered as massive bands or dendritic mineralization areas. Figures 40 and 41 are excellent examples of how the massive pyrite follows structural zones of weakness in the coal. In some cases, pyrite has actually replaced the lignite. Both relatively large areas of coal (.1 to 40 mm in length) and minute coal structures, such as cell walls, which had been replaced by pyrite, were noted (Figures 42 and 43).

The dendritic pyrite forms (Figure 44) are probably an example of how iron sulfide solutions followed zones of weakness in the coal and precipitated pyrite or marcasite. The massive pyrite forms are secondary in origin, forming after compaction and consolidation of the lignite.

As was mentioned earlier, pyrite was observed in

Figure 35. SEM (SEI) photograph of fine delicate flakes of what is probably authigenic illite (1800 X, 1 cm = 6 microns).

Figure 36. SEM (SEI) photograph of a large illite grain as viewed in overburden sample (1000 X, 1 cm = 10 microns).

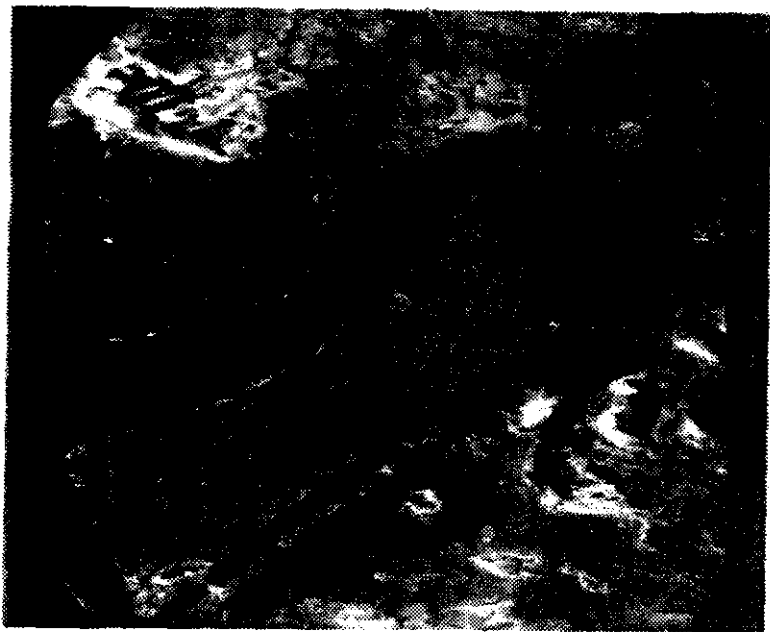
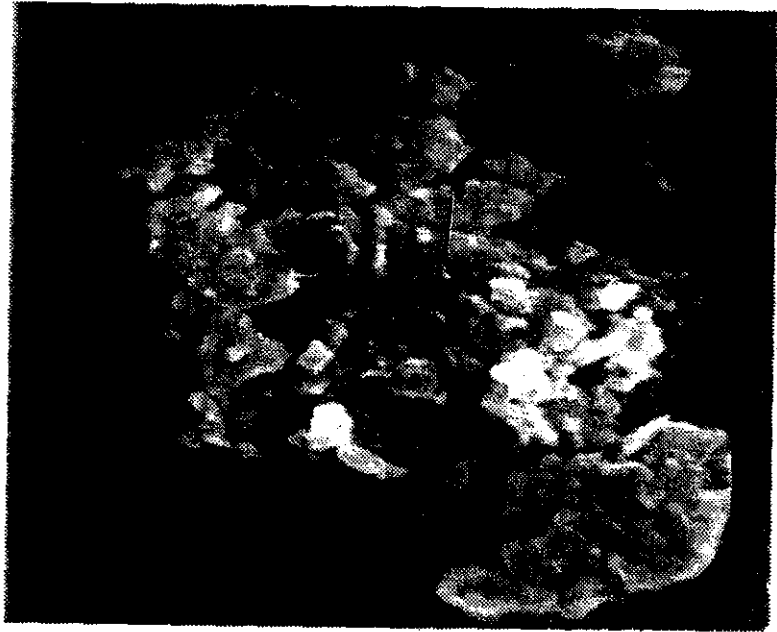


Figure 37. SEM (SEI) photograph of a rounded montmorillonite grain (1300 X, 1 cm = 9 microns).

Figure 38. SEM (SEI) photograph of pyrite framboids (220 X, 1 cm = 52 microns).

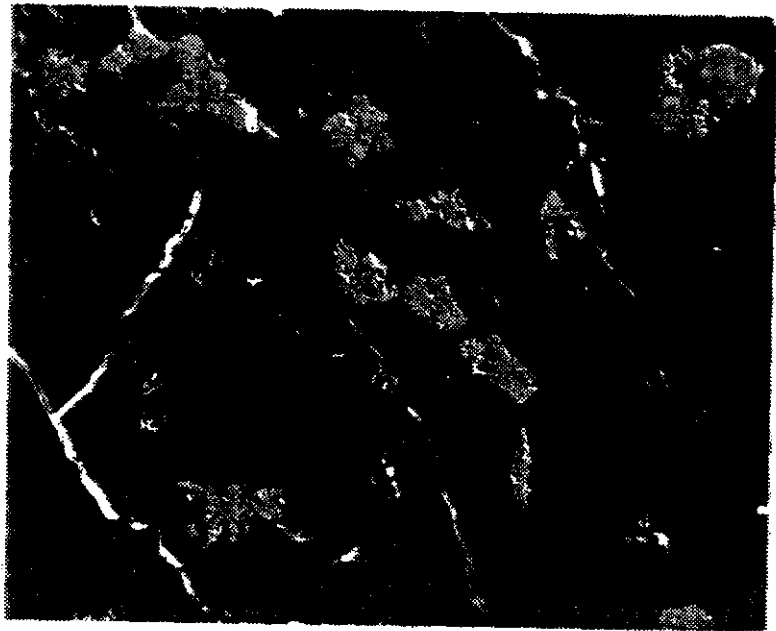


Figure 39. SEM (SEI) photograph showing close-up view of pyrite crystallites, each about 2 microns in diameter (3200 X, 1 cm = 3.2 microns).

Figure 40. SEM (SEI) photograph of massive pyrite layers which are characteristic of an epigenetic origin (220 X, 1 cm = 48 microns).

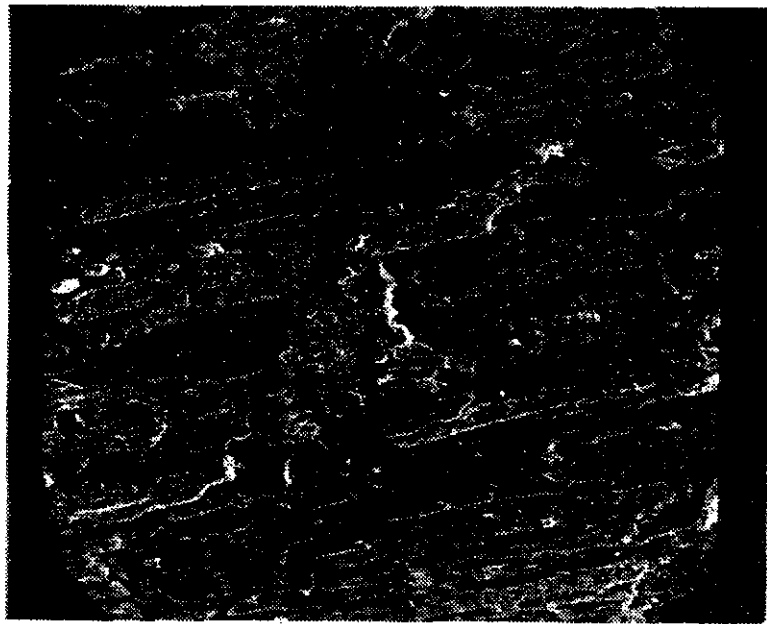
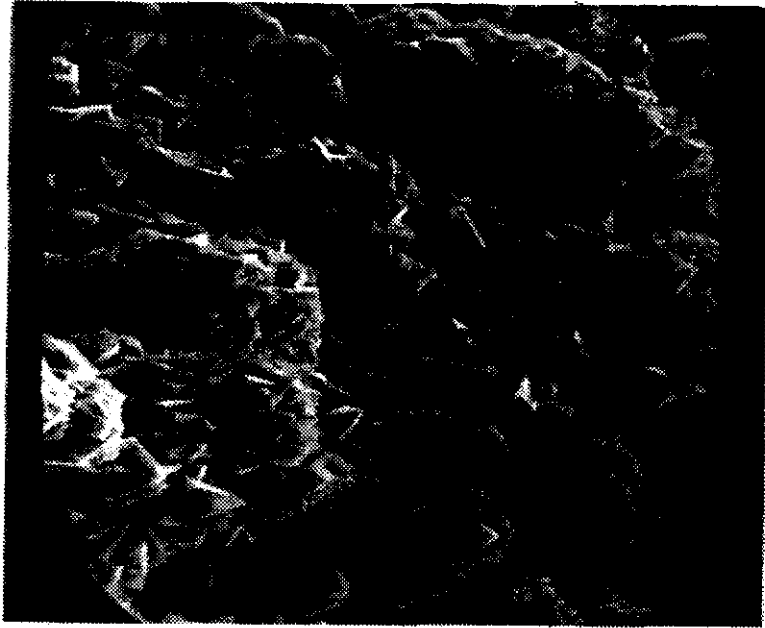


Figure 41. SEM (SEI) photograph showing close-up view of the pyrite bands in Figure 40. Note the 1-3 micron pyrite crystallites (1800 X, 1 cm = 6 microns).

Figure 42. SEM (SEI) photograph showing epigenetic pyrite replacing coal (60 X, 1 cm = 150 microns).

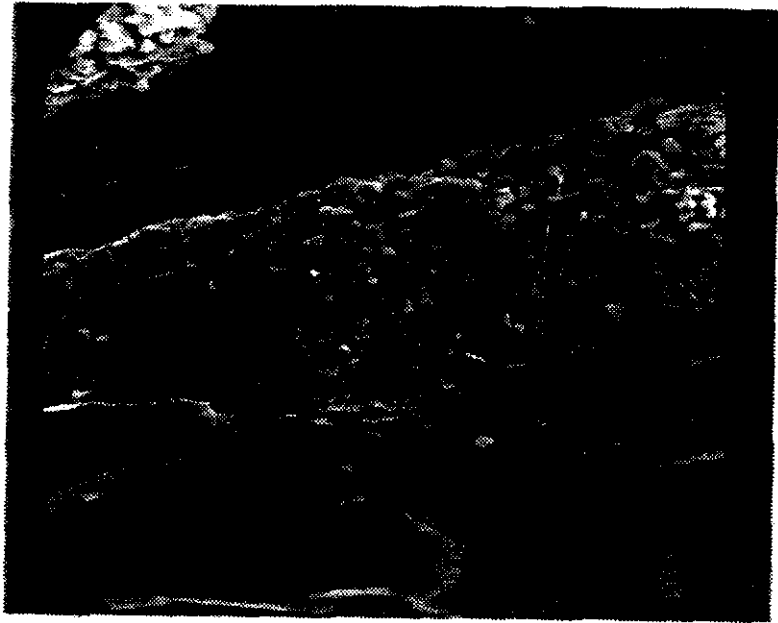
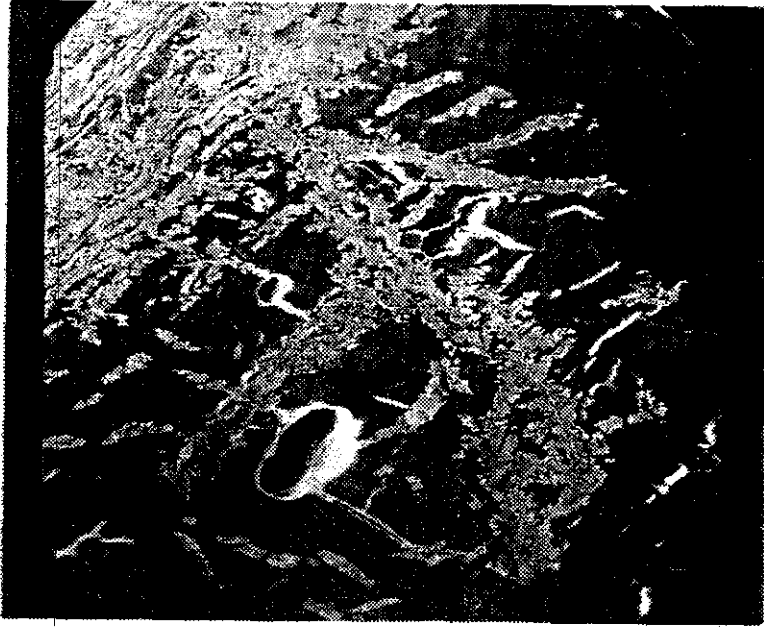


Figure 43. SEM (SEI) photograph showing pyrite replacing cell wall structures; dark material inside pyrite borders is coal (1800 X, 1 cm = 6 microns).

Figure 44. SEM (SEI) photograph showing dendritic pyrite replacing coal or following microfractures in coal (100 X, 1 cm = 52 microns).



association with quartz, possibly as overgrowth material over quartz grains. Pyrite was also seen occurring with kaolinite (Figure 45) and gypsum (Figure 46).

Gypsum. All of the sulfate minerals observed in the course of this study, which include gypsum, barite, celestite, and jarosite, are secondary products which have formed from the elemental constituents in the lignite. Gypsum is a common alteration product found mainly near fractures or weathered surfaces. There were two forms of gypsum noted in the Harmon lignite. The first form consisted of distinct crystals or agglomerations of crystals, ranging from .1 to 20 mm in width or length (Figure 47). This crystalline form of gypsum was normally found only where a lignite surface had been exposed to atmospheric conditions for a period of time. Several instances of gypsum associated with pyrite and siderite were observed (Figure 48).

The second type of gypsum observed was nearly undetectable because it is very finely sized and interspersed in the coal. Sizes of these particles may be less than 1 micrometer in diameter. Some of this gypsum appears to be secondary in nature, being found filling cracks and cavities in the lignite (Figure 49). Most of this fine gypsum, however, was not as obvious to detect as that in the above figure. The coal organic matrix would often show very strong calcium and sulfur peaks in the SEM/EMPA elemental spectra, which may have been indicative

Figure 45. SEM (SEI) photograph of bright subrounded pyrite grain, surrounded by dull gray kaolinite (800 X, 1 cm = 13 microns).

Figure 46. SEM (SEI) photograph of small angular grains of pyrite and elongate laths of gypsum as viewed on a lignite fracture surface (550 X, 1 cm = 18 microns).

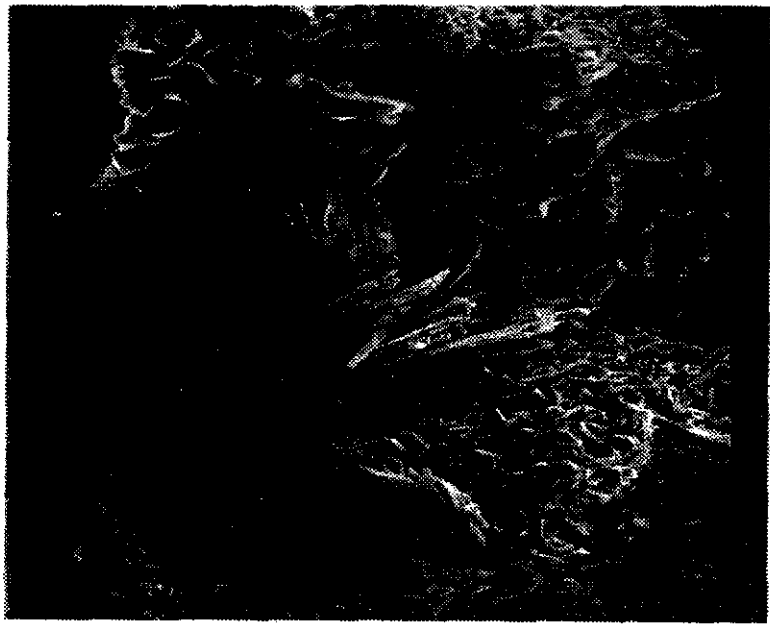
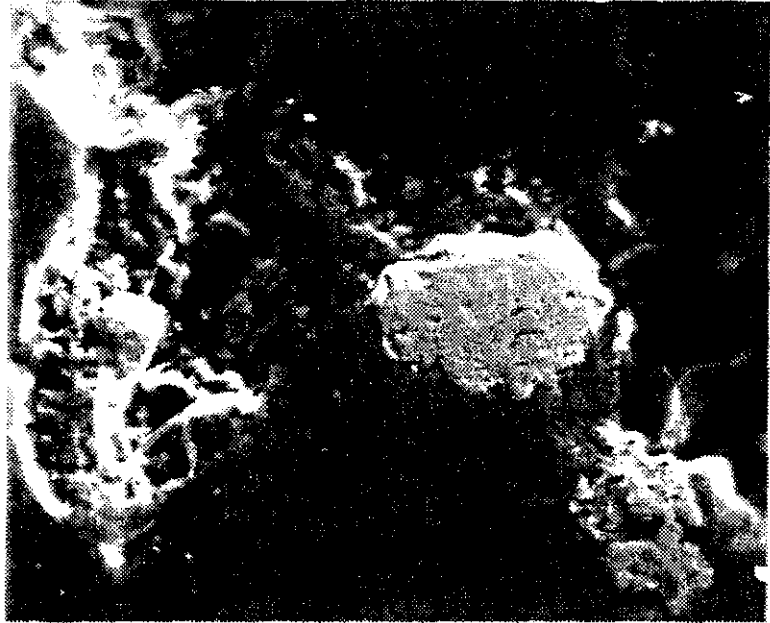
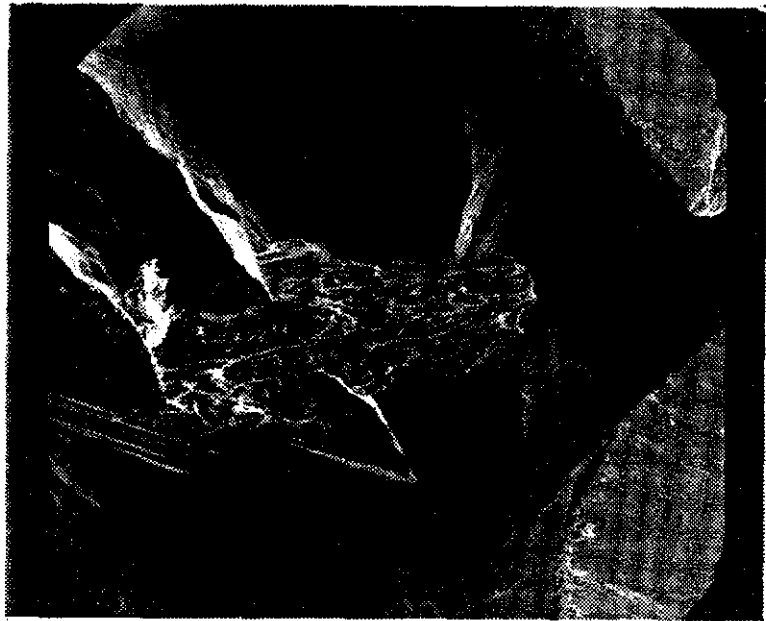
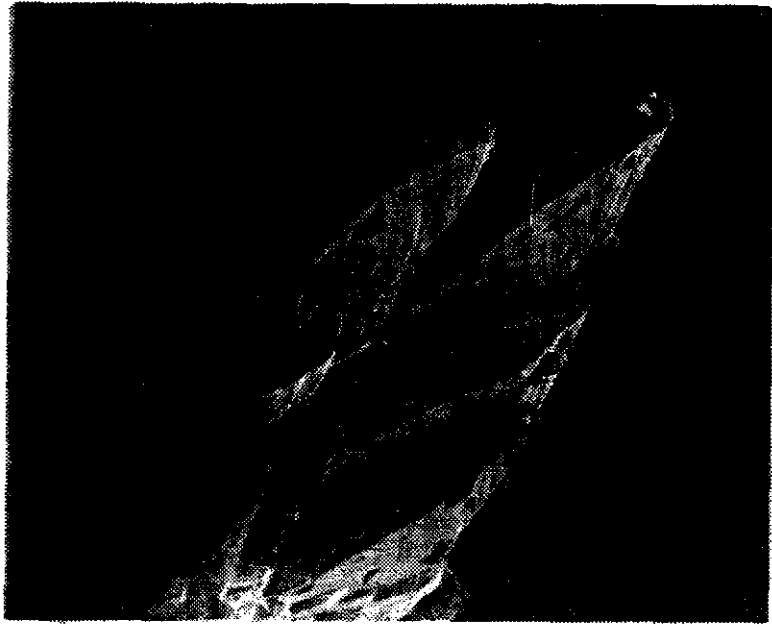


Figure 47. SEM (SEI) photograph of authigenic gypsum crystals on coal fracture surface (150 X, 1 cm = 75 microns).

Figure 48. SEM (SEI) photograph of rough textured siderite (center) intergrown with smooth surfaced gypsum crystals (300 X, 1 cm = 33 microns)



of very finely interspersed gypsum ($\text{CaSO}_4 \cdot 2\text{H}_2\text{O}$) crystals in the coal.

Barite. Barite (barium sulfate) was observed in two distinct forms. The first form was found replacing coal or infilling structural zones of weakness (Figure 50). This type appeared as massive barite mineralization areas 200 to 700 microns in diameter. The second form was limited to lignite surfaces that had been exposed to atmospheric conditions for a period of time. This form was characterized by delicate crystal platelets or laths on coal surfaces (Figure 51).

Celestite and Jarosite. Celestite (strontium sulfate) and jarosite (potassium iron sulfate) were both observed as delicate crystals or agglomerations of crystals on coal fracture surfaces. Neither of these minerals was seen in polished sections of coal. Celestite consisted of very small crystal laths (<2 microns) which were intimately grown on a lignite surface (Figure 52). The relatively high atomic weight of strontium gave celestite a bright appearance in the secondary electron image. Jarosite was seen as very small rectangular flakes (< 1 micron) on a coal fracture surface.

Carbonate Minerals. The carbonate minerals that were observed are calcite, dolomite, and siderite (iron carbonate). Calcite was seen as tiny 2-20 micrometer subangular grains in pure coal lithobodies and as 60 micrometer grains in overburden samples. Cleavage planes

Figure 49. SEM (SEI) photograph showing light gray gypsum mineralization in coal; possibly authigenic in origin (1200 X, 1 cm = 11 microns).

Figure 50. SEM (SEI) photograph of massive barite mineralization in coal particle (130 X, 1 cm = 65 microns).

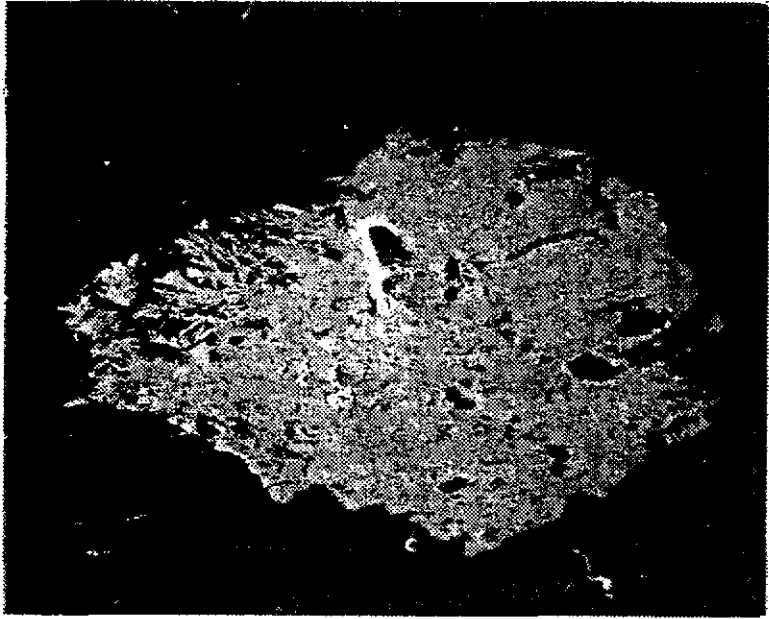
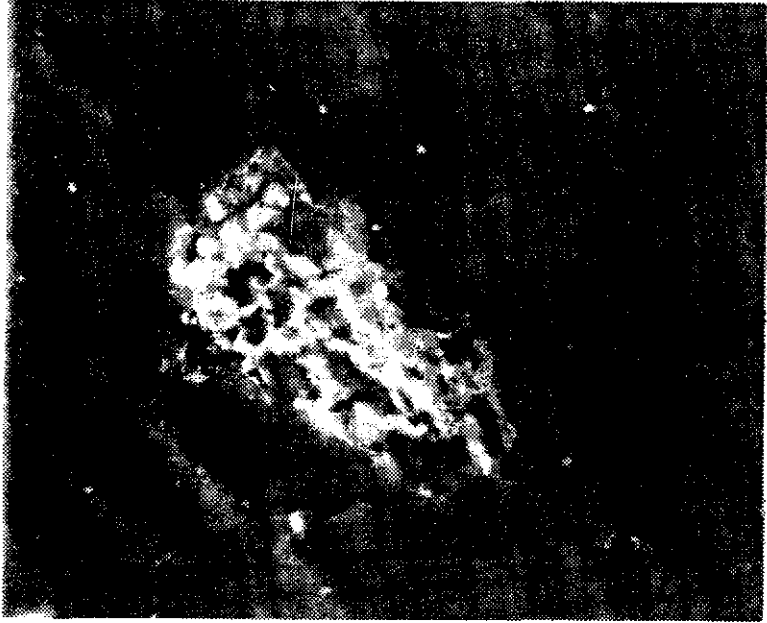
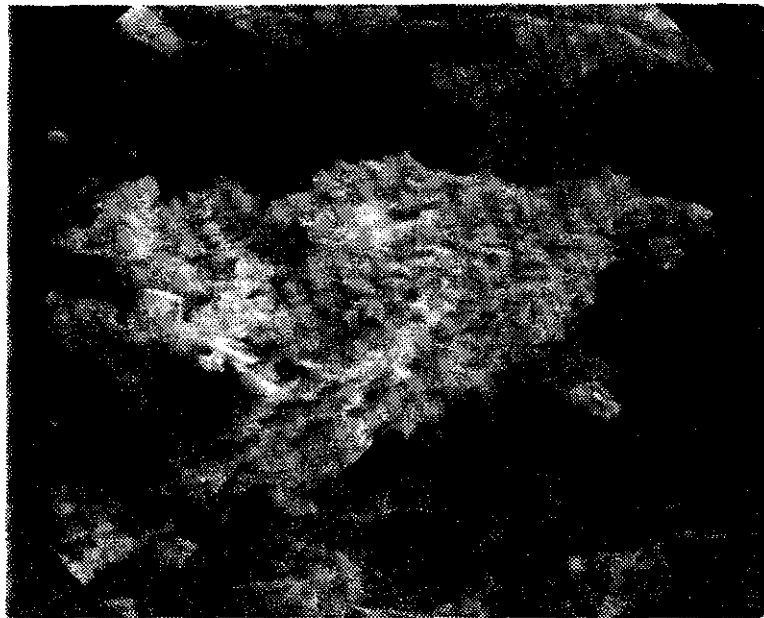
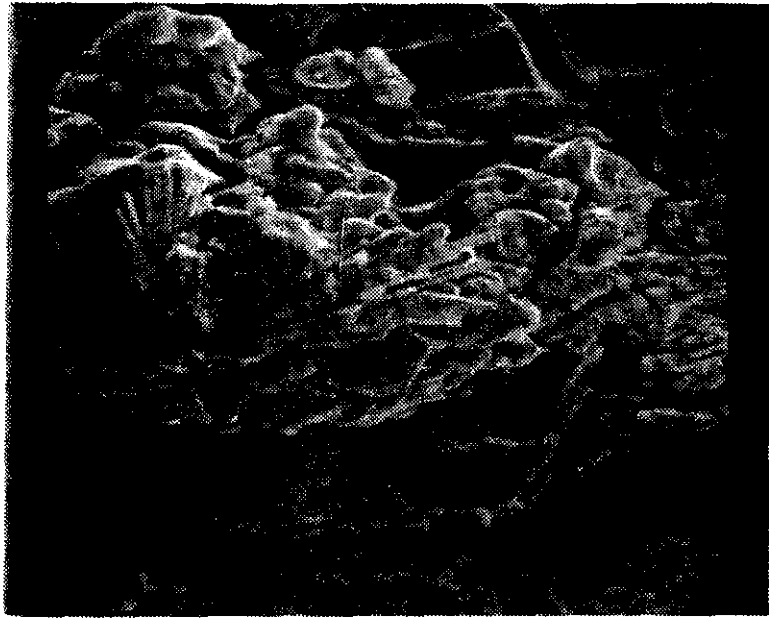


Figure 51. SEM (SEI) photograph of epigenetic barite crystals on lignite fracture surface (1000 X, 1 cm = 10 microns).

Figure 52. SEM (SEI) photograph showing celestite crystals (bright) on coal fracture surface (2000 X, 1 cm = 5 microns).



were usually evident on the calcite surfaces.

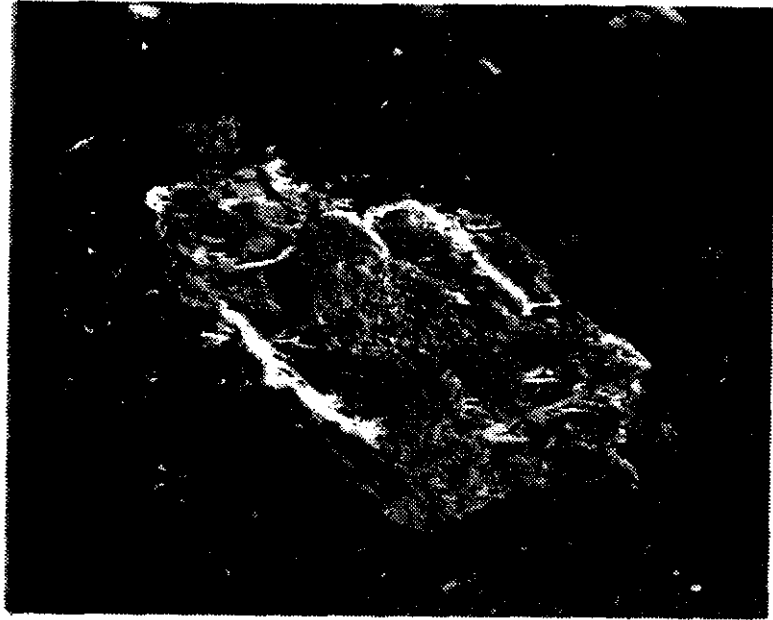
Dolomite was found only in parting or overburden samples as 60-70 micrometer subangular grains. Characteristic cleavage planes were usually noticeable. In one instance dolomite appeared to be replacing quartz in a detrital quartz grain (Figure 53).

Siderite did occur rarely as isolated 20 micrometer grains, but was more common at fracture surfaces exposed to atmospheric conditions. Several whole crystals were observed intergrown with gypsum crystals on fracture surfaces of lignite (Figure 54). In such cases, the siderite either precipitated at the same time as the gypsum or replaced the gypsum. The crystals are elongate in form, averaging 90 micrometers in length and have a rugged or rough surface texture.

Rutile(?) and Titanium Bearing Minerals. Titanium-bearing minerals and rutile(?) were only associated with detrital-rich lithologic layers such as silt-clay partings or lithologic layers lying adjacent to mineral rich partings. Rutile (or anatase) occurred as 5 to 10 micrometer subangular grains. They were highly weathered and appeared brighter relative to adjacent material because of the high atomic weight of titanium. Amorphous titanium compounds or extraneous titanium cations probably existed as very fine particles (< 1 micrometer) in some of the lithobodies that had high inorganic contents. This form was detected only by analyzing x-ray photon energies of coal

Figure 53. SEM (SEI) photograph of quartz and dolomite occurring together in single grain; smooth surfaced darker material is dolomite (500 X, 1 cm = 20 microns).

Figure 54. SEM (SEI) photograph showing siderite crystal (rough texture) protruding from gypsum crystal (360 X, 1 cm = 28 microns).



maceral matrix and no discrete particles were ever encountered.

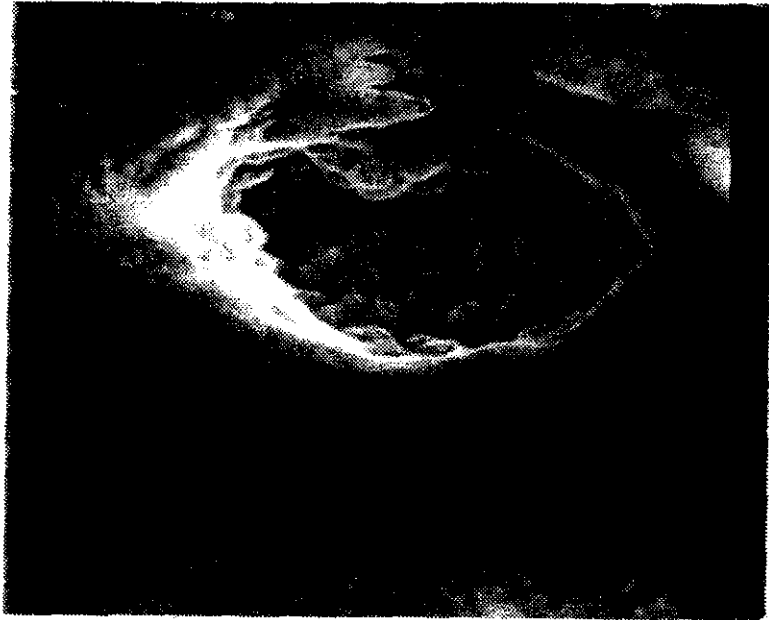
Phosphates or Phosphorus-Bearing Minerals. Unusual calcium-aluminum-phosphorus-bearing compounds were encountered in both the Blue and White pits. Most of this material could not be readily observed using SEM imaging, but was detected using the microprobe x-ray analyzer. Closures on the elemental analyses average to 30-40 percent. Although the chemical structure of this compound is not known for certain, for simplicities sake these compounds are categorized as phosphate-bearing minerals. Phosphates are not uncommon in coal and are very common in modern-day soils. Their presence in the Harmon lignite bed was unexpected but not incredible (Stach et al., 1982; Brown, 1978; Lindsay and Vlek, 1977).

The phosphates that were observed appeared as dull 6-20 micrometer patches or as individual 2-3 micrometer oval or subspherical particles (Figures 55). The surface texture of the individual "pellet-like" particles was very smooth. The delicate form of these particles may indicate an authigenic origin.

Muscovite, Biotite, and Feldspar. The minerals muscovite, biotite, and feldspar were only observed in parting or overburden lithologies. Muscovite occurred as elongate flakes, 15-50 microns long and 5-15 microns in width. Its form greatly resembled that of illite (Figure 56). Biotite, which resembled muscovite in form, was noted

Figure 55. SEM (SEI) photograph showing oval, pellet-like particles of calcium-aluminum-phosphate minerals in cavity of coal (1800 X, 1 cm = 6 microns).

Figure 56. SEM (SEI) photograph of muscovite flakes in center of photo (900 X, 1 cm = 13 microns).



as elongate flakes 50 by 15 microns in dimension. The biotite mineral grains appeared slightly more altered than the muscovite grains (Figure 57). Feldspar grains were observed as 20-40 micrometer subangular grains, similar in form to quartz.

Vermiculite, Chlorite, and Zircon. Vermiculite and chlorite were observed as very fine-grained particles less than 2 micrometers in size. These minerals, which were rarely encountered, were identifiable only by EDS analyzation. Zircon was encountered only once in the entire course of this study. The grain observed was 16 micrometers in diameter and subrounded in shape.

Organically Bound Inorganics. Inorganic constituents not only occurred as discrete minerals but also as organically bound elements. The primary scope of this report pertains to discrete mineral phases; however, some information was collected which involved organically bound inorganics. Table 8 provides a tentative or preliminary look at average compositional data for 40 lignite macerals analyzed in both the Blue and White pits. This data was obtained by a modified approach which shows relative concentrations of organically bound constituents using a standard ZAF correction procedure for minerals. In both pits the major organically bound elements are sodium, magnesium, sulfur, and calcium. Pearson correlation analysis of the oxide data from these macerals revealed that the following elemental oxide pairs form a

Figure 57. SEM (SEI) photograph of elongate strands of biotite as seen in a silt-clay parting (1100 X, 1 cm = 9 microns).

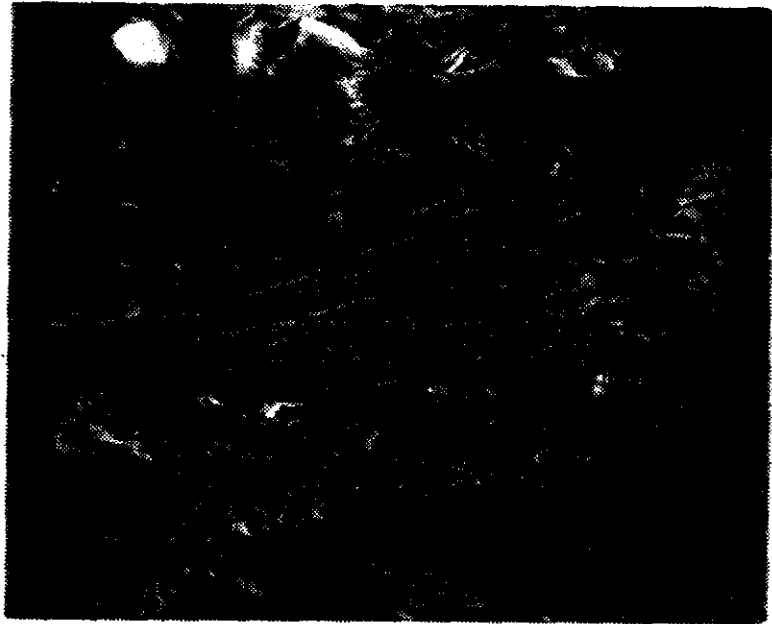


TABLE 8. Average compositions for lignite macerals in the Blue and White Pits. The values were calculated from a ZAF correction procedure and represent normalized weight percents of oxide components. The chemical data was collected from an EDS scan of one square micrometer of moisture-free coal.

Component	Blue Pit	White Pit
Na ₂ O	9.46	11.35
MgO	14.41	10.80
Al ₂ O ₃	5.27	9.05
SiO ₂	4.14	3.06
P ₂ O ₅	0.06	1.98
SO ₃	26.88	33.56
ClO	0.50	0.16
K ₂ O	0.25	0.25
CaO	36.61	28.14
TiO ₂	0.65	0.32
Fe ₂ O ₃	1.66	0.82
BaO	0.13	0.51

statistically valid correlation: 1) MgO and SO₃; 2) CaO and SO₃; and 3) (for just the White Pit) P₂O₅ and Al₂O₃.

The statistical correlations seem to agree with observations made throughout the course of the microprobe analysis. It was repeatedly observed that magnesium, calcium, and sulfur were the primary inorganic constituents in the coal organic matrix. In particular, numerous lithologic layers showed parallel high calcium and sulfur peaks on the spectral analysis.

INTERPRETATION OF DETRITAL AND AUTHIGENIC MINERALS

Textural relationships were used to determine the origin of the minerals (Table 9). Most of the quartz as well-sorted, subangular-subrounded coarse silt. The grains consistently increased in size and abundance closer to silty-clay partings. Several instances of rutilated quartz grain were observed in coal lithobodies and silt-clay partings. These characteristics are evidence for a detrital origin of the majority of the quartz observed in this study. Additional support for this conclusion is that, except for smaller sizes, quartz grains contained within coal lithobodies were fairly similar to those within silt-clay partings. The silt-clay partings are considered known detrital deposits. Only a few quartz grains had the appearance of being authigenic in origin.

It was much more difficult to designate an origin for the major clay minerals. Clay aggregates which formed bands, lenticular bodies, or layers were most likely detritally deposited. Other possible detrital occurrences were isolated subangular to subrounded silt-sized particles. These types of clay minerals also increased in abundance nearer to detrital silt-clay partings.

Clay particles that were observed as flakes or plates intimately associated with the coal, or as infillings of cell cavities and other maceral voids were labeled

TABLE 9. Origin of minerals.

<u>Detrital</u>	<u>Authigenic</u>
Quartz	Kaolinite
Kaolinite	Pyrite
Illite	Gypsum
Calcite	Barite
Dolomite	Celestite
Muscovite	Jarosite
Biotite	Calcite
Rutile	Dolomite
Titanium mineral	Phosphate mineral
Feldspar	Siderite
Chlorite	
Vermiculite	
Zircon	

authigenic.

Kaolinite was observed in equal degree as both authigenic and detrital. Several good examples of kaolinite infilling maceral voids were noted.

Illite was found to be primarily detrital in origin. The abundance of micas and feldspar in some of the silt-clay partings may suggest that the illite was an authigenic weathering product of originally detrital aluminosilicates.

Pyrite is considered to be mostly authigenic in origin. Certain diagnostic morphologies allowed pyrite to be classified as either syngenetic or epigenetic. Most of the pyrite occurred as framboids which appear in the early stages of coal development. Therefore, this form was categorized as syngenetic. Pyrite was also observed as massive bands and dendritic forms which filled coal pores and cavities and in some cases actually appeared to replace organic coal macerals. These characteristics are strong evidence for an epigenetic origin.

All of the gypsum encountered in hand specimens and microscopic sections was interpreted to be authigenic. The delicate crystalline nature of some of the gypsum was strong evidence for secondary authigenic origin. The fine gypsum particles, that were postulated to exist as submicron particles in the coal macerals, would also be authigenic products. These particles may represent an early stage of the inorganic precipitation of calcium sulfate.

Barite, celestite, and jarosite were all seen as

delicate secondary crystal growths on coal fractures surfaces or in coal cavities. Based on this observation, these minerals are most likely authigenic in origin.

Carbonate minerals can have a dual origin much the same as some of the clay minerals. Several examples of well-rounded silt sized (4-60 microns) calcite and dolomite grains were observed in silt-clay partings and inorganic rich coal lithobodies. These occurrences are characteristic of a detrital origin. In contrast these same minerals were viewed as crystalline overgrowths around quartz grains in fracture cavities, signifying a probable authigenic origin. Crystals of siderite were found intergrown with gypsum crystals suggesting strongly an authigenic origin for the few siderite crystals that were encountered.

Rutile(?) and titanium-bearing minerals were probably detrital in origin since they only occur in silt-clay partings or lithologic layers lying adjacent to mineral-rich partings. These particles may represent a heavy mineral fraction of sediment deposited in the peat bog or swamp during the peat stage of formation. An alternative origin may be that they are weathered remnants of some other originally detrital titanium mineral.

The phosphate minerals occurred as fine delicate particles with smooth surfaces and either oval or spherical shapes. Several of these particles were seen lining the inside of cavities in the coal. The origin of these minerals, therefore, is most likely authigenic.

Muscovite, biotite, and feldspar were only observed as discrete subangular grains in parting or overburden lithologies. These minerals may have originated as detrital silt deposits.

Vermiculite and chlorite were classified as detrital in origin. They were only observed in detrital silt-clay deposits and overburden, and are either detrital particles or alteration products of detrital particles. The one grain of zircon that was detected was probably detrital in origin. This conclusion was based on the particles subrounded shape and knowledge of zircon as a common heavy mineral constituent in sedimentary environments.

In summary, textural relationships of the minerals in the Harmon lignite allowed for their classification as either detrital or authigenic (Table 9).

Formation of Detrital Minerals

At this stage of the report, some important questions can be answered regarding how mineral matter was emplaced in the coal and what are some of the controlling factors for their occurrence. It was essential to separate first, even if only in a speculative sense, detrital minerals from authigenic minerals because of the contrast in these two processes of mineral genesis.

The three most abundant minerals of the Harmon lignite at Gascoyne were quartz, illite, and kaolinite. They totalled 88% of the mineral matter by weight. It was

determined that these minerals were primarily detrital in origin. This result leads to the conclusion that the majority of the ash component in the Gascoyne lignite was emplaced in the coal by detrital deposition. Additional support for this deduction was found in the occurrence of the minerals and their distribution. Detrital quartz and clays were commonly associated with detrital macerals such as inertodetrinite and liptodetrinite. The sizes of the detrital minerals were mostly in the silt ranges and varied as would be expected in a depositional environment in which there were fluctuations of the energy of transport and deposition.

Quartz and clays were consistently more abundant in lithobodies adjacent to inorganic-rich lithobodies such as silt-clay partings and overburden. Such a distribution can be explained by a low energy peat or swamp environment which is transgressed by a higher energy environment such as flood waters of a fluvial or lacustrine environment. The relatively mineral poor plant accumulations would gradually receive a greater influx of mineral matter until the energy of the inundating waters would be great enough to deposit a continuous blanket of fine-grained sediments. The actual flooding might take place gradually or even in pulses, and the waters might recede in the same way. If the flood waters recede fairly quickly, then normal deposition of plant materials would bury the silt layer, which, after compaction and coalification, would become a mineral

parting.

In summary, the environment of deposition of the Harmon lignite was the major controlling factor for the present mineral composition. Cecil and others (1982) came to a similar conclusion in their study of higher rank coals. They noticed that processes acting during peat stages of formation, most greatly affected the eventual mineral content. Those processes, however, were not limited to detrital depositional processes but also included authigenic mineral formation and alteration of existing minerals.

Early Stage Authigenic Formation

Some mineral species of the Harmon lignite were interpreted as having been emplaced through authigenic processes during the early peat stage. Pyrite was most likely a product of early stage authigenic formation. Recent studies (Cohen et al., 1984; Altschuler et al., 1983) have shown that pyrite begins forming syngenetically as small framboids during the peat stage of coal formation. The controlling factor for the framboidal pyrite observed in the Harmon lignite was probably the chemistry of the interstitial waters.

Optimum conditions for pyrite formation consist of a near neutral pH (pH=7), anaerobic environment, and sufficient source of sulfur and iron. These conditions allow for sulfate reducing bacteria to remain active creating sufficient concentrations of sulfate ions to

combine with iron ions in solution. High acidity, or low pH, in the interstitial waters inhibits the activity of sulfate reducing bacteria and also causes leaching of minerals (Cecil et al., 1982; Cecil et al., 1978). Thus, pH may be the controlling factor for framboidal pyrite observed in the coal.

Some of the kaolinite may also have been a product of early stage authigenic formation. Kaolinite formation is favored in low temperature and low pressure acidic environments (Deer et al., 1962), but is also commonly a product of weathering and transportation.

The phosphate minerals may also have formed during early peat stages. They may have been organically derived from the degrading plants. Phosphate minerals are common in modern day soils.

Late-Stage or Post-Compaction Authigenic Formation

Several mineral species clearly formed during late stages of the coalification process or after compaction and consolidation of the seam were complete. Pyrite is an obvious example. Pyrite occurs as crystallites in veins which follow fractures and cavities in already compacted and coalified lignite. Solutions rich in iron sulfides derived from dissolved framboids, may have circulated through the coal, depositing the massive pyrite in available spaces. This type of pyrite was referred to earlier as epigenetic pyrite.

Gypsum, barite, celestite, siderite, and jarosite were formed during this stage of Harmon lignite development. Delicate crystal forms lining coal cavities and fractures were evidence for a post-compaction/consolidation formation of these minerals.

Again, the controlling factor for the formation of the above minerals was probably the nature of the interstitial solutions. The elements were already available, bound within an existing mineral phase or within the organic structure of the coal.

ENVIRONMENT OF DEPOSITION

The nature of the mineral matter in the Harmon lignite provides evidence for the depositional environment of the coal. Observations from this study give support for an extensive quiet-water swamp facies. The swamp facies was extensive in lateral dimensions and may have been part of a shallow lacustrine environment. A lacustrine environment was chosen instead of a marine because no chloride minerals and very few carbonate minerals were identified.

Inundations and regressions of a freshwater body appear to have greatly influenced the mineralogy the Harmon lignite. For the most part, the coal lithobodies were sparse in minerals. Mineral grains are more abundant nearer silt-clay partings which were probably the result of moderately rapid inundations. The swamp facies also appears to have been subjected to periods or episodes of drying, after regression. It was shown earlier that fusain quantities were greater at the tops of some of the seams. This is usually indicative of a drying out of the swamp environment (Kleesattel, 1985). In short, the Harmon silt-clay partings indicate rapid fluctuations of water levels. This observation, coupled with the laterally extensive lignite deposits, depicts a very low relief and low energy depositional environment.

The average size and distribution of the major detrital

minerals also supports a low energy lacustrine environment (Table 10). Quartz, illite, and kaolinite were dominantly detrital fine silt, probably transported into the swamp by circulating waters. Wind may also have carried some of the silt to the swamp. Periods of transgressions gave rise to higher concentrations of detrital minerals. In the lignite bed this was noticed by the increase in mineral matter in lithologic layers adjacent to clay partings. Mineral partings represent a complete inundation of the swamp by the transgressing lacustrine waters.

TABLE 10. Average sizes of major minerals
in the Gascoyne White and Blue Pits.
(Average diameter in micrometers)

Lithotype	Quartz	Pyrite	Kaolinite	Gypsum	Illite
Blue Pit					
GBO-1	65	90	--	--	--
GBA-5	194	--	140	87	50
GBA-4	17	74	11	--	17
GBA-3	38	19	57	32	--
GBA-2	23	15	15	--	--
GBA-1	46	31	23	--	--
GBP-4	18	--	10	--	--
GBB-4	29	100	27	--	--
GBB-3	39	--	22	--	--
GBB-2	38	23	103	--	--
GBB-1	64	45	26	--	36
GBP-3	19	--	--	--	13
GBP-2	89	--	47	--	--
GBP-1	500	--	600	--	--
GBC-3	41	--	136	--	5
GBC-2	25	700	109	--	--
GBC-1	25	160	227	125	--
*Av. Coal	44	130	68	81	24
**Av. All	75	130	104	81	24
White Pit					
GWA-3	75	30	51	--	30
GWA-2	41	34	25	--	--
GWA-1	73	45	--	100	74
GWB-5	48	23	73	--	--
GWB-4	34	35	34	--	--
GWB-3	33	29	61	--	45
GWB-2	10	110	95	500	--
GWB-1	44	24	20	25	--
GWP-1	18	20	45	--	3
GWC-4	45	83	15	--	--
GWC-3	--	59	213	--	--
GWC-2	46	55	44	--	--
GWC-1	38	--	30	--	--
*Av. Coal	40	46	60	208	38
**Av. All	40	46	60	208	38
Total av. for both pits	42	88	64	145	31

*Average for all of the lithologic layers which are pure coal;
silt-clay partings are excluded.

**Average for all of the lithologic layers.

APPLICATION TO UTILIZATION

A key parameter in characterizing lignite for purposes of utilization is the ash content and composition. Methods of characterization in the past relied mostly on a simple weight percent of total ash for the coal. This method gave no indication of what minerals were present. The SEM/EMPA system used in this study proved to be an effective means of characterizing coal in more detailed fashion. Knowing the quantities and types of minerals present in a coal can be an aid in discerning combustion characteristics. Another important advantage of the SEM/EMPA system is that mineral associations within a single coal particle can be determined.

The distribution of the minerals in the Gascoyne mine may be helpful in explaining the variable ash deposition properties of coal within the mine. It was shown earlier that the Blue and White pit lignites are notably different in ash deposition behavior and mineral composition. The difference in mineral composition is primarily the amount of quartz and clay minerals in the middle "B" seam. In similar fashion, the ash deposition variability may be related to the mineral composition, since the other characteristics of the two coals are fairly similar.

Knowledge of the vertical distribution of mineral matter at Gascoyne also proves to be useful. Distinct

lithologic layers had unique mineral compositions. Several lithobodies in both pits had very high mineral contents and yet are mined and mixed with the cleaner coal lithobodies. If economically feasible and efficient, such layers, rich in inorganics, could be avoided during mining operations.

Of additional interest to coal applications, is the problem of sodium. No important sodium-bearing minerals were identified. Thus, any problems with sodium fouling during combustion of the coal studied must be due to organically bound sodium in the Harmon lignite.

CONCLUSIONS

1. The scanning electron microscope/microprobe system (SEM/EMPA) is an effective tool in determining the identity, quantity, and origin of discrete mineral phases in coal. SEM/EMPA methods developed in this study provide an alternative to x-ray diffraction for the study of minerals in coal.
2. The most abundant minerals identified in the Harmon bed lithobodies, in order of decreasing abundance are: quartz, illite, kaolinite, montmorillonite, pyrite, gypsum, and barite. Quartz, illite, and kaolinite comprise 88% of the total mineral matter. Other minerals that were encountered only in trace amounts are: siderite, rutile(?), jarosite, dolomite, calcite, feldspar, muscovite, biotite, and chlorite. Unknown mineral phases that were observed are titanium-bearing minerals and phosphate minerals.
3. Study of lithologic layers or lithobodies is an effective means of subdividing the Harmon lignite for the purpose of megascopic and microscopic observation of stratigraphic units. The Harmon lithobodies have varying mineral contents. In vertical distribution, quartz and clay minerals are more abundant in lithologic layers that lie adjacent to clay-silt

partings, overburden, and underclay. Middle portions of the 3 seams in the White and Blue pits have lower mineral concentrations. In lateral distribution, there are variations in inorganic contents between the Blue and White pits. This variation is primarily due to differences in the amounts of quartz and clay in the B seam.

4. Observed associations between specific minerals and macerals are as follows: 1) pyrite (corpohuminite, ulminite, micrinite); 2) quartz (inertodetrinite); 3) clay minerals (liptinite, corpohuminite, ulminite, sporinite, resinite, inertodetrinite, fusinite). The Blue Pit has higher amounts of detrital macerals (inertodetrinite and liptodetrinite) and detrital minerals (quartz and clays) than the White Pit.

5. Lithologic layers with high ash concentrations also have higher concentrations of discrete mineral phases. The three most abundant minerals in the Gascoyne lignite, quartz, illite, and kaolinite, are primarily detrital in origin. These results infer that the controlling factor for the present mineral content of the Harmon lignite was probably depositional environment.

6. Authigenic processes during early peat formation, late coalification, and after compaction contributed in a minor yet significant fashion to the mineral content. Framboidal pyrite and possibly some kaolinite and phosphate minerals formed authigenically during early peat stages. Massive pyrite, gypsum, barite, celestite, siderite, and jarosite were the products processes occurring during late coalification or after seam compaction and consolidation.

7. Judging from its mineralogic content, the Harmon lignite was probably deposited as part of a lacustrine depositional environment. Periodic transgression and regression of the freshwater body would explain best the types of minerals observed and their distributions.

8. SEM/EMPA techniques are a useful method of characterizing the mineral content of coal. This method can detect variations in mineral content which are not normally observed using other standard methods of characterization such as proximate/ultimate analysis. Selective mining could be done to exclude lithobodies having large amounts of problem-causing minerals. Variations in ash deposition behavior between the White and Blue pits may be caused by the variation in types and quantities of mineral phases.

FUTURE RESEARCH

Future research should be undertaken to improve the SEM/EMPA technique for identifying and quantifying minerals in coal. The system could be improved so that mineral grains can be sized and identified automatically.

More work is needed in examining the association between minerals and macerals in lignite. This may help answer questions regarding the affect of the coalification process on mineral content, and also provide more evidence for interpreting depositional environments.

Finally, more research is needed to understand the associations that exist between minerals within a single coal particle. This information would be useful when applied to the study of ash fusion.

APPENDICES

APPENDIX A
MACERAL POINT COUNT DATA

Maceral Point Count Data

The data reported here were collected using standard point counting techniques (Stach et al., 1982), and reflected light microscopy. Detailed descriptions of these analyses are given in the discussion of macerals in this report. The abbreviations used in this appendix are as follows:

U = Ulminite
A = Attrinite
D = Desinite
G = Gelinite
CO = Corpohuminite

SP = Sporinite
CU = Cutinite
R = Resinite
SB = Suberinite
AL = Alginite
EX = Exsudatinite
BI = Bituminite
L = Liptodetrinite

F = Fusinite
SE = Semifusinite
M = Macrinite
SC = Sclerotinite
I = Inertodetrinite
IN = Inorganics (minerals)

tr = trace amount (<1%)
HT = Height above base of seam (in meters)

MACERAL DATA FROM THE BLUE PIT

Label	U	A	D	G	CO	SP	CU	R	SB	AL	EX	BI	L	F	SE	MA	MI	SC	I	IN
GBB-4	22.2	12.4	4.6	0.2	2	7	0	3.4	0	0.6	0	0.2	7.4	5.8	4.6	0.4	0	0.2	20.4	8.6
GBB-3	25	15.6	5.4	1	1.4	7.8	1.2	2.4	1.2	1.2	0	1.2	7.2	5.8	2.4	0.6	0.2	0.6	15	4.8
GBB-2	44.4	25	9.2	1.8	1.6	2.8	1	0.8	0	0.8	0.6	2	5.8	0.2	0.8	0	0	0.4	0.8	2
GBB-1	26.8	14	4.4	1.6	0.8	8.4	1.8	3.8	0	0.6	0	1.2	8.2	2.8	1	0.2	0.2	0.2	11	13
GBC-3	28.6	4.6	3.6	1.2	2	1.4	0.8	1.2	0	0	0.4	0.4	2	11	9.6	0.2	0.6	0.8	30.2	1.4
GBC-2	69	8	2.4	2.4	7.4	0.4	0	1	0.4	0.4	0	0.4	2.4	0.2	1.2	0	1.6	0.6	0.2	2
GBC-1	30.4	24	7.8	1.2	1.2	4.8	1.6	2.4	0	1.6	0	1	11	1.2	0.8	0	0	0.6	5.4	4
GBA-5	35.2	20	23.4	0.8	1.6	4	0	1.4	0	0.2	0	0	3.4	1.8	2.2	0.4	0	0.8	3.4	1.4
GBA-4	53	10.4	11.8	0.6	8	1	0.6	1.6	0	0	0	0	2.6	3	2	0.2	0.8	0.4	2.2	1.2
GBA-3	42.6	14	15.8	0.6	4.8	4.6	0.6	1.4	0.2	1	0	0	4.4	1.2	3.4	0.2	0	0.4	1.2	3.6
GBA-2	40.6	16.4	5	0.4	6	5.6	0.2	2.6	0	0.8	0	0.8	4.4	5.8	1.6	0.6	0	0.8	3.8	3.2
GBA-1	40.2	15.6	5.8	0.4	3.2	3.4	0	1.4	0	0	0	1.2	8	4.4	0.8	0	0	0.2	10.8	4.6

MACERAL DATA FROM THE WHITE PIT

Label	U	A	D	G	CO	SP	CU	R	SB	AI	EX	BI	L	F	SE	MA	MI	SC	I	IN
GWA-3	47	9.8	7.6	1.6	4	1.2	0.2	1.2	0	2.6	0.8	1.6	5.2	2.6	3.4	0.8	0.6	0.4	7.6	1.8
GWA-2	44	11.6	19.2	2.6	1.8	3	0.8	1.4	0	2.2	0.6	1.4	5.4	0.8	1.8	0	0	0.8	1.8	0.8
GWA-1	44.2	11.2	12.6	2.4	6.4	2.8	1	0.8	0	1	0.6	1.4	5.6	0.6	4.2	0	0	0.8	2.2	2.2
GWB-5	31.8	15	14	2.4	1.6	3.2	0	2.2	0.6	2.6	0	2.2	5.2	4.2	2.2	0.2	1	0.4	9.2	2
GWB-4	23.4	27.8	13	1.8	0.6	7.6	0.4	3.6	0.2	2	0.4	1.2	4.2	0.4	1	0	0.2	0.4	8.6	3.2
GWB-3	45.4	16.2	5.6	1.4	0.8	3.4	0	1	0.2	3.2	0	3.2	3.6	2.8	2	0.4	0.2	0.6	5.8	4.2
GWB-2	43.4	20.4	14.2	3.4	2	1	0	2.2	0.4	0.6	0	1	2.2	0	1	0	1	0.2	0.4	5.6
GWB-1	42.8	14.4	19	1.2	3	1.2	0.8	1	0	0.8	0	3	3.2	0.8	1.8	0	3	0.4	1.4	2.2
GWP-1	16.8	6.6	3.6	0.8	2.2	7.2	0.2	2.2	0	1.2	0	1	2.4	4.4	0.6	0.2	0	0	10.8	39.8
GWC-4	15.6	19.6	9.4	0.6	1.4	2.2	0.6	2.4	0.6	1	1	1	4.6	1.8	0.8	0.2	0.4	0	15	21.8
GWC-3	50.6	13.8	11.8	1.2	5	1.6	0	2.8	0.6	1	0	1	3.2	0.2	2.2	0	1	0.4	1.8	1.8
GWC-2	39.4	20.4	16.6	1.4	2.2	4.2	0.4	1.8	0.6	1.2	0	1.8	2.2	1	2.2	0	0.8	0.6	1	1.8
GWC-1	17.2	18.2	12	1.8	1.8	1.6	0	1	0.6	1.4	0	1.4	3	6.8	3.6	2.4	1	0.8	23.2	2.2

APPENDIX B
SEM/EMPA SAMPLE DESCRIPTIONS

SEM/EMPA Sample Descriptions

These descriptions of the discernable lithologic units of the Harmon lignite bed were compiled from hand specimen and SEM/EMPA examination. Only the lithobodies from the White and Blue pits are described in this appendix. The information pertains to the character of the minerals and organic matrix. Each unit is listed by its position relative to the base of the seam. The abbreviations used in this appendix are as follows:

G = Gascoyne
B = Blue Pit
W = White Pit
A = A-seam
B = B-seam
C = C-seam

Gascoyne Mine Blue Pit, C and B Seams
Located at the Northwest End of the Pit

Sample I.D.: GBC-1

Height: 0-.5m

Description:

Quartz (1.99%): Subangular detrital grains; 20-30 microns in diameter.

Kaolinite (3.45%): Large aggregates up to 500 microns in diameter.

Gypsum (.72%): Unusually large 100-150 micron grains.

Pyrite and Iron Sulfide (.98%): Massive pyrite forms; also very fine iron sulfate particles.

Comments: Trace amounts of titanium minerals and illite present; high sulfur and calcium coal organic matrix, massive pyrite forms seen in hand specimens yet only trace amounts found in microprobe.

Sample I.D.: GBC-2

Height: .5-1.43 m

Description:

Quartz (.80%): Subangular 20-30 micron grains.

Pyrite (trace): Small isolated framboids and one massive pyrite form.

Kaolinite (.80%): Patchy aggregates 100-110 microns diameter; also fine particles dispersed through coal.

Barite (1.36%): Large 300 micron particle made up of small framboid-like particles or grains.

Comments: Sparse in mineral matter and high in anthraxylon content.

Sample I.D.: GBC-3

Height: 1.43-1.60 m

Description:

Quartz (1.57%): Angular-subangular grains 20-30 microns diameter; rugged and pitted appearance.

Kaolinite (1.96%): Aggregates seen infilling fusinite pores, dull, large particles common.

Illite (.41%): 5 micron particles, finely

disseminated. Ca-Al-Phosphate (2.51%): Very dull, fine 4 micron particles finely disseminated.

Sample I.D.: GBP-1
 Height: 1.60-1.71 m
 Description:

Quartz (75.95%): Rutilated quartz common, some clay coatings evident, well-rounded; 500-600 microns grains, smooth surface.
 Kaolinite (.96%): Large detrital aggregates.
 Titanium mineral (1.28%): Possibly a mix of quartz and rutile.
 Rutile (1.59%): Small grains often associated with quartz.
 Comments: Mostly detrital silt-sized quartz, large amount of organic matter.

Sample I.D.: GBP-2
 Height: 1.71-1.81 m
 Description:

Quartz (7.54%): 100 micron grains, clay coatings.
 Kaolinite (5.55%): 10-20 micron grains; dispersed; some grains 90-100 microns.
 Illite (1.23%): Small dispersed detrital grains.
 Comments: High calcium maceral, silty coal grains.

Sample I.D.: GBP-3
 Height: 1.81-1.92 m.
 Description:

Quartz (40.12%): Clay coating on 20-50 micron grains; passible calcite coatings.
 Illite (20.10%): Finely dispersed, 10-15 micron grains.
 Comments: Abundance of large clay-silt grains .1-.4 mm in diameter; high calcium coal, tan-brown color in hand specimen, with visible ancient rootlets or branches.

Sample I.D.: GBB-1
 Height: 1.92-2.2 m
 Description:

Quartz (10.24%): Various sized grains 30-110 microns, subangular-subrounded grains; tiny 1-5 micron grains common.
 Kaolinite (3.29%): Rounded blebs or aggregates, 15-40 microns.
 Illite (1.33%): Small dispersed grains, 3-20 microns.
 Comments: Calcium-rich macerals commons, possibly

finely dispersed gypsum crystals. Gray lenticular clay bands visible in hand specimen.

Sample I.D.: GBB-2

Height: 2.2-2.81 m

Description:

Quartz (.37%): 10-70 micron rounded-subangular grains.

Pyrite (.70%): Tiny framboids, 20-50 microns diameter.

Kaolinite (.74%): Rounded aggregates 20-150 microns.

Comments: High sulfur and calcium coal, very hard in hand specimen with abundant massive woody vitrain.

Sample I.D.: GBB-3

Height: 2.81-4.18 m

Description:

Quartz (2.85%): 20-50 micron subrounded grains, smooth surface texture.

Kaolinite (2.03%): 10-60 micron isolated grains; layerings of platelets visible.

Gypsum (.36%): Occurs with Kaolinite commonly; 60 micron grains.

Zircon: 30 micron subrounded detrital grain.

Comments: Very strong calcium component in macerals.

Sample I.D.: GBB-4

Height: 4.18-4.68

Description:

Quartz (7.22%): Rounded-subangular 20-30 micron grains.

Pyrite (trace): Trace 100 micron grain.

Kaolinite (5.7%): Platelet stackings observed on 10-20 micron grains; angular grain common.

Comments: Pyrite from plant cell walls or cell fillings; high calcium coal; gray colored bands noted in hand specimen.

Sample I.D.: GBP-4

Height: 4.68-4.78 m Parting between B and A seams

Description:

Quartz (23.90%): Well-rounded, 20 micron grains.

Illite (54.83%): Massive patches 40-100 microns diameter.

Muscovite (5.59%): Flakes 40-60 microns long and 5-10 microns wide.

Comments: In hand specimen appears as white-gray silty clay, brown plant fragments abundant, iron-stained; iron coatings on coal grains noted in SEM.

Gascoyne Blue Pit, A Seam
Located at the East End of the Pit

Sample I.D.: GBA-1

Height: 0-.19 m

Description:

Quartz (3.01%): Subangular-well-rounded grains, 15-40 microns diameter, some 50-100 micron grains observed.

Pyrite (.81%): Framboids 10-30 microns, some replacement of plant cell structure.

Montmorillonite (.41%): Rounded dull grains 30-40 microns.

Kaolinite (trace): Stacked platelets visible in grains.

Comments: Abundant fusain as distinct layers.

Sample I.D.: GBA-2

Height: .19-.59 m

Description:

Quartz (.46%): Subangular-well-rounded 20-30 micron grains, some 50-100 micron grains.

Kaolinite (1.85%): Small particles 2-10 microns and large dull particles 50-60 microns; swirling deformed Kaolinite stackings observed.

Montmorillonite (1.31%): Rounded grains 20-40 microns.

Comments: Quartz and kaolinite found together in same grain in a few cases.

Sample I.D.: GBA-3

Height: .59-1.10 m

Description:

Quartz (.43%): Angular grains 10-60 microns.

Kaolinite (.43%): Dull grains 50-60 microns diameter, grains are aggregates of smaller particles in platelets.

Pyrite (6.17%): Framboids very abundant, 20-50 diameter.

Gypsum (.41%): Several 30-40 micron grains.

Comments: Pyrite seen several times rimming quartz and kaolinite grains, calcite detected as .91% mineral content.

Sample I.D.: GBA-4

Height: 1.10-1.55 m

Description:

Quartz (1.46%): Angular-rounded 10-25 micron grains.
 Kaolinite (.49%): 10-20 micron grains.
 Illite (.51%): 10-25 micron subrounded grains.
 Comments: Traces of tiny calcite grains, very mineral-sparse overall, high vitrain content.

Sample I.D.: GBA-5
 Height: 1.55-1.85 m
 Description:

Quartz (.79%): Larger 100-200 micron subangular-subrounded detrital grains.
 Gypsum (.70%): 60-100 micron isolated grains.
 Illite (1.44%): Larger detrital grains 140 microns, subrounded.
 Calcite (.42%): Isolated 40-50 micron grains.
 Comments: Pyrite encrusted on some quartz grains, traces of pyrite, kaolinite, dolomite (75 micron grains) identified.

Sample I.D.: GBO-1
 Height: 1.85 + Overburden
 Description:

Quartz (38.77%): Detrital subrounded grains averaging 60 micron diameter.
 Illite (26.47%): 50-100 micron detrital grains.
 Biotite (6.35%): Elongate laths 10-20 microns wide by 100 microns long.
 Comments: Clays (kaolinite, montmorillonite, illite, etc.) have varied sizes from less than one micron to aggregates greater than 200 microns. Calcite and dolomite detrital angular grains, 50-100 microns diameter.

Gascoyne White Pit, C Seam
Located at North End of Pit

Sample I.D.: GWC-1

Height: 0-1.31 m

Description:

Quartz (.38%): Subangular-subrounded grains 10-70 microns diameter.

Kaolinite (1.91%): Varied sizes, 10-100 micron grains, detrital appearance.

Comments: Minerals very sparse and dispersed, fairly high vitrain content.

Sample I.D.: GWC-2

Height: 1.31-1.97 m

Description:

Quartz (.97%): Detrital grains 20-40 microns, several larger 100 micron grains.

Pyrite (trace): Several isolated 30-80 micron framboids.

Kaolinite (3.11%): Mostly 50-80 micron aggregates of 1-5 micron particles.

Comments: Isolated barite, gypsum, and dolomite grains seen, very low vitrain content of coal.

Sample I.D.: GWC-3

Height: 1.97-2.4 m

Description:

Quartz (.40%): Subrounded 20 micron grains.

Pyrite (1.13%): Framboids 25-40 microns diameter, massive patches 120 microns.

Kaolinite (2.79%): Patches or areas of authigenic infilling of maceral structure and bedding plane structures, also isolated 60 micron rounded grains.

Comments: sparse in minerals, high sulfur coal, phosphates present.

Sample I.D.: GWC-4

Height: 2.40-3.02 m

Description:

Quartz (10.17%): Detrital grains 40-100 microns diameter, well-rounded.

Pyrite (.71%): Framboids often associated with quartz and kaolinite.

Kaolinite (3.01%): Infillings of cellular or maceral structures, also 10 micron small rounded grains.

Comments: Calcium aluminum phosphates present as

fine disseminated material, pyrite seen encircling quartz grains.

Sample I.D.: GWP-1

Height: 3.02-3.11 m

Description:

Quartz (28.81%): Subangular-subrounded grains, 15-20 microns diameter.

Kaolinite (2.03%): Rounded 20-40 micron aggregates.

Pyrite (trace): Framboids 20 microns diameter.

Illite (18.95%): Tiny 5 micron laths.

Ti-minerals (2.26%): Possibly rutile and unknown titanium minerals as .5-10 micron particles.

Gascoyne White Pit, A and B Seams
Located at the South End of the Pit

Sample I.D.: GWB-1

Height: 0-.46 m

Description:

Quartz (.81%): Angular 44 micron grains.
Pyrite (.77%): Dispersed 10-40 micron framboids.
Kaolinite (2.83%): Evenly dispersed rounded grains,
mostly 10-20 micron diameter, some 1-10 microns.
Gypsum (trace): 30 micron crystals.

Sample I.D.: GWB-2

Height: .46-1.15 m

Description:

Quartz (.41%): Small 10 micron grains.
Pyrite (3.89%): Massive epigenetic pyrite, some
seen replacing coal, framboids less common as
100-120 micron aggregates.
Kaolinite (trace): 120 micron aggregate, vermicular
stacking of platelets in particles.
Jarosite (.40%): Tiny 5-20 micron flakes.

Sample I.D.: GWB-3

Height: 1.15-2.04 m

Description:

Quartz (.81%): Mostly angular grains 20-75 microns
diameter.
Pyrite (trace): Some pore fillings.
Kaolinite (.41%): Dispersed 15-40 micron rounded
grains.
Illite (1.26%): Strands 80 microns long 1-5 microns
long.
Comments: Some microcrystalline quartz noted.

Sample I.D.: GWB-4

Height: 2.04-2.79 m

Description:

Quartz (1.55%): Angular-subrounded grains, 20-25
microns.
Kaolinite (.39%): 20-60 micron isolated rounded
grains.
Pyrite (trace): 30-40 micron framboids.
Gypsum (.34%): Less than 5 micron grains, some
nearly invisible.

Sample I.D.: GWB-5
 Height: 2.79-4.01 m
 Description:

Quartz (2.0%): Angular-subrounded 25 micron grains, some grains 60-110 microns.
 Pyrite (.76%): Framboids 15-80 microns.
 Kaolinite (.40%): Rounded aggregates 30-120 microns.
 Illite (.41%): Finely disseminated grains.

Sample I.D.: GWA-1
 Height: 4.01-4.76 m
 Description:

Quartz (1.57%): Detrital grains 60-100 microns.
 Pyrite (.75%): Scattered isolated framboids, 50 micron diameter.
 Illite (1.23%): Angular-subrounded grains mostly 40-50 microns, some 60-100 micron grains.
 Comments: Illite seen wrapped around coal particles.

Sample I.D.: GWA-2
 Height: 4.76-5.76 m
 Description:

Quartz (1.22%): Subrounded-subangular grains mostly 25-35 microns, some 100 micron grains.
 Pyrite (trace): Framboids common, 20-45 micron diameter.
 Comments: Unusually sparse in minerals (1.22%). Minerals that are present are very tiny in size.

Sample I.D.: GWA-3
 Height: 5.76-6.25 m
 Description:

Quartz (1.99%): Average diameter of 42 microns, subangular-rounded grains.
 Pyrite (trace): Near spherical framboids, 20 microns.
 Kaolinite (.40%): Subrounded 70-100 micron aggregates and 20 micron laths.
 Illite (1.85%): Laths 10-50 microns diameter.
 Titanium mineral (.49%): Near invisible particles.

REFERENCES CITED

- Akers, D.J., McMillon, B.G., and Leonard, J.W., 1978, Coal minerals bibliography: U.S. Department of Energy, Fossil Energy Research, Report FE-2692-5, 222 p.
- Altschuler, Z.S., Schnepfe, M.M., Silber, C.C., and Simon, F.O., 1983, Sulfur diagenesis in Everglades peat and origin of pyrite in coal: *Science*, v. 221, no. 4607, p. 221-227.
- Annual Book of ASTM Standards, 1983a, Gaseous fuels: coal and coke: Section 5, v. 05.5, D 3172-73 (1979), Proximate analysis of coal and coke, p. 394.
- Annual Book ASTM Standards, 1983b, Gaseous fuels: coal and coke: Section 5, v. 05.5, D 3176-74 (1979), Ultimate analysis of coal and coke, p. 406-409.
- Annual Book of ASTM Standards, 1980, Gaseous fuels: coal and coke: Part 26, D 2797-72 (1980), Preparing coal samples for microscopical analysis by reflected light, p. 363-371.
- Annual Book of ASTM Standards, 1979a, Gaseous fuels: coal and coke: Part 26, D 2797-72, Preparing coal samples for microscopical analysis by reflected light, p. 350-362, D 3174-73, Ash in the analysis sample of coal and coke, p. 373-374.
- Augustyn, D., Iley, M., and Marsh, H., 1976, Optical and scanning electron microscope study of brown coals: *Fuel*, v. 65, no. 1, p. 25-38.
- Ball, C.G., 1936, Possible relations of mineral matter in coal to the time of coalification: *Illinois State Acad. Sci. Trans.*, 28, 181.
- Ball, C.G., 1935, Mineral matter of No. 6 bed coal at West Frankfort, Franklin County, Illinois: *Illinois Geological Survey, Report of Investigation*, no. 33, 106 p.
- Benson, S.A., Kleesattel, D.R., and Schobert, H.H., 1984, Selection and characterization of low-rank coal samples: *ACS Div. Fuel Chem. Preprints*, v. 29, no. 1, pp. 108-113.

- Benson, S.A., Zygarlicke, C.J., and Karner, F.R., 1984, Occurrence of detrital, authigenic and adsorbed inorganic constituents in lignite from the Beulah Mine, North Dakota: Proceedings: Symposium on the geology of Rocky Mountain coal: North Dakota Geological Society Publication 84-1, p. 12-27.
- Benson, W.E., 1952, Geology of the Knife River area, North Dakota: U.S. Geol. Surv. Open File Report, 323 p.
- Boenteng, D.A.D., and Phillips, C.R., 1976, Examination of coal surfaces by microscopy and the electron microscope: Fuel, v. 55, no. 4, p. 318-322.
- Brown, J.L., 1978, Precipitation of calcium orthophosphate at slightly alkaline pH: unpublished Doctoral Dissertation, University of Minnesota, 291 p.
- Carlson, C.G., and Anderson, S.B., 1970, Sedimentary and tectonic history of North Dakota Part of Williston Basin: American Association of Petroleum Geologists Bulletin, v. 49, no. 11, p. 1833-1846.
- Cecil, C.B., Stanton, R.W., Allshouse, S.D., and Finkelman, R.B., 1978, Geologic controls on mineral matter in the upper Freeport coal bed: Proceedings: Symposium on coal cleaning to achieve energy and environmental goals, p. 110-125.
- Cecil, C.B., Stanton, R.W., Allshouse, S.D., Finkelman, R.B., and Greenland, L.P., 1979, Geologic controls on element concentrations in the upper Freeport coal bed: ACS, Div. Fuel Chem., Preprints of paper presented at Honolulu, Hawaii, v. 24, no. 1, p. 230-235.
- Cecil, C.B., Stanton, R.W., Dulong, F.T., and Renton, J.J., 1982, Geologic facts that control mineral matter in coal: in Filby, R.H., ed., Atomic and nuclear methods in fossil energy research: Plenum Press, New York, p. 323-335.
- Chemical Rubber Company Handbook of Chemistry and Physics, 1982, 63rd edition, Weast, R.C., and Astle, M.J., eds., CRC Press, Inc., Boca Raton, Florida, p. B-202-B-207.
- Clayton, L., Carlson, C.G., Moore, W.L., Groenewold, G.H., Holland, F.D., Jr., and Moran, S.R., 1977, The Slope (Paleocene) and Bullion Creek (Paleocene) formations of North Dakota: North Dakota Geological Survey Report of Investigation No. 59, 14 p.

- Cohen, A.D., Spackman, W., and Dolsen, P., 1984, Occurrence and distribution of sulfur in peat-forming environments of Southern Florida: *International Jour. Coal Geol.*, v. 4, p. 73-96.
- Davis, A., Russel, S.J., Rimmer, S.M., and Yeakel, J.D., 1984, Some genetic implications of silica and aluminosilicates in peat and coal: *International Journal of Coal Geology*, v. 3, p. 293-314.
- Deer, W.A., Howie, R.A., and Zussman, J., 1966, *An introduction to the rock-forming minerals*: John Wiley and Sons Inc., New York, 528 p.
- Deer, W.A., Howie, R.A., and Zussman, J., 1962, *Rock-forming minerals, Volume 3 (Sheet Silicates)*: John Wiley and Sons Inc., New York, 270 p.
- Dutcher, R.R., editor, 1976, *Field description of coal*: ASTM Spec. Tech. Publ. 661, 70 p.
- Falcone, S.K., Schobert, H.H., Rindt, D.K., and Braun, S., 1984, Mineral transformations during ashing and slagging of selected low-rank coals: *ACS, Div. Fuel Chem., Preprints*, v. 29, no. 4, p. 76-83.
- Finkelman, R.B., 1983, *The inorganic geochemistry of coal: an SEM view*: unpublished paper written for: Exxon Production Research Company, Houston, Texas, 27 p.
- Finkelman, R.B., 1982, Modes of occurrence of trace elements and minerals in coal: an analytical approach: In *atomic and nuclear methods in fossil energy research*, R.H. Filby, editor, Plenum Press, New York, p. 141-149.
- Finkelman, R.B., 1980, *Modes of occurrence of trace elements in coal*: PH.D. Dissertation, University of Maryland, College Park, MD., 300 p.
- Finkelman, R.B., 1978, Determination of trace element sites in the Waynesburg coal by SEM analysis of accessory minerals: *Scanning Electron Microscopy*, v. I, SEM Inc., AMF O'Hare, IL, p. 143-148.
- Finkelman, R.B., and Stanton, R.W., 1978, Identification and significance of accessory minerals from a bituminous coal: *Fuel*, v. 57, p. 736-768.
- Fowkes, W.W., 1978, Separation and identification of minerals from lignites: in *Karr, C., Jr., ed., Analytical methods for coal and coal products, Volume II*: Academic Press, Inc., p. 293-314.

- Francis, W., 1961, Coal: its formation and composition, 2nd edition,: London, Edward Arnold Publishers, 806 p.
- Gluskoter, H.J., 1965, Electric low-temperature ashing of bituminous coal: Fuel, v. 44, no. 4, p. 285-291.
- Greer, R.T., 1977, Coal microstructure and the significance of pyrite inclusions: Scanning Electron Microscopy, 1977, v. I, SEM Inc., AMF O'Hare, IL, p. 79-93.
- Groenewold, G.H., Hemish, L.A., Cherry, J.A., Rehm, B.W., Meyer, G.N., and Winczewski, L.M., 1979, Geology and geohydrology of the Knife River and adjacent areas of west-central North Dakota: North Dakota Geological Survey Report of Investigation No. 64, 402 p.
- Gronhovd, G.H., Wagner, R.J., and Whittmaier, A.J., 1967, A study of the ash fouling tendencies of a North Dakota lignite as related to its sodium content: Transactions of the Society of Mining Engineers, September, p. 313-322.
- Guyen, N., and Lee, L., 1983, Characterization of mineral matter in East Texas lignites: Texas Energy and Natural Resources Advisory Council, Energy Development Fund, Report No. TENRAC/EDF-103, 64 p.
- Harvey, R.D., and Ruch, R.R., 1984, Overview of mineral matter in U.S. coals: ACS, Div. Fuel Chem., Preprints, v. 29, no. 4, p. 76-83.
- Houghton, R.L., Thorstenson, D.C., Fisher, D.W., and Groenewold, G.H., 1984, Hydrogeochemistry of the upper part of the Fort Union Group in the Gascoyne lignite strip-mining area, North Dakota: U.S. Geological Survey, Open File Report No. 84-131, 184 p.
- Huggins, F.E., Kosmack, D.A., Huffman, G.P., and Lee, R.J., 1980, Coal mineralogies by SEM automatic image analysis: Scanning Electron Microscopy, 1980, I, SEM Inc., AMF O'Hare, IL, p. 531-540.
- Hughes, R.E., 1971, Mineral matter associated with Illinois coals: University of Illinois, Doctoral Dissertation Urbana-Champaign, Illinois, 145 p.
- Hurley, J.P., and Benson, S.A., 1984, Comparative elemental associations in lignites having significant within-mine variability of sodium content: ACS Div. Fuel Chem., Preprints, v. 29, no. 5, pp. 210-216.

- Hurley, J.P., Miller, B.G., and Jones, M.L., 1985, Correlation of coal characteristics and fouling tendencies of various coals from the Gascoyne Mine: Proceedings for the 13th Biennial Lignite Symposium, Bismarck, North Dakota, May 1985, DOE/FE-60181-136.
- International Committee for Coal Petrology, 1963, 1971, 1975, Handbook of coal petrology: 2nd ed., supplements 1 and 2, Centre National de la Recherche Scientifique, Paris, France.
- Jacob, A.F., 1976, Geology of the upper part of the Fort Union Group (Paleocene), Williston Basin, with reference to uranium: North Dakota Geological Survey, Report of Investigation No. 58, 49 p.
- Kemezys, M., and Taylor, G.H., 1964, Occurrence and distribution of minerals in some Australian coals: Jour. Inst. Fuel, v. 37, no. 284, p. 389-397.
- Kepferle, R.C., and Culbertson, W.C., 1955, Strippable lignite deposits, Slope and Bowman counties North Dakota: U.S. Geol. Surv. Bull. 1015-E, p. 123-182.
- Kerr, P.F., Hamilton, P.K., Pill, R.J., Wheeler, G.V., Lewis, D.R., Burkhardt, W., Reno, D., Taylor, G.L., Mielenz, R.C., King, M.E., and Schieltz, N.C., 1950, Analytical data on reference clay materials: American Petroleum Institute, Preliminary Report No. 7, Project 49, Clay Mineral Standards, Columbia University, New York, p. 52-56.
- Kleesattel, D.R., 1985, Petrology of the Beulah-Zap lignite bed, Sentinel Butte formation (Paleocene) Mercer County, North Dakota: University of North Dakota unpublished Master's Thesis, 187 p.
- Kleesattel, D.R., 1984, Distribution, abundance, and maceral content of the lithotypes in the Beulah-Zap bed of North Dakota: Proceedings: Symposium on the geology of Rocky Mountain coal: North Dakota Geol. Soc. Publ. 84-1, p. 28-40
- Leonard, A.G., Babcock, E.J., and Dove, L.P., 1925, The lignite deposits of North Dakota: North Dakota Geological Survey Bulletin No. 4, 240 p.
- Lindsay, W.L., and Vlek, P.L.G., 1977, Phosphate minerals: in Dinaver, R.C., Nagler, J., and Nauseef, J.H., eds., Minerals in soil environments: Soil Science Society of America, Madison, WI, p. 339-670.

- Mackowsky, M-Th., 1968, Mineral matter in coal: in Coal and coal-bearing strata, Murchison, D.G., and Westall, T.S., eds., American Elsevier, New York, p. 309-321.
- Miller, R.N., 1984, The methodology of low-temperature ashing, in Finkelman, R.B., Fiene, F.L., Miller, R.N., and Simon, F.O., eds., Interlaboratory comparison of mineral constituents in a sample from the Herrin (No. 6) coal bed from Illinois: U.S. Geological Survey Circular 932, p. 9-15.
- Mott, R.A., 1948, Journal of the Institute of Fuel, v. 22, no. 2.
- Moza, A.K., Austin, L.G., and Johnson, G.G., Jr., 1979, Inorganic element analysis of coal particles using computer evaluation of scanning electron microscopy images: Scanning Electron Microscopy, I, SEM Inc., AMF O'Hare, IL, p. 473-476.
- Moza, A.K., Strickler, D.W., and Austin, L.G., 1980, Elemental analysis of upper Freeport coal particles: Scanning Electron Microscopy, IV, SEM Inc., AMF O'Hare, IL, p. 91-96.
- O'Gorman, J.V., and Walker, P.L., Jr., 1972, Mineral matter and trace elements in U.S. coals: U.S. Office of Coal Research, Research and Development Report No. 61, Interim Report No. 2, U.S. Gov't Printing Office, Washington, D.C., 184 p.
- O'Gorman, J.V., and Walker, P.L., Jr., 1971, Mineral matter characteristics of some american coals: Fuel, v. 50, p. 135-151.
- Parkash, S., Carlson, D., and Ignasiak, B., 1982, Petrographic composition and liquefaction behavior of North Dakota and Texas lignites: Fuel, v. 62, no. 6, p. 627.
- Parr, S.W., 1932, The analysis of fuel, gas, water, and lubricants: McGraw-Hill, New York, 49 p.
- Paulson, L.E., Beckering, W., and Fowkes, W.W., 1972, Separation and identification of minerals from Northern Great Plains Province lignite: Fuel, v. 51, July, p. 224-227.
- Pough, F.H., 1976, A field guide to rocks and minerals: Houghton Mifflin Company, Boston, 317 p.

- Rao, C.P., and Gluskoter, H.J., 1973, Occurrence and distribution of minerals in Illinois coals: Circular 476, Illinois State Geol. Surv., Urbana, 56 p.
- Raymond, R., Jr., and Gooley, R., 1979, Electron probe microanalyzer in coal research: in Karr, C., Jr., ed., Analytical methods for coal and coal products, Volume III: Academic Press, p. 337-356.
- Royse, C.F., 1970, A sedimentological analysis of the Tongue River-Sentinel Butte interval (Paleocene) of Williston Basin, western North Dakota: Sedimentary Geology, v. 4 p. 19-80.
- Royse, C.F., 1967, Tongue River-Sentinel Butte contact in western North Dakota: North Dakota Geological Survey Report of Investigation No. 45, 53 p.
- Russel, S.J., and Rimmer, S.M., 1979, Analysis of mineral matter in coal, coal gasification ash, and coal liquefaction residues by scanning electron microscopy and x-Ray diffraction: in Karr, C., Jr., ed., Analytical methods for coal and coal products, Volume III: Academic Press, p. 133-162.
- Schopf, J.M., 1960, Field description and sampling of coal beds: Geol. Surv. Bull. 1111-B. 67 p.
- Sondreal, E.A., and Ellman, R.C., 1975, Fusibility of ash from lignite and its correlation with ash composition: ERDA Report of Investigation, GFERC/RI-75/1, 121 p.
- Sondreal, E.A., Kube, W.R., and Elder, J.L., 1968, Analysis of the Northern Great Plains Province lignites and their ash: a study of variability: Bureau of Mines Report of Investigations 7158, 94 p.
- Sondreal, E.A., Tufte, P.H., Beckering, W., 1977, Ash fouling in the combustion of low rank western U.S. coals: Combustion Science and Technology, v. 16, p. 95-110.
- Sprunk, G.C., and O'Donnell, H.J., 1942, Mineral matter in coal: U.S. Bureau of Mines, Technical Paper 648, 67 p.
- Stach, E., Mackowsky, M-Th., Teichmuller, M., Taylor, G.H., Chandra, D., and Teichmuller, R., 1982, Coal petrology: Gebruder Borntraeger, Berlin, Stuttgart, Germany, 535 p.
- Stadnichenko, T., Zubovic, P., and Sheffey, N.B., 1961, Beryllium content of American coals: Geol. Soc. Amer. Bull. 1084-K, p. 253-295.

- Stanton, R.W., and Finkelman, R.B., 1979, Petrographic analysis of bituminous coal: optical and SEM identification of constituents: Scanning Electron Microscopy, 1979, v. I, SEM Inc., AMF O'Hare, IL, p. 465-471.
- Stopes, M.C., 1919, On the four visible ingredients in banded bituminous coals: Proc. Roy. Soc. B, 90, p. 470-487, London.
- Thiessen, R., and Francis, W., 1929, Terminology in coal research: Fuel, v. 8, no. 8, p. 385-405.
- Thiessen, R., and Sprunk, G.C., 1935, Microscopic and petrographic studies of certain American coals: U.S. Department of the Interior, Technical Paper 564, 71 p.
- Ting, F.T.C., 1972, Petrified peat from a Paleocene lignite in North Dakota: Science, v. 177, p. 165-166.
- Valkovic, V., 1983, Trace elements in coal: CRC Press Inc., Volume I, 210 p.
- Vassamillet, L.F., 1972, Examination of medium rank coals by SEM in 7th conference on electron probe analysis: Electron Probe Analysis Soc. Am., p. 55-A-B.